

This electronic thesis or dissertation has been downloaded from the King's Research Portal at <https://kclpure.kcl.ac.uk/portal/>



## **UVA-induced oxidative stress and DNA damage in human skin cells and photoprotection by antioxidant compounds**

Delinassios, George

*Awarding institution:*  
King's College London

The copyright of this thesis rests with the author and no quotation from it or information derived from it may be published without proper acknowledgement.

### **END USER LICENCE AGREEMENT**



**Unless another licence is stated on the immediately following page** this work is licensed

under a Creative Commons Attribution-NonCommercial-NoDerivatives 4.0 International

licence. <https://creativecommons.org/licenses/by-nc-nd/4.0/>

You are free to copy, distribute and transmit the work

Under the following conditions:

- Attribution: You must attribute the work in the manner specified by the author (but not in any way that suggests that they endorse you or your use of the work).
- Non Commercial: You may not use this work for commercial purposes.
- No Derivative Works - You may not alter, transform, or build upon this work.

Any of these conditions can be waived if you receive permission from the author. Your fair dealings and other rights are in no way affected by the above.

### **Take down policy**

If you believe that this document breaches copyright please contact [librarypure@kcl.ac.uk](mailto:librarypure@kcl.ac.uk) providing details, and we will remove access to the work immediately and investigate your claim.

This electronic theses or dissertation has been downloaded from the King's Research Portal at <https://kclpure.kcl.ac.uk/portal/>



**Title:** UVA-induced oxidative stress and DNA damage in human skin cells and photoprotection by antioxidant compounds

**Author:** George Delinassios

The copyright of this thesis rests with the author and no quotation from it or information derived from it may be published without proper acknowledgement.

#### END USER LICENSE AGREEMENT



This work is licensed under a Creative Commons Attribution-NonCommercial-NoDerivs 3.0 Unported License. <http://creativecommons.org/licenses/by-nc-nd/3.0/>

You are free to:

- Share: to copy, distribute and transmit the work

Under the following conditions:

- Attribution: You must attribute the work in the manner specified by the author (but not in any way that suggests that they endorse you or your use of the work).
- Non Commercial: You may not use this work for commercial purposes.
- No Derivative Works - You may not alter, transform, or build upon this work.

Any of these conditions can be waived if you receive permission from the author. Your fair dealings and other rights are in no way affected by the above.

#### Take down policy

If you believe that this document breaches copyright please contact [librarypure@kcl.ac.uk](mailto:librarypure@kcl.ac.uk) providing details, and we will remove access to the work immediately and investigate your claim.

# UVA-induced oxidative stress and DNA damage in human skin cells and photoprotection by antioxidant compounds

Thesis presented for the degree of Ph.D.

By

George Delinassios

Photobiology Group

St John's Institute of Dermatology

Division of Genetics and Molecular Medicine

King's College London School of Medicine

University of London

**May 2012**

Total word count: 36,559

### **Signed Declaration**

The *in vitro* work presented here is my own and all experiments were performed by me. The only exceptions are the PCR data obtained from human skin experiments carried out by my colleague, Dr Angela Tewari. These are included so that *in vitro* and *in vivo* comparisons can be made.

George Delinassios

## Abstract

Solar ultraviolet radiation (UVR), especially UVA (320-400nm), is a potent inducer of oxidative DNA damage in human skin cells. Such damage has mutagenic and carcinogenic potential. It is therefore important to understand the mechanisms that control its extent, and develop means of protecting against such damage. The main purpose of this work was to develop reliable quantitative methods to measure UVR-induced oxidative stress, assess its biological consequences and its inhibition, in human skin cells *in vitro*. Most of this work studied the effects of UVA radiation, as this is the major (>95%) component of solar UVR and readily generates reactive oxygen species (ROS). Particular focuses of this work were the measurement of UVA-induced ROS, as well as the formation of two of the most intensively studied DNA photolesions, the guanine-derived lesion 8-oxo-7,8-dihydroguanine (8-oxoGua), and the cyclobutane pyrimidine dimer (CPD). These were assessed by an enzyme specific comet assay. Vitamin E was used as a model antioxidant and treatment of HaCaT keratinocytes pre- but also post-irradiation was found to reduce ROS levels, as well as UVA-induced 8-oxoGua and CPD formation. The post-UVR protection offered by vitamin E eliminated any possible sunscreen effects. Real-time PCR data of UVA-induced genes showed that vitamin E inhibited expression of heme oxygenase 1 (HO1) but not matrix metalloproteinase 12 (MMP12). Of three other antioxidants tested, only one (lanosterol) had an inhibitory effect on ROS and 8-oxoGua, but not on CPD formation. Studies with agents that modified ROS levels showed a clear link between ROS and 8-oxoGua but not CPD. Overall, the data showed that antioxidants have the potential to protect against potentially mutagenic epidermal DNA photodamage, an endpoint which, along with gene expression, can be readily applied to the *in vivo* human situation.

## Table of Contents

Abstract .....	3
Table of Contents .....	4
Tables .....	9
Figures.....	10
Acknowledgments.....	15
List of abbreviations.....	16
<b>Chapter 1: Introduction.....</b>	<b>19</b>
1.1    Solar radiation .....	20
1.1.1    Historical perspective.....	20
1.2    Light and photobiology .....	22
1.3    Importance of action spectra and UVR sources.....	22
1.4    Ultraviolet radiation and its effects on human health .....	23
1.4.1    UVA.....	27
1.4.2    UVB .....	33
1.5    CPD.....	34
1.5.1    UVA-induced CPD.....	35
1.6    DNA repair .....	37
1.7    Photoprotection .....	38
1.7.1    Sunscreens.....	38
1.8    Positive effects of UVR .....	40
1.9    Oxidative stress .....	41
1.9.1    Measurement of oxidative stress.....	42
1.10    Antioxidants .....	43

1.10.1	Antioxidants against UVR-induced oxidative stress .....	45
1.11	Vitamin E .....	48
1.12	Aims of thesis.....	52
<b>Chapter 2: Materials and Methods .....</b>		<b>54</b>
2.1	Materials.....	55
2.2	Cell culture and antioxidant treatments.....	59
2.2.1	HaCaT keratinocytes .....	59
2.2.2	Primary human skin fibroblasts .....	59
2.2.3	MRC5V1 fibroblasts .....	60
2.3	Spectroscopy .....	60
2.4	Antioxidant treatments .....	61
2.4.1	Vitamin E .....	61
2.4.2	N-acetyl cysteine.....	62
2.4.3	Stiefel compounds.....	63
2.5	Irradiation.....	65
2.5.1	UVA.....	65
2.5.2	UVB .....	67
2.5.3	UVC .....	69
2.6	Cell viability/survival assays.....	70
2.6.1	MTT-time course assay .....	70
2.6.2	Trypan blue exclusion assay .....	71
2.7	Reactive oxygen species production .....	71
2.8	Single-cell gel electrophoresis (comet assay) .....	73
2.8.1	8-oxoGua detection .....	74
2.8.2	CPD detection .....	74

2.8.3	DNA unwinding and electrophoresis .....	75
2.9	A mechanistic approach to study UVA-induced DNA damage .....	77
2.10	Gene expression studies .....	78
2.10.1	RNA isolation.....	78
2.10.2	cDNA synthesis.....	79
2.10.3	Real Time RT-PCR.....	79
2.10.4	Analysis of real-time PCR data.....	80
2.11	Total glutathione (GSH) measurement.....	81
2.12	Immuno-Slot-Blot (ISB) for the detection of UVA-induced CPD.....	82
2.12.1	Densitometry .....	83
2.13	Statistical analysis .....	83
<b>Chapter 3:</b>	<b>Results.....</b>	<b>84</b>
3.1	Study of UVB-induced DNA damage for technique development.....	86
3.1.1	UVB-induced DNA damage on HaCaT keratinocytes.....	86
3.2	Optimisation of hOGG1, T4endoV and vitamin E concentrations for the comet assay .....	90
3.2.1	Cell viability.....	94
3.3	Time-course experiments to establish DNA repair time-points for specific types of UVA-induced DNA damage.....	95
3.4	Pre- and post-UVR effect of vitamin E against UVA-induced DNA damage and oxidative stress .....	98
3.4.1	Vitamin E pre-treatment protects against UVA-induced ROS formation and DNA damage .....	98
3.4.2	Post-UVR treatment with vitamin E also offers significant protection against ROS formation and DNA damage .....	103



3.4.3	Vitamin E does not protect against UVC-induced formation of CPD but does protect against the formation of 8-oxoGua and ALS/SB.....	108
3.4.4	Vitamin E treatment prior to UVA significantly protects against T<math>\rightarrow</math>T formation.....	111
3.4.5	Vitamin E increases total GSH levels in HaCaT keratinocytes and protects against UVA-induced GSH depletion.....	114
3.5	Assessment of NAC in the protection against UVA-induced DNA damage	116
3.5.1	NAC protects against UVA-induced ROS and GSH depletion.....	117
3.5.2	NAC protects against UVA-induced 8-oxoGua formation but not against CPD.....	120
3.6	Real time PCR for detection of HO-1 and MMP-12 induction by UVA .....	123
3.6.1	In vivo study for the UVA1-induced expression of HO1 and MMP12	136
3.7	ROS pathways inhibitors study.....	139
3.8	Stiefel compounds testing against UVA-induced DNA damage and oxidative stress.....	146
<b>Chapter 4: Discussion .....</b>		<b>154</b>
4.1	UVR-induced DNA damage .....	155
4.1.1	UVA vs UVB-induced CPD formation .....	155
4.2	Time-course assay for UVA-induced 8-oxoGua, CPD and ALS/SB .....	157
4.3	Vitamin E photoprotection .....	159
4.4	NAC photoprotection.....	167
4.5	UVA-induced HO1 and MMP12 gene expression .....	167
4.6	Role of mitochondrial respiratory chain complex I and NADPH in UVA-induced DNA damage .....	170
4.7	Stiefel compounds with antioxidant potential.....	174

4.8	General conclusions .....	176
4.9	Further perspectives .....	181
	Bibliography.....	183
	Appendix .....	218

## Tables

Table 2.1:	General reagents.....	55
Table 2.2:	Tissue culture growth medium constituents.....	56
Table 2.3:	Antibodies, enzymes and primers .....	57
Table 2.4:	Molecular biology kits .....	57
Table 2.5:	Stock solutions .....	58
Table 2.6:	Optical properties of antioxidant compounds and their solvents used in thesis.....	58
Table 2.7:	Spectroradiometric distribution of emission spectrum of the UVASPOT.....	67
Table 2.8:	Spectroradiometric distribution of emission spectrum of the FS20 Westinghouse SunLamp.....	68
Table 3.1:	HaCaT cell viability following UVB irradiation .....	86
Table 3.2:	HaCaT cell viability following UVA irradiation.....	94
Table 3.3:	HaCaT cell viability following UVA $\pm$ vit E.....	94
Table 3.4:	HaCaT cell viability following incubation (4 h) with various concentrations of NAC.....	116
Table 3.5:	HaCaT cell viability following incubation (2 h) with various concentrations of rotenone.....	140
Table 3.6:	HaCaT cell viability following incubation (2 h) with various concentrations of DPI.....	140
Table 3.7:	HaCaT cell viability following incubation with various concentrations of the Stiefel compounds .....	146

## Figures

Figure 1.1:	The electromagnetic spectrum .....	24
Figure 1.2:	Some of the effects of UVA and UVB on the human skin .....	26
Figure 1.3:	Human skin penetration by UVR.....	28
Figure 1.4a:	UVA-induced oxidative stress.....	30
Figure 1.5b:	Photosensitization reactions type I and type II .....	30
Figure 1.6:	Chemical structures of 8-oxoGua and its corresponding base, 8-oxodGuo.....	32
Figure 1.7:	Chemical structure of CPD .....	33
Figure 1.8:	Chemical structure of $\alpha$ -tocopherol.....	49
Figure 1.9:	Schematic depicting the chemical action of $\alpha$ -tocopherol reacting with a free radical.....	51
Figure 2.1:	Absorption spectrum of vitamin E (0.1 mg/ml in <i>n</i> -hexane) .....	61
Figure 2.2:	Absorption spectrum of NAC (1 mM solution, in PBS) .....	62
Figure 2.3:	Absorption spectrum of farnesol (10 $\mu$ M in EtOH) .....	63
Figure 2.4:	Absorption spectrum of guggulsterone (5 $\mu$ M in DMSO) .....	64
Figure 2.5:	Absorption spectrum of lanosterol (5 $\mu$ M in EtOH) .....	64
Figure 2.6:	Emission spectrum of the UVASPOT .....	66
Figure 2.7:	Emission spectrum of the FS20 Westinghouse SunLamp.....	68
Figure 2.8:	Schematic representation of the basic steps of the comet assay .....	76
Figure 3.1:	Comets formed due to UVB radiation with two doses (50 and 100 mJ/cm <sup>2</sup> ).....	87
Figure 3.2a:	Effect of UVB irradiation on the formation of 8-oxoGua, CPD and ALS/SB detected by the hOGG1- and the T4endoV-modified comet assay .....	88

Figure 3.2b: Effect of UVB irradiation on the formation of 8-oxoGua and CPD formation as detected by the hOGG1- and the T4endoV-modified comet assay (background corrected) .....	89
Figure 3.3: Optimisation of hOGG1 concentration by the comet assay .....	91
Figure 3.4: Optimisation of T4endoV concentration by the comet assay .....	92
Figure 3.5: Optimisation of vitamin E concentration (without the use of any DNA repair enzymes) .....	93
Figure 3.6: Induction and repair of UVA-induced 8-oxoGua and CPDs, over 10 h ..	96
Figure 3.7: Comparison of ROS production between control (EtOH) and pre-UVR treated (+ vit E) groups .....	99
Figure 3.8a: Effect of pre-UVR incubation with vit E on 8-oxoGua, CPD and ALS/SB formation detected by the hOGG1 and the T4endoV-modified comet assay .....	101
Figure 3.8b: Effect of pre-UVR incubation with vitamin E on 8-oxoGua and CPD formation as detected by the hOGG1- and the T4endoV-modified comet assay (background corrected) .....	102
Figure 3.9: Comparison of ROS production between control (EtOH) and post-UVR treated (+ vit E) groups .....	104
Figure 3.10a: Effect of post-UVR incubation with vitamin E on 8-oxoGua, CPD and ALS/SB formation as detected by the hOGG1- and the T4endoV-modified comet assay .....	106
Figure 3.10b: Effect of post-UVR incubation with vitamin E on 8-oxoGua and CPD formation as detected by the hOGG1- and the T4endoV-modified comet assay (background corrected) .....	107
Figure 3.11a: Effect of pre-incubation with vitamin E on UVC-induced formation of CPD, 8-oxoGua and ALS/SB. Mean percentage of tail DNA HaCaT cells exposed to	

UVC for 10 sec.....	109
Figure 3.11b: Effect of pre-incubation with vitamin E on UVC-induced formation of CPD and 8-oxoGua. Mean percentage of tail DNA HaCaT cells exposed to UVC for 10 sec (background corrected) .....	110
Figure 3.12: UVB-irradiated (0-1 J/cm <sup>2</sup> ) CT-DNA was analyzed with the immuno-slot blot assay by using a T<math>\rhd</math>T-specific mAb.....	112
Figure 3.13: Genomic DNA of UVA-irradiated (20 J/cm <sup>2</sup> ) HaCaT keratinocytes was analyzed with immuno-slot blot assay by using a T<math>\rhd</math>T-specific mAb.....	113
Figure 3.14: Effect of UVA on total GSH levels in HaCaT keratinocytes .....	115
Figure 3.15: Comparison of ROS production between control and NAC-treated groups.....	118
Figure 3.16: Effect of NAC on total GSH levels in HaCaT keratinocytes.....	119
Figure 3.17a: Effect of pre-UVR incubation with NAC on 8-oxoGua, CPD and ALS/SB formation as detected by the hOGG1- and T4endoV-modified comet assay .	121
Figure 3.17b: Effect of pre-UVR incubation with NAC on 8-oxoGua and CPD levels (background corrected) .....	122
Figure 3.18: Time-course assay for HO1 induction following UVA irradiation (20 J/cm <sup>2</sup> ).....	124
Figure 3.19a: Real-time PCR analysis of HO1 expression in three different cell lines, 3 h after UVA irradiation.....	126
Figure 3.19b: Real-time PCR analysis of HO1 expression in three different cell lines, 3 h after UVA irradiation.....	127
Figure 3.20: Real-time PCR analysis HO1 expression in HaCaT keratinocytes ( $\pm$ vit E pretreatment) 3 h after UVA irradiation.....	128
Figure 3.21: Real-time PCR analysis of HO1 expression in MRC5V1 fibroblasts ( $\pm$	

vit E pretreatment), 3 h after UVA irradiation.....	129
Figure 3.22: Time-course assay for MMP12 induction following UVA irradiation (20 J/cm <sup>2</sup> ).....	130
Figure 3.23a: Real-time PCR analysis of MMP12 expression in three different cell lines, 12 h after UVA irradiation (20J/cm <sup>2</sup> ).....	132
Figure 3.23b: Real-time PCR analysis of MMP12 expression in three different cell lines, 12 h after UVA irradiation (20J/cm <sup>2</sup> ).....	133
Figure 3.24: Real-time PCR analysis of MMP12 expression in HaCaT keratinocytes (± vit E pretreatment) 12 h after UVA irradiation.....	134
Figure 3.25: Real-time PCR analysis of MMP12 expression in MRC5V1 fibroblasts, 12 h after UVA irradiation.....	135
Figure 3.26: Real-time PCR analysis of HO1 expression <i>in vivo</i> , 6 and 24 h following UVAI irradiation (relevant to untreated) .....	137
Figure 3.27: Real-time PCR analysis of MMP12 expression <i>in vivo</i> , 6 and 24 h following UVAI irradiation (relevant to untreated) .....	138
Figure 3.28: Effect of rotenone and DPI in intracellular UVA-induced ROS production.....	141
Figure 3.29: Effect of rotenone on UVA-induced DNA damage detected by the T4endoV- and hOGG1-modified comet assay .....	143
Figure 3.30: Effect of DPI on UVA-induced DNA damage detected by T4endoV- and hOGG1-modified comet assay .....	144
Figure 3.31: Effect of pre-incubation with rotenone (rot) and DPI on UVA-induced DNA damage detected by the T4endoV- and hOGG1-modified comet assay (background corrected) .....	145
Figure 3.32: Effect of lanosterol (10, 20 and 40 µM) in intracellular UVA-induced	

ROS production.....	148
Figure 3.33: Effect of guggulsterone (5, 10 and 20 $\mu$ M) in intracellular UVA-induced ROS production.....	149
Figure 3.34: Effect of lanosterol on UVA-induced DNA damage detected by T4endoV- and hOGG1-modified comet assay .....	151
Figure 3.35: Effect of guggulsterone on UVA-induced DNA damage detected by T4endoV- and hOGG1-modified comet assay .....	152
Figure 3.36: Effect of pre-incubation with lanosterol (lan) and guggulsterone (gug) on UVA-induced DNA damage detected by the T4endoV- and hOGG1-modified comet assay (background corrected).....	153
Figure 4.1: Emission spectrum of the UVASPOT, together with the absorption spectrum of a vit E solution (0.1 mg/ml in <i>n</i> -hexane) .....	160
Figure 4.2: UVA effects on human skin cells based on literature and findings of this thesis.....	180



## Acknowledgments

I express my sincere gratitude and respect to my first supervisor Professor Antony Young, for being patiently by my side during these years, guiding and supporting me through my work and also for his continuous challenges that have contributed to my personal and professional development. I would also like to thank my second supervisor Dr Marcus Cooke for his helpful input into my research, giving me the opportunity to learn valuable techniques in his laboratory in Leicester University, and for his helpful input into my research. I express my appreciation to Dr Tiago Duarte for teaching me the comet assay, and Mahsa Karbaschi for her assistance with the immuno-slot blot assay in Leicester University.

I gratefully acknowledge financial support from Stiefel Laboratories, UK. I also acknowledge financial support from the Department of Health via the National Institute for Health Research (NIHR) comprehensive Biomedical Research Centre award to Guy's & St Thomas' NHS Foundation Trust in partnership with King's College London and King's College Hospital NHS Foundation Trust.

My gratitude also goes to my colleagues in the photobiology group over the last 4 years. Specifically, I would like to thank Dr Olivier Reelfs for his valuable advice and critical input on experimental design and data analysis; Dr Kazuyo Kaneko for helping me through my first steps during my PhD by sharing her tissue culture protocols and always finding time to assist me with all the naïve queries I had in the beginning; Dr Angela Tewari, for allowing me to compare her *in vivo* data on HO-1 and MMP-12 induction with my *in vitro* results.

Last but not least, I thank my family for encouraging me throughout my studies and mentally helping me to cope with all the difficulties arisen during this period.

## List of abbreviations

8-oxoGua: 8-oxo-7,8-dihydroguanine

8-oxodGuo: 8-oxo-7,8-dihydro-2'-deoxyguanosine

°C: Centigrade

BER: Base Excision Repair

BSA: Bovine Serum Albumin

Ca<sup>2+</sup>: Calcium

cDNA: Complementary Deoxyribonucleic Acid

CO<sub>2</sub>: Carbon dioxide

CPD: Cyclobutane Pyrimidine Dimer

Ct: Threshold cycle

CT-DNA: Calf thymus DNA

DAPI: 4',6-diamidino-2-phenylindole

dH<sub>2</sub>O: Distilled water

DMEM: Dulbecco's Modified Eagle's medium

DMSO: Dimethyl Sulfoxide

DNA: Desoxyribonucleic Acid

DPI: Diphenylene Iodonium

dNTP: Deoxyribonucleotide Triphosphate

EDTA: Ethylenediaminetetraacetic Acid

EEE: Erythemally Effective Energy

EtOH: Ethanol (100%)

FCS: Fetal Calf Serum

FITC: Fluorescein Isothiocyanate

Fpg: Formamidopyrimidine Glycosylase

GO: Gene Ontology

h: Hour

H<sub>2</sub>O<sub>2</sub>: Hydrogen peroxide

HCl: Hydrochloric acid

HO1: Heme Oxygenase 1

hOGG1: human 8-oxoguanine DNA Glycosylase 1

IL-: Interleukin

MAPK: Mitogen-Activated Protein Kinase

MED: Minimal Erythematol Dose

MMP1: Matrix Metalloproteinase 1

MMP12: Matrix Metalloproteinase 12

mg: Milligram

MgCl<sub>2</sub>: Magnesium chloride

min: Minute

mL: Millilitre

mRNA: Messenger RNA

NAC: N-acetyl cysteine

NaCl: Sodium chloride

NER: Nucleotide Excision Repair

NF-κB: Nuclear Factor kappa-light-chain-enhancer of activated B cells

ng: Nanogram

NH<sub>4</sub>SO<sub>4</sub>: Ammonium sulphate

NO: Nitric Oxide

OGG1: 8-Oxoguanine Glycosylase 1

PBS: Phosphate Buffer Saline

PCR: Polymerase chain reaction

pH: potential of Hydrogen

PI: Propidium iodide

RNA: Ribonucleic Acid

ROS: Reactive Oxygen Species

RPMI 1640: Roswell Park Memorial Institute medium

RQ: Relative Quantification

RT-PCR: Reverse Transcription-Polymerase Chain Reaction

sec: Seconds

SPF : Sun Protective Factor

SSR : Solar Simulating Radiation

T4endoV : T4 endonuclease V

TE: Tris-EDTA buffer

TNF $\alpha$ : Tumor Necrosis Factor Alpha

U/ $\mu$ L: Unit per microliter

UCA: Urocanic Acid

US: United States

UV: Ultraviolet

UK: United Kingdom

v/v: Volume/Volume

V: Volt

Vit E:  $\alpha$ -tocopherol

w/v: Weight/Volume

$\mu$ L: Microliter

$\mu$ M: Micromolar

## **Chapter 1: Introduction**

## **1.1 Solar radiation**

### **1.1.1 Historical perspective**

Human fascination with the sun and sunlight began from the dawn of mankind. The human race recognized its importance for vision, warmth and, eventually, agriculture and health. The sun has been an important aspect of all major civilizations, including the Egyptians, who worshipped the god Ammon Ra that presumably gave the naming of the word “radiation” (Bovie, 1918b), Assyrians, Babylonians and Greeks (god Helios). The life-sustaining powers of the sun have been prominently displayed in ancient mythology and traditional culture.

Around 450 BC, the Greek philosopher Anaxagoras faced trial and was imprisoned for claiming that the sun was not a god, but a big fiery rock and its light was reflected by the moon. A little later, close to 400 BC, the Athenian physician Hippocrates understood the sun’s healing powers and prescribed heliotherapy (sunbathing) for the treatment psychological and medical disorders.

During the following century, Greek scholars studied optics, creating theories that attempted to explain vision, colour, light, and astronomical phenomena. Despite the fact that most of those theories were proven wrong, they initiated a gradual understanding of the relationship between the sun and living organisms (Hockberger, 2002).

During the second century BC, Ptolemy, a Greek astronomer based in Alexandria (Egypt), wrote several books about optics, but only one of these survived to the modern world. His work was mostly dedicated to the study of reflection and refraction, using

mirrors of different shapes (Smith, 1996). Coming to the early modern period, during the 17<sup>th</sup> century, Sir Isaac Newton made some important observations; when a narrow beam of sunlight hit a glass prism at an angle, some was reflected, while some passed through the glass, coming out as different coloured bands (“colour rainbow”). He hypothesised that light consists of particles of various colours, moving at different speeds. Furthermore, Newton was the first to use the term “spectrum” (Latin for “appearance”) explaining his research in optics. Continuing to the 19<sup>th</sup> century, physicists accomplished a number of important theoretical and practical contributions that assisted in clarifying light’s properties. Specifically, in 1842, Becquerel managed to photograph the solar spectrum, using a slit to diffract sunlight, and a lens to focus the image onto a glass plate. He demonstrated that the emitted light was of longer wavelength than the incident light (fluorescence); this was the first indication of the spectrum of ultraviolet radiation (UVR) (Valeur and Brochon, 2001). Later on, more breakthroughs in the emerging science of photobiology followed. In the early 1860s, while he was a Professor of Natural Philosophy at King's College London, James Clerk Maxwell was the first to hypothesise that light was an electromagnetic wave. Hertz later confirmed this theory by showing that light travels in waves at discrete wavelengths. In the beginning of the 20<sup>th</sup> century, discoveries in photophysics from Planck, Einstein and Bohr and other major scientists led to today’s knowledge that radiation is comprised of photons that are released from molecules after absorbing light. Electrons of different atoms absorb energy from photons and in turn emit it at different wavelengths (Hockberger, 2002).

## 1.2 Light and photobiology

Light/UVR is made up of photons (the smallest available “light packets”) and is propagated in the form of waves, so in a sense it is both a particle and a wave. The spatial period of the wave as it advances, is defined as wavelength and is measured in nanometres (nm). Photons at different wavelengths have different energies; the longer the wavelength, the lower the energy.

Photobiology is the science dedicated in studying the effects of light, including UVR, either harmful, or beneficial. The significance of photobiology as a discipline is easy to appreciate just by looking at the Nobel prizes awarded in the field, starting from the early 1900s (Phototherapy of *lupus vulgaris* and other diseases.), until 2008 (Discovery and development of the green fluorescent protein). The importance of photobiology is also highlighted by the fact that photobiologists can be found in numerous disciplines, varying from physics, biology, medicine and chemistry, to agriculture, ecology and meteorology. In addition, photo(chemo)therapy is widely used to treat skin diseases.

## 1.3 Importance of action spectra and UVR sources

Since the biological effects induced by UVR depend on the wavelengths of the radiation source, it is necessary to have spectral emission data in order to properly determine the hazard. These data consist of spectral irradiance ( $\text{W/m}^2/\text{nm}$ ) measurements of the source, measured with a spectroradiometer. The total irradiance ( $\text{W/m}^2$ ) is obtained by summing over all wavelengths emitted. The biologically-weighted irradiance is determined by multiplying the spectral irradiance at each wavelength by the biological or hazard weighting factor, termed action spectrum (which quantifies the relative



efficacy at each wavelength for causing the effect), and summing over all wavelengths (Cridland and Driscoll, 2009). All these factors are obtained from action spectra. Therefore, it is important for all studies concerned with UVR-induced damage on human tissue, to include detailed information about their UVR sources. This would enable researchers to replicate experiments easier and compare results in a more robust manner.

Another common problem that must be addressed in photobiology is the fact that studies often differ in specifying doses based either on physical (spectra/irradiance) or a biological (erythema) basis.

#### **1.4 Ultraviolet radiation and its effects on human health**

UVR ranges from 10 nm to 400 nm in the electromagnetic radiation spectrum (Figure 1.1). UVR is composed of UVA (315-400 nm), UVB (280-315 nm) and UVC (100-280 nm), based on the official designations of the Commission Internationale de l'Éclairage (CIE). However, in dermatological photobiology, UVR is commonly divided into UVA (320-400 nm), UVB (290-320 nm) and UVC (200-290 nm) (Diffey, 2002). Since advances in photobiology indicated a clearer distinction between UVB and UVA wavelengths, UVA was further subdivided to UVAI (320-340 nm) and UVAIL (340-400 nm). This is because the shorter wavelength UVAIL is more like UVB in terms of photobiological mechanisms.

From as early as the 1900s, photobiologists had concluded that UVR was important in damaging macromolecules and cell nuclei in particular (Bovie, 1918a). In studies in

1918, Bovie and Hughes were the first to describe specific UVR-induced alterations in the rate of cell growth and demonstrated that nuclear chromatin was particularly sensitive. They concluded with the insightful comment that the effects of UVR could be determined by energy absorption in molecules (Cleaver, 2002; Bovie and Hughes, 1918).

Since the skin is the largest human organ, it is constantly exposed to the potentially dangerous effects of UVR. Although UVC damages the skin (superficial layers), the longer UVR wavelengths, UVB and UVA, are more relevant to human exposures due to the elimination of wavelengths below 300 nm by the stratospheric ozone layer (Frederick et al., 1989).

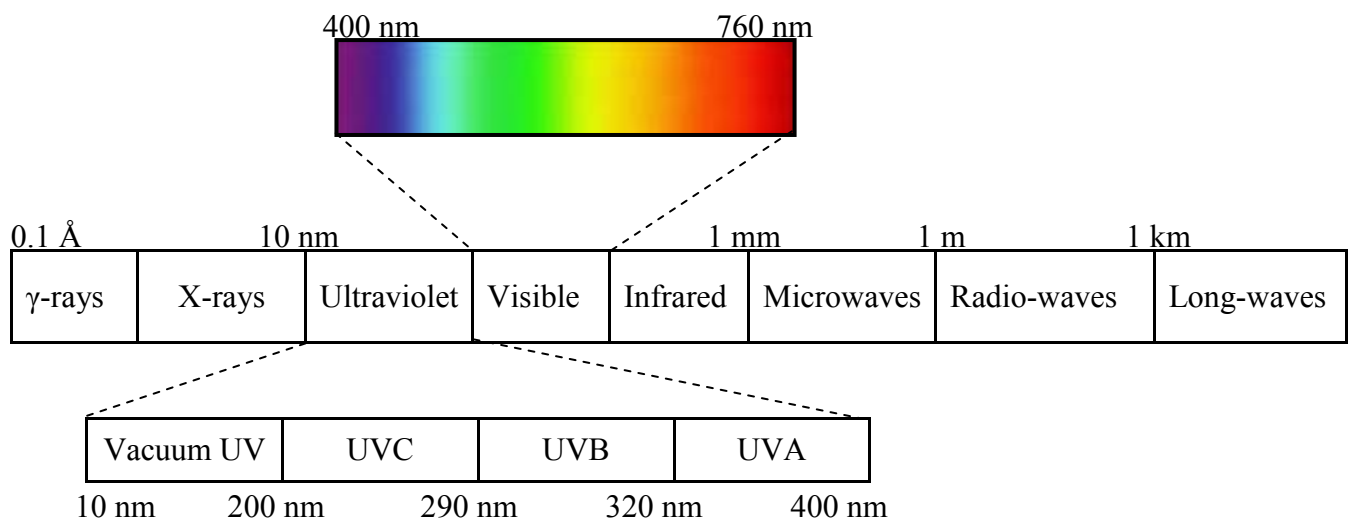


**Figure 1.1: The electromagnetic spectrum**

The UVR component of the terrestrial solar spectrum comprises approximately 5% of the total solar radiation. The majority (>95%) of solar UVR is UVA, and most (~75%) of this is UVAI (340-400 nm). This emphasizes the need to study the biological effects of UVA.

Although the short- and long-term consequences of solar UVR exposure have been well established (Marrot and Meunier, 2008), we lack detailed knowledge of spectral effects and their mechanisms, especially with long-term effects.

Exposure of skin to UVR may result in acute and chronic damage. Short-term overexposure causes sunburn (erythema), while chronic overexposure leads to an increased risk of skin cancer and photoageing (Meewes et al., 2001). In 1992, solar radiation was classified by the International Agency for Research on Cancer (IARC) as a Group 1 carcinogen, with a well-established link to cutaneous malignant melanoma and non-melanocytic skin cancer (World Health Organisation, 1992). UVR has also been linked with eye melanoma (Guenel et al., 2001) and non-Hodgkin's lymphoma (Tavani et al., 2006). It is therefore clear that UVR constitutes a great occupational hazard, especially in susceptible populations.

Sunlight can also suppress the immune function of skin (immunosuppression) and promote skin cancer formation (Streilein et al., 1994). Immunosuppression has been demonstrated in all patients with basal or squamous cell carcinomas (Rangwala and Tsai, 2011). Most UVR immunosuppression studies have used UVB, but recently UVA has been found to also play an important role (Damian et al., 2011; Halliday and Rana, 2008). One of the most well-studied chromophores, urocanic acid (UCA) (Gibbs and

Norval, 2011) has been recognised as an important initiator of the complex cascade leading to cell immunosuppression (Kaneko et al., 2008), but its mechanism of action is not completely understood (Gibbs et al., 2008). However, there is also evidence that DNA damage and the cyclobutane pyrimidine dimer (CPD; see section 1.6) in particular is important in immunosuppression (Kripke et al., 1992). In general, the mechanisms of UVR-induced immunosuppression still remain unclear (Norval, 2006).

A simplified schematic summarizing UVR effects on human skin is presented in Figure 1.2.

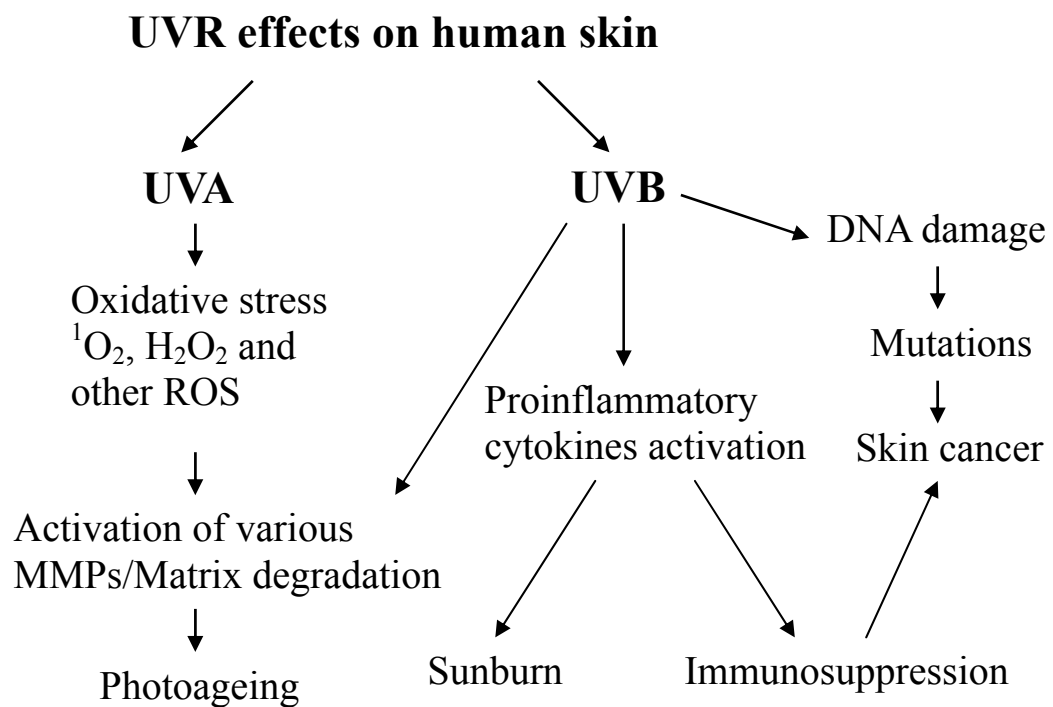


**Figure 1.2:** Some of the effects of UVA and UVB on the human skin

### 1.4.1 UVA

The nature of the DNA damage induced by UVR strongly depends on the wavelength of the incident photons that reach the cell (Douki et al., 2003). Since an increase in wavelength also means an increase in skin and tissue penetration (Bruls et al., 1984; Tewari et al., 2012a), the abundance of UVA (and particularly UVAI), in solar UVR means that it is very important to study its effects on skin.

During the last 20-30 years UVA attracted great interest, mainly due to its dominant role in the cosmetic industry. Sunlamps and sunbeds that are now widely used in the UK and other countries use a spectrum particularly high in UVA content. From as early as the 70s, tanning devices have been very popular. In 1985, the US Food and Drug Association (FDA) approved UVA emitting lamps for use in cosmetic skin tanning. UVA radiation was originally thought to cause tanning without any harmful effects to the skin. Actually, before 1990, only UVB, and not UVA, was considered to be carcinogenic. A lot of progress has been made since then in the understanding of the harmful effects of UVA radiation, but artificial tanning still remains a controversial subject. Although some older studies failed to demonstrate a clear danger, more recent research has established a correlation between sunbed use and skin cancer (Young, 2004; Gallagher et al., 2005). Furthermore, in 2005, the International Agency for Research on Cancer (IARC) assembled a “Working Group” of international experts on skin cancer and UVR to review the potential association between sunbed use and skin cancer. Meta-analysis of epidemiological data by the Working Group provided evidence between exposure to artificial UVR and increased risk of skin cancer, especially melanoma in people under 35 years of age (Autier et al., 2011).

The major reason UVA has drawn so much attention is that this spectral region penetrates the skin deeper than UVB readily reaching beyond the basal layer of the epidermis to the dermis, with the potential to damage dermal collagen and elastic fibres (Tewari et al., 2012b) (Figure 1.3).

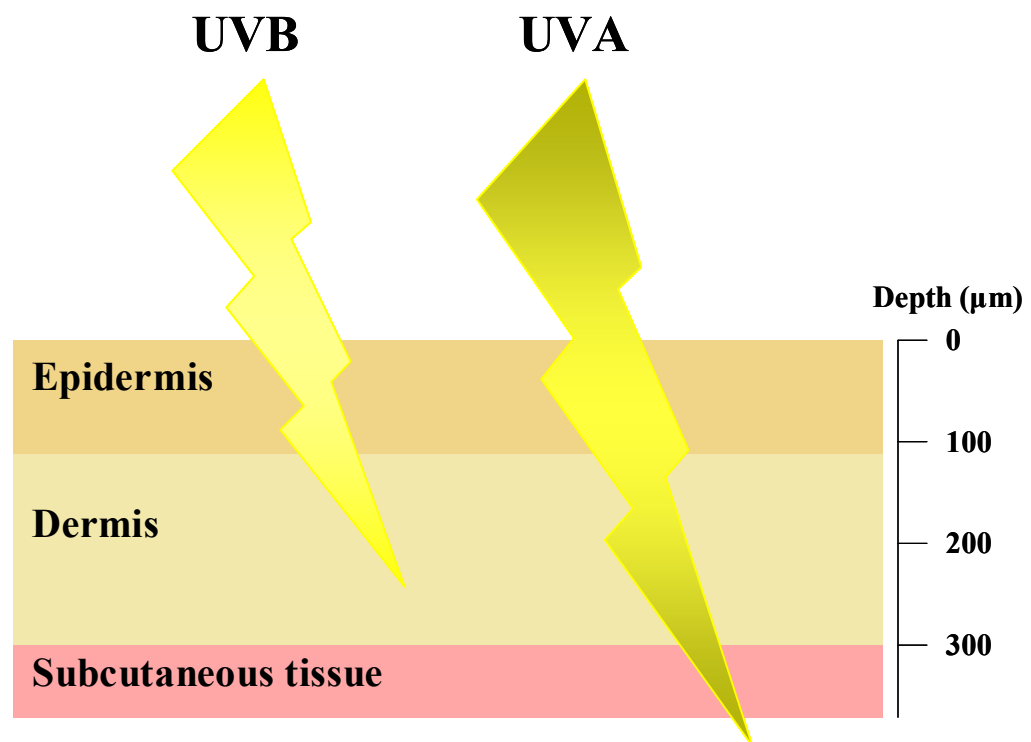


**Figure 1.3: Human skin penetration by UVR**

Approximate depth for UVA and UVB penetration in the human skin is based on a study by Bruls and colleagues in 1984 (Bruls et al., 1984).

UVA leads to free radical production, which can modify DNA along with other cellular components and may even lead to photocarcinogenesis (Baier et al., 2007; Agar et al., 2004; de Gruijl, 1995). Reactive oxygen species (ROS) are widely known as mediators of UVA-induced photodamage but the exact mechanism of their generation in UVR-irradiated skin is not fully understood. UVA-induced production of ROS is summarized in Figure 1.4a. Although UVA can cause an increase in electron leakage from the mitochondrial respiratory chain and enhance ROS production, the most prevalent theory about UVA oxidatively-induced photodamage involves photosensitization by endogenous chromophores in the human skin (Scharffetter-Kochanek et al., 1997). These chromophores absorb photons, reaching a photoexcited state, known as the triplet state. The sensitised chromophore can then damage human skin either through direct reaction with molecules such as DNA bases (type I photosensitisation; Figure 1.4b I), or by reacting with oxygen (type II photosensitisation; Figure 1.4b II), leading to free radical formation (Wondrak et al., 2006). UVAI, a particularly potent inducer of oxidative stress (Phillipson et al., 2002) has been found to induce the generation of singlet oxygen ( $^1\text{O}_2$ ), which causes skin ageing and cancer, and is an established mediator of photodamage (Baier et al., 2007; Davies, 2004).

$^1\text{O}_2$  is an excited state molecule that is formed by direct energy transfer between the excited sensitizer and ground state triplet oxygen, as illustrated in Figure 1.4 (reaction II A). Formation of the superoxide radical anion ( $\text{O}_2^{\cdot-}$ ), as a precursor of hydrogen peroxide ( $\text{H}_2\text{O}_2$ ) occurs through electron transfer, giving rise to a sensitizer radical cation (reaction II B), or after intermediate reduction of the sensitizer by a substrate with subsequent single electron reduction of oxygen (reaction I).

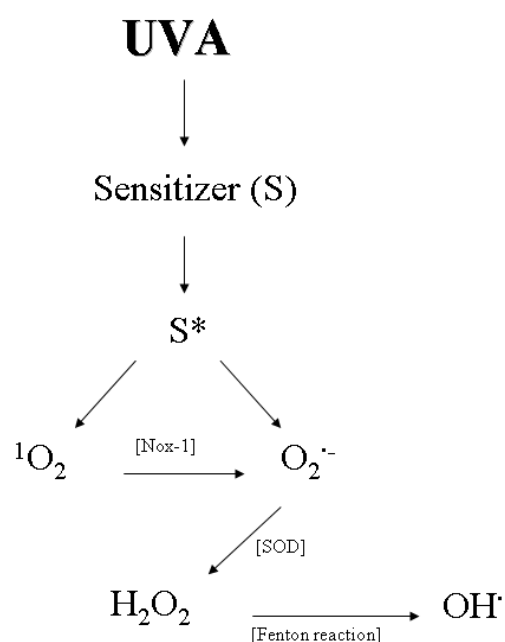


**Figure 1.4a: UVA-induced oxidative stress**

After UVA absorption, the excited photosensitizer ( $S^*$ ) generates  $^1O_2$ , which plays a key role in UVA-induced ROS production; The high redox potential of  $^1O_2$  allows it to react with all major classes of biomolecules, leading to protein oxidation, lipid peroxidation and DNA damage, and it triggers the generation of other ROS.

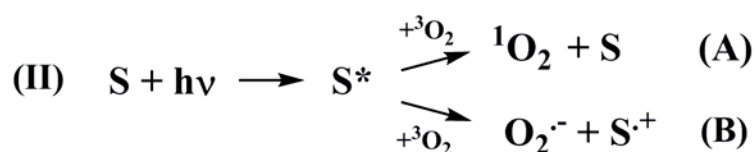
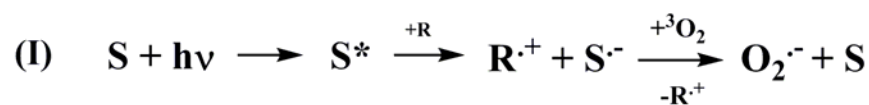


**Figure 1.5b: Photosensitization reactions type I and type II**

Photon absorption by chromophores in the electronic ground state ( $S$ ) induces formation of photoexcited states ( $S^*$ ). These can interact directly with substrate molecules ( $R$ ), like DNA bases (type I reaction) or activate molecular oxygen by electron or energy transfer reactions (type II reactions). *Adapted by Wondrak et al (Wondrak et al., 2006)*



As mentioned above, UVA can cause direct and indirect DNA damage, and its mutagenicity has been attributed to oxidatively generated modification of DNA nucleobases (Kassam and Rainbow, 2009). One of the most intensively studied lesions is the guanine-derived lesion 8-oxo-7,8-dihydroguanine (8-oxoGua), and its corresponding base, 2'-deoxyribonucleoside, 8-oxo-7,8-dihydro-2'-deoxyguanosine (8-oxodGuo) (Figure 1.5). This lesion is a possible cause of UVA mutagenesis, and its presence has been studied in both human DNA and urine (Kappes et al., 2006; Kielbassa et al., 1997; Cooke et al., 2001).

Several studies have focused on the activation of mitogen-activated protein kinases (MAPK) through UVA-induced ROS, and mainly through singlet oxygen (Bachelor and Bowden, 2004). Down-stream of MAPK and other signalling cascades, UVA irradiation has also been shown to activate various transcription factors such as AP-1 and NF $\kappa$ B, affecting crucial pathways involved in carcinogenesis (Reelfs et al., 2004; Wu et al., 2008). Furthermore, UVA induces the expression of several genes such as heme oxygenase 1 (HO1), matrix metalloproteinase 1 (MMP1) and tumour necrosis factor  $\alpha$  (TNF $\alpha$ ), that are also involved in photocarcinogenesis through immunosuppression or the degradation of extracellular matrix proteins (Klotz et al., 2003; Wondrak et al., 2006). It has also been proposed that UVA may increase intracellular oxidative stress without the intervention of ROS, by increasing the ratio of GSSG/GSH (He et al., 2003).

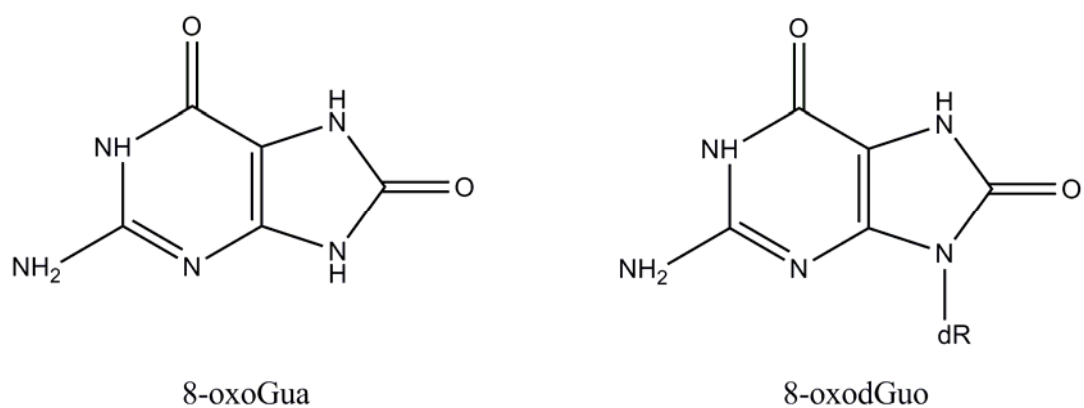


**Figure 1.6: Chemical structures of 8-oxoGua and its corresponding base, 8-oxodGuo**

Designed with ChemDraw Ultra

8-oxoGua has been used in various studies as a biomarker of oxidatively induced DNA damage. It is mostly repaired by the base excision repair (BER) pathway and is specifically recognized by the formamidopyrimidine glycosylase (Fpg) in *Escherichia coli* and the human oxoguanine glycosylase 1 (hOGG1) protein in humans (Girard and Boiteux, 1997).

In general, mutations by UVA-induced DNA damage typically consist of T-G transversions, called "UVA fingerprint" lesions (Agar et al., 2004). Furthermore, UVA has been shown to induce fewer immediate mutations than UVB, but more long-term mutations ("delayed mutations") (Dahle and Kvam, 2003). UVA-induced mutations have been reported by various workers (Huang et al., 2009; Mitchell and Fernandez, 2012). Evidence also exists showing that indirect oxidatively-induced DNA damage due to UVA, may promote melanoma formation (Panich et al., 2011; von Thaler et al., 2010). Recent epidemiological data also strengthen the link between UVA and melanoma cancers (Autier et al., 2011).

### 1.4.2 UVB

For many years, it was thought that UVB was far more carcinogenic to the skin than UVA. Of course, when comparing similar physical doses between the two, UVB radiation is much more damaging. This is because UVB is highly mutagenic and is directly absorbed by macromolecules such as proteins, lipids and DNA (Marrot and Meunier, 2008). UVB-induced DNA damage has therefore been considered as a key factor leading to mutations in genes associated with cancer, hence initiating the formation of tumours. UVB has also been found to induce genomic instability (an effect shared with UVA), and it can also cause delayed mutations (Dahle et al., 2005).

UVB radiation has been shown to give rise to dimeric photoproducts between adjacent pyrimidine bases. Two major types of these modifications are produced, known as cyclobutane pyrimidine dimers (CPD; Figure 1.6) and pyrimidine (6-4) pyrimidone photoproducts (6-4 PP) (Mouret et al., 2006; Marrot and Meunier, 2008). 6-4PP may change into an isomeric secondary product, the Dewar valence isomer, after subsequent absorption of UVA (Matsunaga et al., 1991; Chadwick et al., 1995). The role of these dimeric lesions in carcinogenesis may be due to high proportion of p53 mutations, mostly C to T and CC to TT transitions, detected at bipyrimidine sites in skin tumours (Mouret et al., 2008).

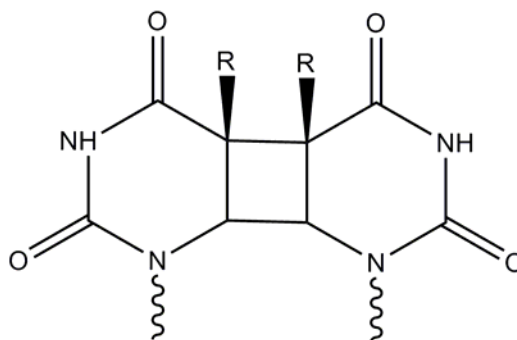


Figure 1.7: Chemical structure of CPD

## 1.5 CPD

As mentioned previously, UVR produces specific DNA damage, and the CPD is one of the most important and well-studied photolesions. UVR causes the formation of CPD and 6-4PP at dipyrimidine sites, where two pyrimidine bases are juxtaposed in tandem in the nucleotide sequence of DNA. These photolesions are formed through a photochemical reaction, whose efficiency is wavelength-dependent, following direct absorption of UVR by DNA bases (Markovitsi et al., 2004).

The importance of CPD is highlighted by the recent conclusion that they are the principal lesion responsible for most DNA damage-dependent biological effects of solar UVR (Besaratina et al., 2011). CPD, 6-4PP and also the Dewar isomer, cause UVR-specific mutations. Specifically, UVR-induced CPD formation can lead to non-melanoma skin cancers (You et al., 2001), since they may strongly contribute to the mutation spectrum in the p53 gene of non-melanoma skin cancers (Pfeifer and Besaratina, 2012).

However, CPD also have non-mutagenic consequences such as initiating cytokine release (Wolf et al., 2000) and photoimmunosuppression, which is thought to be important in skin cancer (Halliday, 2005; Walker and Young, 2007). They have also been associated with the induction of matrix metalloproteinase-1 (MMP1) which may play a major role in photoageing (Dong et al., 2008). CPD are readily induced by direct absorption of UVB (as well as UVC) by DNA, and are thought to be an important trigger for erythema (Young et al., 1998).

A noteworthy observation was the fact that DNA pyrimidines' absorbance spectrum overlaps with the UVB spectral range. This means that pyrimidines can act themselves as chromophores (Sage, 1993). The importance of pyrimidine photolesions is outlined by the fact that CPD and 6-4 PP are the most abundant DNA lesions in epidermal cells following UVB radiation (Clingen et al., 1995; Young et al., 1996). It is now known that, in mammalian cells proficient in DNA repair, the vast majority of UVB-induced mutations are caused by CPD. In general, bipyrimidine photoproducts are repaired by nucleotide excision repair (NER). However, when left unrepaired they can form the classic "UVB signature" mutations that require the methylation of cytosines (C→T or CC→TT) and lead to various skin cancers (Rochette et al., 2009; Ziegler et al., 1996).

### **1.5.1 UVA-induced CPD**

During the last 10-15 years, a lot of focus has been drawn to the production of CPD due to UVA irradiation. Since recent *in vitro* and *ex vivo* studies have drawn attention to the fact that UVAI can readily induce the formation of CPD, especially of thymine dimers (T<>T) (Mouret et al., 2006; Jiang et al., 2009; Mouret et al., 2010), the mechanisms by which these photolesions are produced, has been a matter of considerable debate (Douki et al., 2003). In a 1999 study, Douki and his colleagues observed the production of UVA-induced CPD. They hypothesized that CPD could be formed in cellular DNA in part by photosensitization by endogenous chromophores upon UVA irradiation (Douki et al., 1999). Unlike UVB, UVA (and particularly UVAI) induces the production of thymine dimers (T<>T), but very few C<>C, C<>T, and no 6-4PP. At first, an indirect photosensitized triplet energy transfer mechanism with UVAI was suggested to explain the high yield of UVA-induced CPD (Cadet et al., 2009; Mouret et al., 2006). However,

the latest research has indicated that this may not be the case. CPD formation (and specifically T<>T) is now thought to be a direct photochemical mechanism, without any involvement of endogenous photosensitizers (Jiang et al., 2009; Mouret et al., 2010). This –now reported- CPD formation by direct absorption had been hinted as early as 1981, based on the weak absorption of DNA in the UVA region (Sutherland and Griffin, 1981).

Another interesting point to notice is the lack of 6-4PP formation following UVA irradiation. This suggests that the photochemical process is different from that with UVB and UVC wavelengths, but this difference remains to be elucidated.

An interesting observation from some studies using quantitative techniques, has been that UVA-induced CPD are produced in larger amounts than 8-oxoGua in human skin and in primary cultures of human cutaneous cells (Courdavault et al., 2004; Mouret et al., 2006). Recent studies also concluded that UVA-induced CPD formation is similar for keratinocytes and melanocytes, but suggested a cell-specific preference for UVA-induced 8-oxoGua, which was more prominent in melanocytes (Mouret et al., 2012). However, discrepancies in the UVA-induced mutation spectrum among various research groups might result from differences in the UVA sources and doses used (Ikehata and Ono, 2011).

Although recent findings contradict a direct involvement of ROS in UVA-induced CPD, there is evidence suggesting a key role in their formation. Protection offered by certain antioxidants against CPD formation could mean an indirect role of ROS in causing damage to DNA repair enzymes or halting repair processes through other mechanisms (Hochberg et al., 2006; Halliday, 2010).

## 1.6 DNA repair

The biological significance of UVR-induced DNA lesions depends on the capacity of the cell to repair the damage caused, before it can permanently affect the human genome. Research on xeroderma pigmentosum (XP) patients (a disease characterized by a deficiency in repairing UVR-induced DNA damage) (Moriwaki and Kraemer, 2001) has been a key factor in understanding how direct DNA damage by UVR may cause skin cancers.

The major system responsible for repairing UVR-induced DNA damage in human cells is NER (Friedberg, 2001). NER is an extremely accurate process that repairs damaged nucleotides (such as CPD and 6-4PP) by excising the damaged area, leaving a single strand gap of about 25-30 nucleotides. Then, the opposite –undamaged- strand is used as a template for resynthesis of the gap by DNA polymerase (de Gruijl, 1999). The overall process in humans is quite complex and involves more than twenty proteins. Briefly, the NER system is divided in two subpathways: the global genome NER (GG-NER), which continuously surveys the entire genome for distorting damage, and the transcription-coupled repair (TCR) that focuses on damage that blocks the activity of elongating RNA polymerases (Hoeijmakers, 2001). The importance of NER is evidenced by the severe disorders occurring in the event of certain genetic mutations, in which NER is compromised. Consequences of such defects result in three rare recessive syndromes: XP, Cockayne syndrome (CS) and the photosensitive form of the brittle hair disorder trichothiodystrophy (TTD) (de Boer and Hoeijmakers, 2000; Kraemer et al., 2007). In conclusion, a deficiency of the DNA repair mechanisms may lead to an accumulation of mutations over time and increase the risk of skin cancer development (Matsumura and Ananthaswamy, 2002).

## 1.7 Photoprotection

The increasing incidence of skin cancer in sun-sensitive, white-skinned populations has initiated much discussion and research on acute and long-term photoprotection. Sunscreens have limitations (Diffey, 2009) and consequently other methods of photoprotection have been sought. These include the use of antioxidants, although it has often been difficult to prove their efficacy for protection of human skin *in vivo* (Cocheme and Murphy, 2010).

In general, sunscreen formulations contain a mix of chemicals that are applied to the outer layer of the human skin. These chemicals act by absorbing or reflecting UVR. Sunscreens are labelled by their sun protective factor (SPF), which is a measure of their ability to prevent erythema after a single exposure to solar simulating radiation (SSR). Recent developments in our understanding of UVA-induced damage to the human skin have increased the necessity of producing better sunscreens, more potent in attenuating UVA radiation.

### 1.7.1 Sunscreens

Protection against UVR has been a major concern since the harmful effects of sunlight became known. In the past, sunscreens focused in the protection against the UVB portion of solar UVR, but during the recent years formulations have been optimized to become protective over a broader spectrum of UVR and maintain greater photostability (Morabito et al., 2011). Sunscreens are comprised of organic and inorganic compounds that act as shields against UVR. Organic components act as chemical sunscreens by absorbing UVR. In contrast, inorganic components act as physical sunscreens by



absorbing, reflecting, or scattering UVR. Sunscreen is applied topically to the skin, covering the dead *stratum corneum*, protecting the skin's multiple living layers.

A problem that has been highlighted lately in the photobiology community is that SPF is an incomplete measure for protection of sunscreens, as it is primarily dependent on UVB protection and does not adequately illustrate UVA protection offered by the product (Bissonnette, 2008). Recently, other indicators to assess protection against non-melanoma skin cancers and to quantify the effectiveness of sunscreens against UVA, such as the UVA-protection factor (UVA-PF) have been proposed (Couteau et al., 2011; Fourtanier et al., 2011).

As oxidative stress and its effects on the human skin are implicated in photodamage, several antioxidants have been tested and incorporated in sunscreens, once it was demonstrated that they can be delivered into the skin percutaneously. Beneficial effects, among other compounds, have been shown for vitamins C and E and  $\beta$ -carotene that have been found to reduce erythema (Edlich et al., 2004). However, it has been stressed that prevention of erythema cannot guarantee the prevention of epidermal DNA photodamage (Young et al., 1998). Epidemiological studies have also shown that sunscreen use can protect against actinic keratoses, squamous cell carcinoma (SCC), and indeed melanoma (Green et al., 2011; Green et al., 1999; Thompson et al., 1993).

In general, recent evidence supports the use of non-sunscreen materials such as botanical extracts, antioxidants, and DNA repair enzymes in sunscreen lotions, as they can add value to the product when applied topically to human skin (Matsui et al., 2009; Oresajo et al., 2010).

## **1.8 Positive effects of UVR**

One of the most important substances necessary for the human organism is vitamin D. Nature has provided humans with two sources to acquire this essential nutrient: solar UVB radiation and diet. Since most foods provide very little vitamin D (with one exception being oily fish), especially in typical Western diets, solar UVB radiation is necessary to obtain vitamin D (Young, 2010). Various studies have shown vitamin D deficiencies in people living in sun-deprived locations (or even sunny places). Manmade interventions to bypass this issue include food fortification, supplementation, and the use of tanning devices with UVB.

One of the most important functions of vitamin D is to maintain blood calcium levels within the normal range in order to maintain neuromuscular function and bone mineralization. During the past few decades, intensive research on vitamin D has revealed that vitamin D is a hormone and not a vitamin. During exposure to sunlight provitamin D in the skin is photolyzed to previtamin D, a thermally labile intermediate that slowly -thermally- converts to vitamin D. Once formed, vitamin D enters the circulation and is hydroxylated first in the liver to 25-hydroxyvitamin D (25-OH-D) and then to the kidney to form the biologically active form 1,25-dihydroxyvitamin D (Webb and Holick, 1988). There are two major forms of vitamin D: vitamin D<sub>2</sub> (ergocalciferol) and vitamin D<sub>3</sub> (cholecalciferol). The former, results from UVB irradiation (280-320 nm) of a yeast sterol, ergosterol (provitamin D<sub>2</sub>), the latter from irradiation of 7-dehydrocholesterol (provitamin D<sub>3</sub>), a sterol that is naturally present in skin cells.

The dermatological community is now aware of the well-established detrimental effects of UVB. Although researchers are also aware of the role of UVB radiation in vitamin D

synthesis and the health benefits it offers, they are concerned about the misuse of information given to the public aiming for financial gain in a field which could be proven to be quite profitable. Therefore, much work remains to be done in risk-versus-benefit assessment of UVR exposure (Young, 2010).

## **1.9 Oxidative stress**

The generation of ROS in the skin results in oxidative stress when their concentration exceeds the antioxidant defense ability of the target cell. Oxidative stress is defined as an imbalance between pro-oxidants and antioxidants in favour of the former (Jones, 2006). Oxidative stress is produced by a variety of reactive oxidants. ROS are short-lived and are continuously generated at low levels as the consequence of normal aerobic metabolism. In general, they are oxygen-centered radicals (free radicals) that contain an unpaired electron. Some of the most important ROS involved in biological processes are the superoxide anion ( $O_2^{\cdot-}$ ), singlet oxygen ( $^1O_2$ ) and hydrogen peroxide ( $H_2O_2$ ). ROS are also produced in phagocytic cells, mainly through the activation of NADPH oxidase, while they attack various pathogenic agents (Bickers and Athar, 2006; Jones, 2006). UVR induces various ROS in human cells, including hydrogen peroxide, superoxide anion, singlet oxygen, and hydroxyl radical (Scharffetter-Kochanek et al., 1997).

Oxidative stress is involved in ageing and plays an important role in the pathophysiology of several diseases, among which are cancer, vascular disorders, as well as degenerative diseases. Furthermore, it is now known that oxidative stress has a big impact on intracellular signaling processes (Kim et al., 2005; Reelfs et al., 2004).

### 1.9.1 Measurement of oxidative stress

The study of the effects of oxidative stress requires methods for its measurement, particularly *in vivo*. Due to their high reactivity and limited lifetime, the detection of free radicals *in vivo* is still difficult, and techniques able to directly assess ROS in human tissue are still scarcely available. Therefore, the majority of techniques developed so far are based on the detection of the end products resulting from the reactions of free radicals with several biomolecules (Milatovic et al., 2011). Until now, considerable effort has been made to validate these assays, but still it is not clear which is most suitable for routine clinical assessment of oxidative stress.

Oxidative stress assays include detection of antioxidant enzyme systems, small molecule antioxidants, antioxidant/oxidant balance, reactive oxidants, and products of oxidative damage. On the pro-oxidant side of the balance, assays are available to measure ROS and products of lipid peroxidation, protein oxidation, and DNA damage. Free radicals can be measured by spin-trapping and electron spin resonance (ESR) spectroscopy (Valgimigli et al., 2001), but these methods are not considered suitable for clinical studies. However, a more recent study with new *in vivo* ESR techniques, has shown that it is now feasible to carry out human studies *in vivo* to get valuable information on effective UVR protection (Herrling et al., 2006). On the other hand, a simple colorimetric assay to measure preformed reactive species in the blood has been developed. It provides a rapid and sensitive way to quantify oxidants that react with phenylenediamine and it could prove extremely helpful at on-site screening of individuals for experimental antioxidant trials (Alberti et al., 2000).

Some of the most popular assays are those measuring products of lipid peroxidation (Bartsch and Nair, 2000). They can measure specific hydrocarbons (by means of gas chromatography, or mass spectrometry) such as ethane and F2 isoprostanes (Roberts and Morrow, 2000), or aldehyde products (thiobarbituric acid reactive substances assay, TBARS).

Other techniques, like antibodies targeted against oxidative lesions, high performance liquid chromatography (HPLC) and enzyme-linked immunosorbent assay (ELISA), have been used to measure oxidative DNA damage. HPLC has been shown to be very accurate in the detection of 8-oxodGuo (Marrot and Meunier, 2008; Cooke et al., 2008b).

From the antioxidant aspect, several assays are available. These are able to measure intracellular concentration of antioxidants such as vitamin C or E, as well as the activity of certain antioxidant systems (eg. catalase and GSH peroxidase activity) (Jones, 2006).

### **1.10 Antioxidants**

Cells are equipped with antioxidant defensive mechanisms that can either act by preventing ROS formation, or by eliminating them. This defense system includes various enzymes such as superoxide dismutase (SOD), catalase (CAT) and glutathione peroxidases (GPx), as well as some non-enzymatic antioxidants like glutathione (Remacle et al., 1992). A broad definition of an antioxidant was given by Halliwell and Gutteridge, as “any substance that, when present at low concentrations compared with those of an oxidizable substrate, significantly delays or prevents oxidation of that

substrate” (Halliwell and Gutteridge, 1999). The purpose of antioxidants is to protect cells from the harmful effects of free radicals, which have been found to damage cells and molecules and have been implicated in cancer and numerous diseases (Dreher and Junod, 1996; Cross et al., 1987). Since ROS are a constant threat, either produced in the human organism, or through environmental exposures such as UVR, air pollution and cigarette smoke, antioxidants are necessary to protect cells from their damaging effects, and therefore, have always been an appealing research topic (Kelly, 2004; Doruk et al., 2011).

Since epidemiology has pointed towards the use of antioxidants as the active ingredients of fruits and vegetables, several compounds have been employed in cancer research, heart diseases, and many other complications arising from an increased oxidative stress in the human organism. During the last two decades, many antioxidant supplementation trials have been conducted. The results have usually been controversial, and most studies could not provide definite evidence that antioxidant supplementation is actually beneficial (Collins and Horváthová E, 2001; Slatore et al., 2008). Even negative outcomes have been observed; one study suggested that  $\beta$ -carotene supplementation increased lung cancer incidence in a group of smokers (The Alpha-Tocopherol Beta Carotene Cancer Prevention Study Group, 1994). However, some studies have shown that antioxidants might be beneficial in cancer patients, increasing tumour response to chemotherapy, and reduce toxicity, or even increase survival (Simone et al., 2007; Block et al., 2007).

Antioxidants have been employed for trials on many diseases in which oxidative stress is implicated. A recent study on pulmonary tuberculosis showed that vitamin E and selenium supplementation can reduce oxidative stress and enhance total antioxidant

status in patients suffering from the disease (Seyedrezazadeh et al., 2008). On the other hand, most trials dealing with atherosclerosis have concluded that antioxidants do not have a supportive role in its chronic suppression (Steinhubl, 2008). Vitamins C and E have been extensively used in an effort to prevent pre-eclampsia, a disease occurring during pregnancy. Data from these studies have been controversial, but overall, antioxidant supplementation has not been found to reduce the risk of the disease (Padayatty et al., 2006; Rumbold et al., 2008).

These examples demonstrate the status of antioxidant trials until today, but also highlight the need to understand the reasons behind the failure of clinical trials to exhibit a clear benefit of antioxidant therapies.

#### **1.10.1 Antioxidants against UVR-induced oxidative stress**

All major antioxidant enzymes as well as low molecular weight antioxidants are present in the human skin (Shindo et al., 1994). Antioxidant capacity of the human epidermis is far greater than that of the dermis, presumably because it is exposed to higher doses of UVR, but also because it is a much more cellular tissue. In the human epidermis, for example, levels of vitamin C (L-ascorbate) are approximately five times higher than in the dermis (Fuchs, 1998).

Overall, a complex antioxidant system provides protection to human skin from photo-oxidative stress. It has been well-established that UVR depletes the skin's natural antioxidant system (Podda et al., 1998). If antioxidant defenses fail along with cellular repair systems, cells are led to apoptosis (programmed cell death). Both UVA and UVB

may induce apoptosis in human cell lines (Godar, 1996), although the exact mechanism of UVR-induced apoptosis is not entirely understood. Most of the work that demonstrates the efficacy of antioxidants has been carried out *in vitro*. There are surprisingly few data that unequivocally demonstrate the efficacy of antioxidants in human skin *in vivo* (Bickers and Athar, 2006).

A study in 2001 found that topically applied vitamin C slightly enhanced levels of mRNA for procollagens I and III; it also enhanced levels of some procollagen processing enzymes in human skin (Nusgens et al., 2001). The outcome was quite interesting, but there are some doubts whether the technique used in the study was able to detect the minor changes reported (Pinnell, 2003). A 2002 trial, employing 8 volunteers, examined the effects of vitamin C supplementation prior to UVR (McArdle et al., 2002). No evidence showing any effect of the supplementary vitamin C on the mild oxidative stress seen in the human skin was obtained. In contrast, a reduction of total glutathione and protein thiols was observed, probably indicating the replacement of some reductants in cells by the supplemented antioxidant. Very recently vitamin C was found to protect against UVA-induced melanogenesis, possibly by boosting antioxidant defense capacity and inhibiting nitric oxide (NO) production (Panich et al., 2011).

Many photoprotection studies have focused on the use of carotenoids, as they exhibit specific antioxidant activity but also influence gene expression.  $\beta$ -Carotene and lycopene are two of the most studied compounds of this group, and have been found to protect the skin against UVR-induced erythema (Stahl and Sies, 2012; Rizwan et al., 2011).



Several studies have documented the photoprotective effects of topically applied vitamin E ( $\alpha$ -tocopherol), but all were conducted on animal skin (Burke et al., 2000; Lopez-Torres et al., 1998). On the other hand, an oral combination of vitamins C and E in high doses protects against UVR-induced erythema in human beings, while either vitamin alone is not effective (Fuchs and Kern, 1998; Eberlein-König et al., 1998). Furthermore, a recent human trial combining vitamins C and E with ferulic acid (possibly acting as a stabilizer), found a substantial protection against acute UVR injury (Murray et al., 2008). The authors proposed that the p53 pathway (induced by UVR, and may lead to DNA repair, cell cycle arrest or apoptosis) is implicated in the outcome of their study, as the antioxidant mixture used reduced p53 activation.

Another *in vivo* study was conducted in 2004 and tested the effects of oral vitamin E and  $\beta$ -carotene supplementation on 16 healthy subjects, following UVR (McArdle et al., 2004). Neither of the supplements was able to provide protection from UVR-induced oxidative stress. A more recent *in vivo* study showed that a combination of tocopherols and tocotrienols reduced UVB-induced erythema in human volunteers (Pedrelli et al., 2011).

Green tea polyphenols have also been suggested as possible photoprotective agents, and animal studies have exhibited their antioxidant capacity (Pinnell, 2003). A human trial in 2001, showed a protective effect on human skin (Elmets et al., 2001). Skin pretreated with green tea polyphenols before UVR exposure, developed less erythema in comparison to untreated skin. Unfortunately this study did not assess the levels of oxidative stress. Another polyphenol, luteolin, was very recently found to protect human skin against UVB-induced CPD. Its protection was attributed to a combination

of UVR-absorbing, DNA-protective, antioxidant, and anti-inflammatory properties (Wölflle et al., 2011).

Several antioxidants have also been found to protect against photoimmunosuppression (Steenvoorden and van Henegouwen, 1997). Lutein (a carotenoid) has been shown to decrease UVB-induced immunosuppression (Lee et al., 2005), while lycium barbarum was shown to protect against solar-simulated UVR-induced immunosuppression in mouse skin (Reeve et al., 2010). Recently, the phytoestrogenic isoflavonoid equol was found to protect against UVA-induced immunosuppression in mouse skin (Widyarini et al., 2012).

An important –and poorly addressed- issue in antioxidant studies is the fact that many of the compounds tested absorb in the UVR region. This makes it difficult to determine if their protective effects are attributed to their antioxidant or to their spectral properties. In general, the photoprotection offered by antioxidants alone would be the equivalent of a weak sunscreen with a maximum SPF of 4; however the combination of antioxidants with traditional sunscreens has been able to provide SPF levels of about 30 (Baran and Maibach, 2004).

## **1.11 Vitamin E**

Since a significant part of this thesis has dealt with vitamin E, an introduction in this potent antioxidant is necessary.

Vitamin E is a lipid-soluble antioxidant that can be found naturally in some foods (such as peanuts, sunflower seeds and almonds) but is also widely available as a dietary

supplement. Vitamin E includes a family of tocopherols and tocotrienols that share a chain-breaking antioxidant activity. Tocopherols and tocotrienols exist in eight chemical forms (four for each “family”):  $\alpha$ -,  $\beta$ -,  $\gamma$  -, and  $\delta$ . These forms differ in the number of methyl groups on the chromanol aromatic ring. Tocopherols have a phytyl tail, whereas tocotrienols have an unsaturated tail (Brigelius-Flohe, 2006). However, notably,  $\alpha$ -tocopherol (Figure 1.7) is the only form of vitamin E that meets human requirements and is capable of reversing deficiency symptoms in humans. The biochemical reason for this “preference” over the other forms remains unknown.

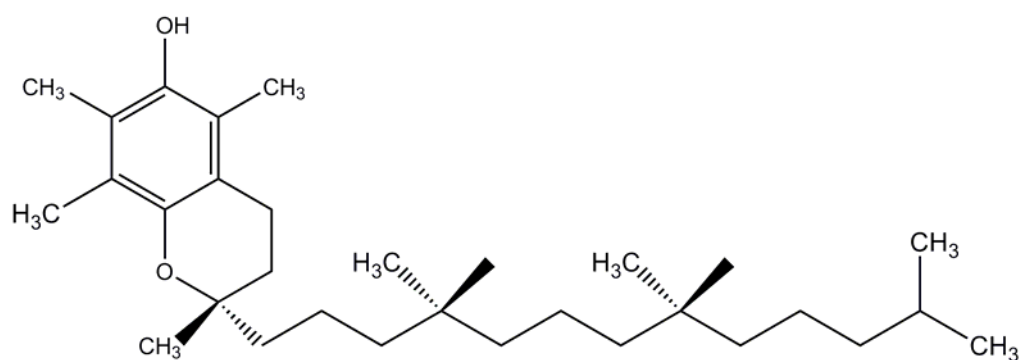


**Figure 1.8: Chemical structure of  $\alpha$ -tocopherol**

Vitamin E is available commercially, both as a natural or a synthetic preparation. Naturally occurring  $\alpha$ -tocopherol is referred in the literature as RRR-  $\alpha$ -tocopherol, or d-  $\alpha$ -tocopherol. Synthetic  $\alpha$ -tocopherol is referred to as all-rac- $\alpha$ -tocopherol, or dl-  $\alpha$ -tocopherol. The esterified forms of vitamin E such as  $\alpha$ -tocopherol acetate,  $\alpha$ -tocopherol succinate and  $\alpha$ -tocopherol nicotinate are also available commercially.

For simplicity's sake,  $\alpha$ -tocopherol from now on, in the rest of the presented thesis, will be referred as vitamin E.

Serum concentrations of vitamin E depend on the liver, which absorbs the nutrient after the various forms are absorbed from the small intestine. Vitamin E is transported in plasma lipoproteins, and the mechanisms of lipoprotein metabolism determine the delivery of vitamin E to tissues.

Vitamin E is considered as nature's most effective antioxidant and is the major chain-breaking antioxidant in body tissues. It presents the first line of defence against lipid peroxidation and protects cell membranes from ROS (Vasavi et al., 1994). The antioxidant activity of  $\alpha$ -tocopherol derives from the free hydroxyl group on the aromatic ring (Figure 1.8). The hydrogen of the aromatic ring is donated to the free radical, giving rise to a relatively stable tocopheryl free radical, which can then in turn combine with another peroxy free radical (Kamal-Eldin and Appelqvist, 1996).

Individuals with plasma concentrations less than 0.5 mg/dL are considered vitamin E-deficient. According to the Food and Nutrition Board of the Institute of Medicine (Washington DC, USA) in 2000, daily dietary vitamin E intakes of about 15 mg in healthy are sufficient to maintain serum vitamin E concentrations in the normal range (Krinsky et al., 2000).

Since free radicals have long been implicated in carcinogenesis, vitamin E has been the focus of numerous studies examining its effect as an anti-carcinogen.

Some studies have also demonstrated a protective effect of vitamin E against esophageal and oral cancers in mice and hamsters (Odeleye et al., 1992; Trickler and Shklar, 1987; Shklar et al., 1990). However, most of the studies have failed to provide conclusive

evidence. In contrast, epidemiological data showed no effect of vitamin E against lung cancer (The Alpha-Tocopherol Beta Carotene Cancer Prevention Study Group, 1994). There have often been inconsistent outcomes about the effects of vitamin E supplements against lipid peroxidation in *in vivo* studies, with some failing to show an effect and others showing a decrease, or even an increase in lipid oxidation; furthermore, it is still not clear to what extent vitamin E supplementation has been successful in raising tissue vitamin E levels (Kelly et al., 2004). Also, vitamin E protection levels, exhibit a large variation depending on experimental models. A very recent trial connected vitamin E supplementation with an increased risk of prostate cancer in healthy men (Klein et al., 2011).

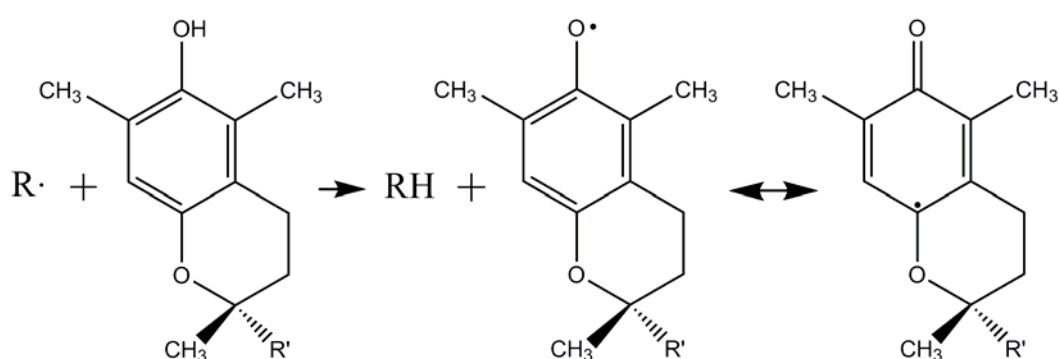


**Figure 1.9:** Schematic depicting the chemical action of  $\alpha$ -tocopherol reacting with a free radical

## 1.12 Aims of thesis

The significance of UVR-induced oxidative stress and its related complications can be appreciated by the fact that publications including these terms increased dramatically in the last decade. From 2001, until 2011, 952 articles were published on this (broad) field, compared to the previous decade that 347 articles were produced (based on a combined search on NCBI Pubmed). Therefore, it is important to shed light on the mechanisms that control the extent of UVR-induced damage.

The main aim of this project was to develop a panel of reliable and quantitative methods to measure UVR-induced oxidative stress and DNA damage in skin cells *in vitro*. The ultimate aim would be to develop techniques that could be applied to the human *in vivo* situation to test the benefits of antioxidants. More specifically, the goals of the thesis were to:

- (a) Identify *in vitro* techniques to measure DNA damage that could be translated to human skin *in vivo*. This was done with a modified comet assay using DNA repair enzymes, in order to establish a method of assessment of specific UVR-induced DNA damage.
- (b) Identify UVR-induced genes that could be used *in vitro* and *in vivo*.
- (c) Evaluate the effects of vitamin E, as a model antioxidant, in decreasing UVR-induced intracellular ROS, DNA damage and gene expression.

- (d) Try to differentiate between antioxidant effects and possible sunscreen effects of agents tested.
- (e) Develop an understanding of the mechanisms of UVA-induced DNA damage.
- (f) Test antioxidant compounds supplied by Stiefel laboratories and assess their effect against UVR-induced DNA damage and the formation of free radicals.

Considerable attention was given to the spectral properties of the UVR sources used in the studies, as this has frequently been the weakest point in photobiological studies.

## **Chapter 2: Materials and Methods**



## 2.1 Materials

Tables 1-5 below list the consumables. All materials/reagents were purchased from the UK, unless otherwise specified.

**Table 2.1: General reagents**

Reagents	Supplier*
3-(4,5-dimethyl-thiazol-2-yl)-2,5-diphenyl tetrazolium bromide (MTT)	Sigma-Aldrich
4'-6-Diamidino-2-phenylindole (DAPI)	Sigma-Aldrich
5-(and-6)-carboxy-2',7'-dichlorodihydrofluorescein diacetate (carboxy-H <sub>2</sub> DCFDA)	Invitrogen
Agarose	BDH
$\alpha$ -tocopherol	Sigma-Aldrich
Bovine serum albumin (BSA)	GE Healthcare
Dimethyl sulphoxide (DMSO)	Sigma-Aldrich
Diphenylene iodonium chloride (DPI)	Sigma-Aldrich
Ethanol	BDH
Ethylenediamine tetraacetic acid (EDTA)	BDH
Isopropanol	BDH
Low-melting point agarose	Trevigen
Methanol	Sigma-Aldrich
N-2-hydroxyethylpiperazine-N'-2-ethanesulphonic acid (HEPES)	Sigma-Aldrich
Potassium chloride (KCl)	BDH
Propidium iodide (PI)	BDH

Rotenone	Sigma-Aldrich
Skimmed milk	Morrison
Sodium chloride (NaCl)	Sigma-Aldrich
Sodium hydroxide (NaOH)	BDH
TaqMan Gene expression assays/PCR mastermix	Applied Biosystems
Triton X-100	Sigma-Aldrich
Trypan blue	Sigma-Aldrich
Tween 20	Sigma-Aldrich

**Table 2.2: Tissue culture growth medium constituents**

<b>Reagent</b>	<b>Supplier</b>
Dulbecco's modified Eagle's medium (DMEM)	Invitrogen
Foetal calf serum (FCS)	Invitrogen
L-glutamine	Invitrogen
Penicillin-streptomycin (P/S)	Invitrogen
Phosphate buffer saline (PBS)	Invitrogen
Trypsin-EDTA	Invitrogen

**Table 2.3: Antibodies, enzymes and primers**

<b>Reagent</b>	<b>Supplier</b>
Anti-thymine dimer mAb, clone KTM53	Kamiya Biomedical, USA
Goat anti-mouse immunoglobulin horse radish peroxidase conjugated	Dako
Glyceraldehyde 3-phosphate dehydrogenase (GAPDH)	Applied Biosystems
Heme oxygenase 1 (HO1)	Applied Biosystems
Human oxoguanine glycosylase 1 (hOGG1)	New England Biolabs
Human $\beta$ 2-macroglobulin (B2M)	Applied Biosystems
Matrix metalloprotease 12 (MMP12)	Applied Biosystems
T4 endonuclease V (T4endoV)	New England Biolabs

**Table 2.4: Molecular biology kits**

<b>Reagent</b>	<b>Supplier</b>
Absolutely RNA microprep kit	Agilent Technologies
DNAeasy blood and tissue	Qiagen
GSH/GSSG kit	Calbiochem
QuantiTect reverse transcription kit	Qiagen

**Table 2.5: Stock solutions**

<b>Solution</b>	<b>Constituents</b>
10X Comet assay enzyme reaction buffer	9.5 g Hepes, 7.4 g KCl, 186 mg EDTA, 200 mg BSA, pH 8, diluted in ddH <sub>2</sub> O
Comet assay electrophoresis buffer	NaOH 10 M, EDTA 200 mM, pH >13, diluted in ddH <sub>2</sub> O
Comet assay lysis buffer	2.5 M NaCl, 100 mM EDTA, 10 mM acid Tris, 1% sodium sarcosinate, pH 10, 1% of Triton 100, and 10% DMSO
Comet assay neutralization solution	0.4 M TrisMABase, pH 7.5

**Table 2.6: Optical properties of antioxidant compounds and their solvents used in thesis**

<b>Compound</b>	<b><math>\lambda_{\max}</math> (nm)</b>	<b>Solvent</b>
$\alpha$ -tocopherol (vitamin E)	295	EtOH
N-acetyl-cysteine (NAC)	215	PBS
Farnesol	215	DMSO
Guggulsterone	285	DMSO
Lanosterol	280	EtOH

## **2.2 Cell culture and antioxidant treatments**

All cell lines used in the project were routinely tested to assess the absence of *Mycoplasma* infection by 4'-6-Diamidino-2-phenylindole (DAPI) staining.

### **2.2.1 HaCaT keratinocytes**

The spontaneously transformed human keratinocyte cell line HaCaT (abbreviation for Human adult low Calcium Temperature) was the main cell line used in the project. This cell line is known to bear two p53 point mutations and it is unclear whether p53 in HaCaT cells is still functional. HaCaT keratinocytes (originally purchased from ATCC, USA) were routinely cultured in Dulbecco modified eagle medium (DMEM; Invitrogen, Paisley, UK) supplemented with 10% foetal calf serum (Sigma-Aldrich, Poole, UK), 100 U/mL penicillin, and 100 µg/mL streptomycin (Invitrogen) and maintained at 37°C in a humidified incubator with 95 % air/5 % CO<sub>2</sub>. For all experiments, cells were cultured to 80% confluence in 25 cm<sup>2</sup> or 75 cm<sup>2</sup> plastic flasks (Corning, USA).

### **2.2.2 Primary human skin fibroblasts**

Human dermal fibroblast cultures (named NH22 for convenience purposes, after the name and age of the individual they were acquired from) were established by outgrowth from an upper non-previously sun-exposed buttock biopsy of a healthy donor (skin type I-II). NH22 fibroblasts were passaged each week (ratio 1:2) in DMEM, supplemented with 10% heat inactivated fetal calf serum and 100 U/ml penicillin and 100 µg/ml streptomycin and maintained at 37°C in a humidified incubator with 95% air/5% CO<sub>2</sub>.

Culture media were replaced every three days. All experiments were carried out between passages 3 and 14, at the same cell density, i.e., about 70% confluence.

### **2.2.3 MRC5V1 fibroblasts**

For some comparative studies, the SV40-transformed human fibroblast cell line MRC5V1 was used. MRC5V1 cells were routinely cultured in DMEM, supplemented with 10% FCS, 100 U/mL penicillin, and 100 µg/mL streptomycin and maintained at 37°C in a humidified incubator with 95 % air/5 % CO<sub>2</sub>.

## **2.3 Spectroscopy**

UVR absorbance properties of the various compounds studied, were determined with a UV/Vis Spectrophotometer (ATI Unicam, UK) between wavelengths 220-360 nm.

## 2.4 Antioxidant treatments

### 2.4.1 Vitamin E

Cells were either pretreated for 24h prior to UVR or treated for 2h after UVR, with 0.1 mM vitamin E ( $\alpha$ -tocopherol, Sigma). Following pilot investigations with a range of vitamin E concentrations from 0.1 to 1 mM, a concentration of 0.1 mM was chosen to provide maximal protection against UVA exposure with minimal cytotoxicity. As stock solutions of vitamin E were diluted in 100% ethanol (following filter sterilisation with 0.2  $\mu$ m pore-size filters), the concentration of ethanol in the medium was 1% and therefore controls were also treated with 1% ethanol. In the case of pretreatment, the media containing vitamin E were removed and each sample was washed three times with Dulbecco's phosphate-buffered saline (PBS; Sigma) to remove any traces of extracellular vitamin E before irradiation. The absorption spectrum of vitamin E is shown in Figure 2.1.

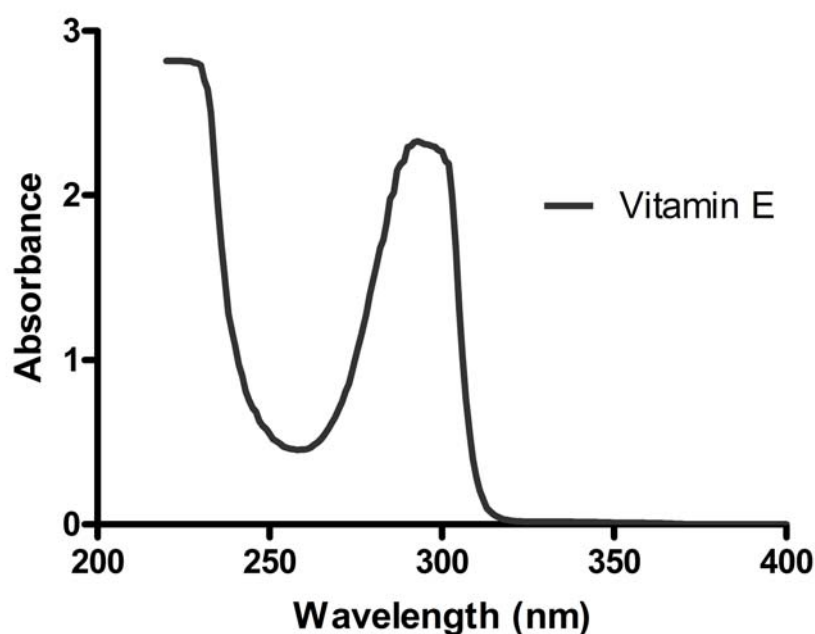


Figure 2.1: Absorption spectrum of vitamin E (0.1 mg/ml in *n*-hexane)

### 2.4.2 N-acetyl cysteine

N-acetyl cysteine (NAC; Sigma) was used as a representative ROS scavenger. It was selected because it does not absorb UVR at wavelengths less than 280 nm (Figure 2.2). Following experiments utilising a range of NAC concentrations from 2-20 mM, concentrations of 10 and 20 mM were determined to provide significant protection against UVA-induced ROS (measured by the H<sub>2</sub>DCFDA assay). Stock solutions of NAC were diluted in PBS. Cells were pretreated with NAC 4 h prior to UVA (time was based on published literature). Media containing NAC were removed prior to irradiation and samples were washed three times with PBS to ensure all traces of extracellular NAC were removed.

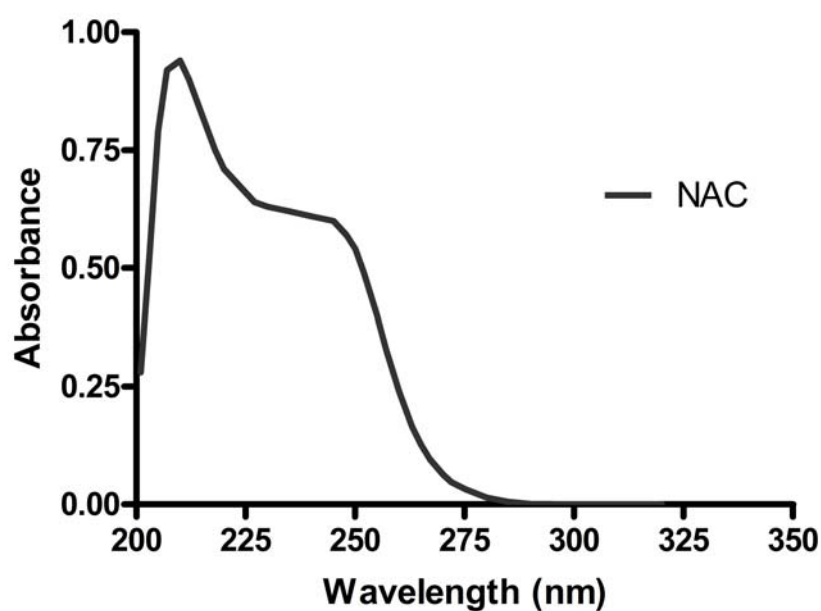


Figure 2.2: Absorption spectrum of NAC (1 mM solution, in PBS)



### 2.4.3 Stiefel compounds

Stiefel laboratories supplied us with three compounds to be tested for antioxidant properties against UVR-induced oxidative stress. The compounds were screened by Stiefel as weak ligands of a skin receptor the company was interested in. These included a pharmaceutical excipient called farnesol (MW: 222.37), a guggulsterone plant extract composed of plant polyphenols (MW: 312.45), and a common wax emulsifier, lanosterol (MW: 426.71). The absorption spectra of these compounds are presented in figures 2.3, 2.4 and 2.5, respectively.

Following investigations utilising various concentrations (in the range suggested by Stiefel laboratories), concentrations between 5 and 80  $\mu\text{M}$  were chosen (please see Results section for further details). Cells were incubated routinely with the compounds for 24 h and were thoroughly washed with PBS prior to irradiation.

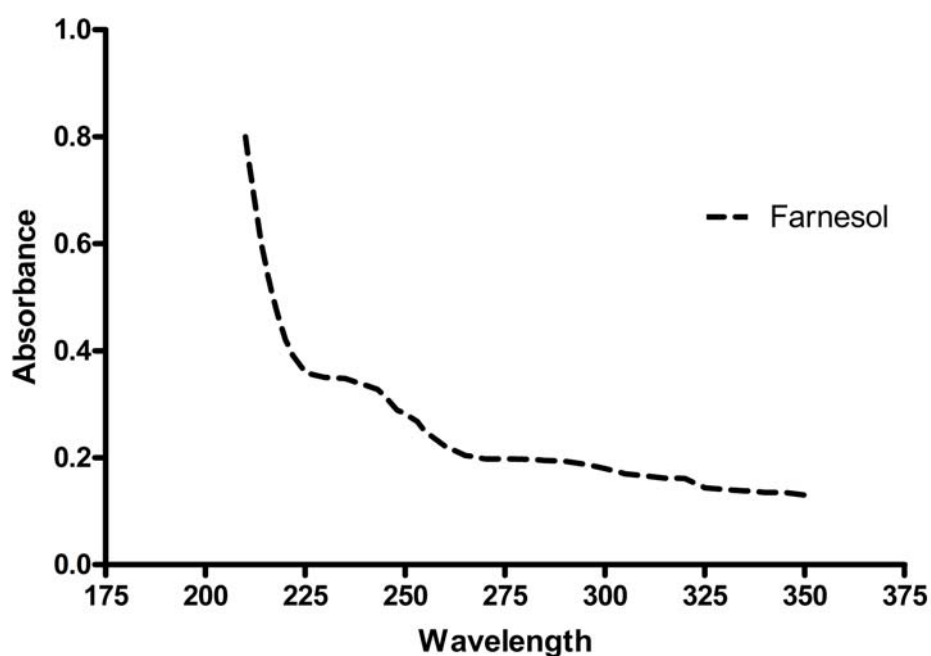


Figure 2.3: Absorption spectrum of farnesol (10  $\mu\text{M}$  in EtOH)

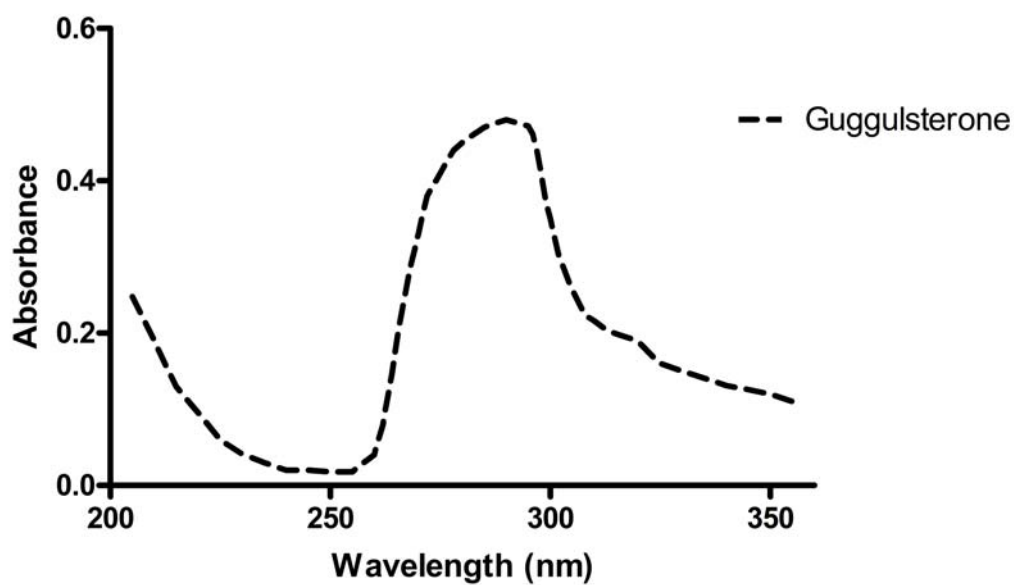


Figure 2.4: Absorption spectrum of guggulsterone (5  $\mu$ M in DMSO)

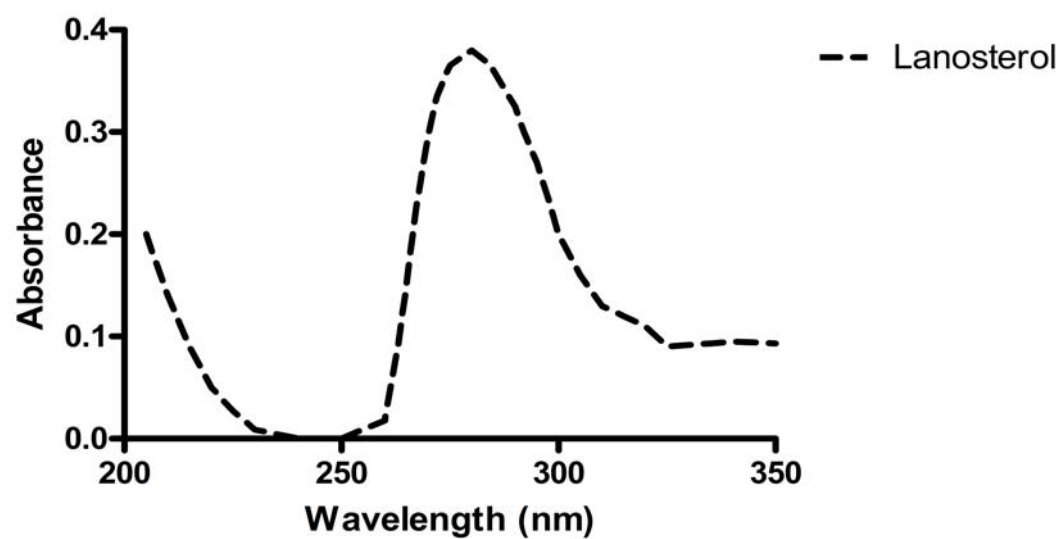


Figure 2.5: Absorption spectrum of lanosterol (5  $\mu$ M in EtOH)

## **2.5 Irradiation**

### **2.5.1 UVA**

The main UVR source was a UVASPOT (400/T, Dr K Hönle UVTechnologie, Munich, Germany), the spectrum of which is shown in Figure 2.6 and described in Table 2.7. The erythral effective energy (EEE) was calculated using the erythral action spectrum of the International Commission on Illumination (CIE) (Webb et al., 2011). Irradiance was routinely determined with an International Light IL 442A radiometer (Newbury Port, MA, USA) with a UVA detector calibrated against the measurements made with a double-monochromator spectroradiometer (Bentham Instruments, Reading, UK), which was calibrated against a UK national standard.

Cells were routinely irradiated in monolayers. Irradiation was always carried out at the same distance from the lamp (17 cm from the source), in cold PBS, with the lid always in place, to avoid contamination. The clear plastic lid was also placed on top of the detector when measuring the irradiance of the source. As the UVA source produced high levels of heat, a cooling platform set at a temperature of 6°C was used, to keep the temperature at ~27°C. Controls (unirradiated samples), and samples with shorter irradiation times, were maintained in PBS at the same temperature for the same time as the longest exposure to ensure that any differences observed occurred because of UVR dose differences, rather than prolonged time in PBS. Cells were always kept on ice, after irradiation, before any processing.

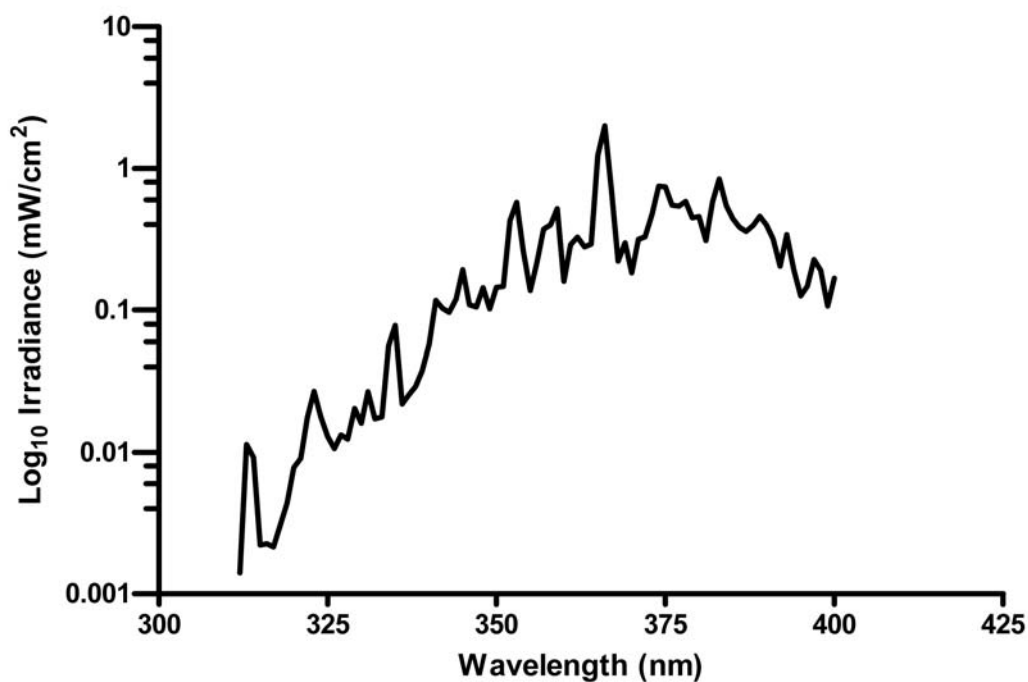


**Figure 2.6: Emission spectrum of the UVASPOT**

Spectrum was determined by a Bentham DM150 double monochromator spectroradiometer (Bentham Instruments, Reading, U.K.) through the plastic lid, at a distance of 39 cm.

Following pilot investigations using various UVA doses from 1 to 40 J/cm<sup>2</sup>, and keeping in mind the physiological relevance of our irradiations, doses ranging from 5 to 20 J/cm<sup>2</sup> were selected as the standard protocol doses for the experiments. These doses ranged from 1/12 to 1/3 of a minimal erythema dose (MED) for a fair skin type.

<b>UVR Region</b>	<b>Wavelength (nm)</b>	<b>% of total irradiance</b>	<b>% EEE</b>
<b>UVA</b>	<b>321-400</b>	<b>99.8</b>	<b>87.5</b>
<i>UVAI</i>	<i>340-400</i>	<i>97.5</i>	<i>78.4</i>
<i>UVAII</i>	<i>321-340</i>	<i>2.3</i>	<i>9.1</i>
UVB (CIE)*	281-315	0.1	10.4
<b>UVB</b>	<b>281-320</b>	<b>0.2</b>	<b>12.7</b>
<b>UVC</b>	<b>200-280</b>	<b>0.0</b>	<b>0</b>
<b>Total UVR</b>	<b>200-400</b>	<b>100</b>	<b>100</b>

**Table 2.7: Spectroradiometric distribution of emission spectrum of the UVASPOT**

See Figure 2.6; Spectra were measured through the plastic lid of a 6-well plate used in the experiments. Respective erythemally effective energies (EEE) were obtained by multiplying with the CIE action spectrum for erythema (Webb et al., 2011). This shows that the majority of the EEE was in the UVAI region. \*official CIE definition of UVB, but cut-off at 320 nm is widely used in dermatology research.

## **2.5.2 UVB**

At an early stage of my project, UVB was used for some studies, to establish technique development, as well as UVB-induced DNA damage. Irradiations were conducted with an FS20 Westinghouse SunLamp (Westinghouse, Pittsburgh, PA), emitting mainly in the UVB range, with peak emission at 313 nm. The spectrum of the FS0 lamp is shown in Figure 2.7 and described in Table 2.8. Irradiance was routinely determined with an International Light IL 442A radiometer, fitted with a UVB detector (SEE1240; Newbury Port, MA, USA), calibrated against the measurements made in the past with a double-monochromator Bentham spectroradiometer. Irradiations were always carried out in the same distance from the lamp (8 cm from the source). Cells in a 6-well plate

were washed twice with PBS and then irradiated in 1 ml of PBS (with  $\text{Ca}^{2+}$  and  $\text{Mg}^{2+}$ ) at doses between 50 and 200  $\text{mJ}/\text{cm}^2$  (equivalent to a range of 1.5-6 MEDs for fair skin).

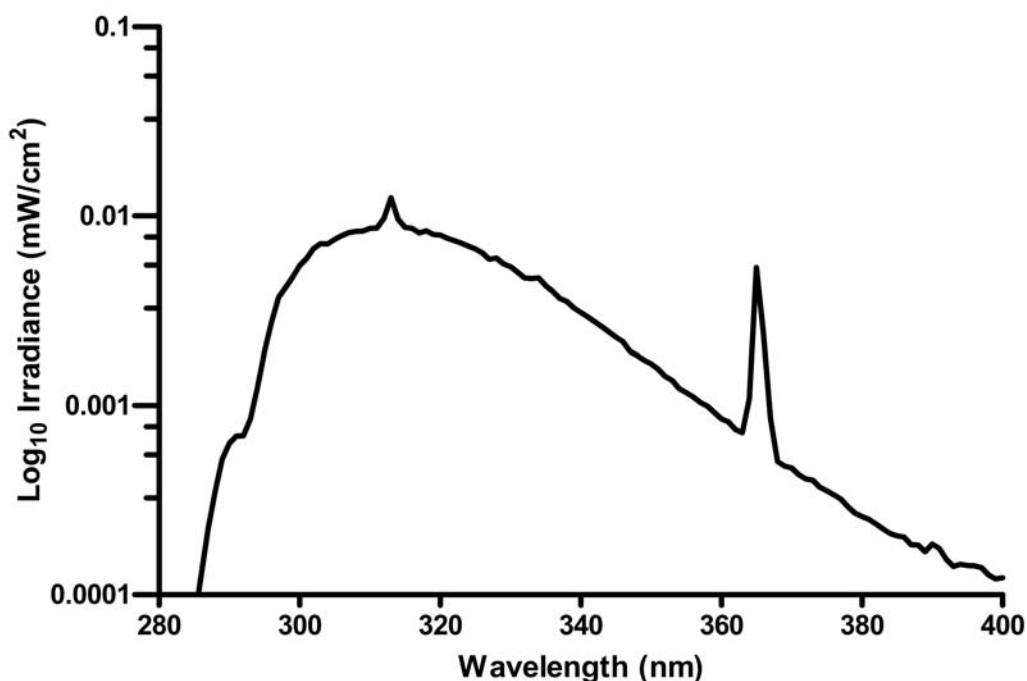


Figure 2.7: Emission spectrum of the FS20 Westinghouse SunLamp

UVR Region	Wavelength (nm)	% of total irradiance	% EEE
UVA	321-400	45.3	0.7
<i>UVAII only</i>	<i>321-340</i>	<i>29.9</i>	<i>0.6</i>
UVB	281-320	54.8	99.4
UVC	200-280	0.0	0.0
<b>Total UVR</b>	<b>200-400</b>	<b>100.0</b>	<b>100.0</b>

Table 2.8: Spectroradiometric distribution of emission spectrum of the FS20 Westinghouse SunLamp

Spectrum was determined by a Bentham DM150 double monochromator spectroradiometer (Bentham Instruments, Reading, U.K.).

### **2.5.3 UVC**

An XX-15s UV Bench Lamp (UVP) was used to generate UVC (254nm). Irradiation of cells was performed at a distance of 25 cm from the lamp, in PBS, without the lid. Exposure was based on time (10 and 20 s), and determined empirically because reliable UVC dosimetry was not available.

## 2.6 Cell viability/survival assays

### 2.6.1 MTT-time course assay

This assay measures the metabolism of 3-(4,5-dimethyl-thiazol-2-yl)-2,5-diphenyl tetrazolium bromide (MTT), a yellow tetrazolium salt, that is reduced by the mitochondria of metabolically active cells to form a blue formazan dye precipitate, which can be extracted using organic solvent (Mosmann, 1983).

Seeding was at  $10^4$  cells/well into flat-bottomed 96-well plates and cells were allowed to recover for 24h at 37°C in a humidified incubator, 5% CO<sub>2</sub>. Media was removed carefully and cells were washed twice with cold PBS (+Ca<sup>2+</sup>, Mg<sup>2+</sup>). Cells were then irradiated in 100 µl of PBS, with the lid on. Control wells were covered with aluminium foil. Eight replicate wells were used for each UVA dose. After radiation, PBS was removed and replaced with normal fibroblast medium (200 µl). After a 19h incubation period, cell viability was assessed. Aliquots (20 µl) of MTT solution (10 mg/ml PBS) were added to each well and the plates were incubated for 4h at 37°C followed by removal of the medium and addition of 100 µl of lysis solution (0.04 M HCl in absolute isopropanol) to each well. Plates were covered with foil and left on a plate shaker for approximately 10 min. The plates were subsequently read on a plate reader at 550 nm. The average absorbance reading was taken from each time point of each plate. Cell survival curves were constructed by plotting cell survival against UVR doses.



### **2.6.2 Trypan blue exclusion assay**

Immediately after UVR or treatment with various compounds, cell viability was determined using the trypan blue exclusion assay to ensure that no significant cytotoxicity was induced. Trypan blue (Sigma, UK) solution was added to aliquots of cell suspensions to a final concentration of 0.04% to estimate the number of viable cells. Viable (unstained) and non-viable (stained) cells were counted in a hemacytometer under an inverted microscope (Olympus, Tokyo, Japan); the percentage of viable cells was calculated for each condition tested.

### **2.7 Reactive oxygen species production**

Detection of total intracellular ROS generation was performed using 5-(and-6)-carboxy-2',7'-dichlorodihydrofluorescein diacetate (carboxy-H<sub>2</sub>DCFDA). Carboxy-H<sub>2</sub>-DCFDA (Invitrogen, Paisley UK) was preferred as it is thought to have better retention in the cell due to a negative charge at physiological pH (Peter, 2007).

Cells were cultured in 6-well plates to a confluence of approximately 80 %. Medium was removed and cells were rinsed (×2) with PBS. Cells were irradiated after the addition of 1 ml PBS containing 9 mM Ca<sup>2+</sup> and 4.9 mM Mg<sup>2+</sup> (Gibco, UK) in each well. Control cells remained in the dark at approximately the same temperature as the irradiated samples (less than ~30°C). After UVR exposure, 2 ml of 5 μM H<sub>2</sub>-DCFDA, diluted in PBS (containing 1 g/L glucose; Gibco) were added to each well. Only PBS was added in control wells. Cells were incubated for 20 min in the dark at 37°C in a humidified incubator with 95% air/5% CO<sub>2</sub>. Plates were subsequently washed twice with PBS to completely remove any dye that had not been internalized by the cells.

Post-UVR loading of H<sub>2</sub>DCFDA in PBS has been reported to be the optimal protocol for this technique in order to avoid an exaggerated response of the dye to UVA (Boulton et al., 2011).

After treatment, cells were trypsinized, centrifuged at  $400 \times g$  for 4 min at 4°C and resuspended in 0.5 ml of PBS + 0.1% (w/v) bovine serum albumin (BSA). Samples were then transferred to FACS tubes and analysed with a Becton Dickinson FACSAria II. The viable proportion of the cell population was quantified by the addition of 2.5 µg/mL propidium iodide (PI) immediately before the analysis.

## 2.8 Single-cell gel electrophoresis (comet assay)

DNA damage was assessed using the alkaline comet assay (pH~13) with specific modifications based on the cell type and the photolesion investigated (Cooke et al., 2008a). The alkaline version of the comet assay was developed by N.P. Singh and colleagues in 1988 (Singh et al., 1988), to measure low levels of strand breaks with high sensitivity. The pH in which the unwinding of the DNA and electrophoresis takes place is extremely important, as it changes what lesions the assay detects. The neutral comet assay (pH 7-8) facilitates the detection of double strand breaks and cross links; At pH between 12.1-12.4, the detects single and double strand breaks, incomplete excision repair sites and cross links; At pH>12.6, the assay detects alkali labile sites (ALS) in addition to all types of lesions mentioned above (Miyamae et al., 1997).

This assay is shown schematically in Figure 2.8. Routinely, ordinary, alcohol-cleaned clear glass microscope slides were pre-coated with agarose, by dipping in a staining jar containing melted 1% standard agarose in H<sub>2</sub>O. The backs of the slides were wiped clean, and they were left to dry. Slides were then stored at room temperature for future use.

Cells were counted before UVR exposure and distributed in the wells of a 9-well (~10<sup>3</sup> cells per well). After irradiation, cells were trypsinised and harvested into PBS, and subsequently transferred into Eppendorf tubes. Cells were then centrifuged at 400 × g for 4 min, at 4°C. Supernatants were discarded and pellets were kept on ice. Cells were mixed with 200 µl of low-melting point agarose (LMA) and 75 µl of the gel was quickly poured on agarose pre-coated slides. Coverslips were placed over the gels, and slides were kept in a tray on ice for 10 min to allow the agarose to set. Coverslips were gently

removed and slides were placed in a tank filled with lysis buffer (2.5 M NaCl, 100 mM EDTA, 10 mM acid Tris, 1% sodium sarcosinate, pH 10, 1% of Triton 100, and 10% DMSO) for 16h at 4°C, in the dark.

After carefully removing lysis buffer, slides were washed with ice-cold ddH<sub>2</sub>O for 10 min (covered to prevent any DNA damage due to light). Slides were immersed in 2 changes of enzyme reaction buffer (9.5 g Hepes, 7.4 g KCl, 186 mg EDTA, 200 mg BSA, pH 8, diluted in ddH<sub>2</sub>O), for 5 min each, at room temperature.

The detection of specific photolesions requires the incorporation of an extra step; after the lysis of agarose-embedded cells, DNA can be digested with lesion-specific endonucleases (DNA repair enzymes of bacterial/phage origin) that recognise the lesions and convert them to strand breaks. Thus, range, specificity and sensitivity of the assay are significantly increased.

### **2.8.1 8-oxoGua detection**

Oxidatively induced DNA damage was measured using the human 8-oxoguanine DNA glycosylase 1 (hOGG1)-modified comet assay. Gels were incubated with hOGG1 [3.2 U/ml (New England Biolabs, UK) - diluted 1:100 in enzyme reaction buffer], or enzyme reaction buffer alone.

### **2.8.2 CPD detection**

Cyclobutane pyrimidine dimers (CPD) were assessed using the T4 endonuclease V (T4endoV)-modified comet assay. Gels were incubated with T4endoV [0.1 U/ml (New

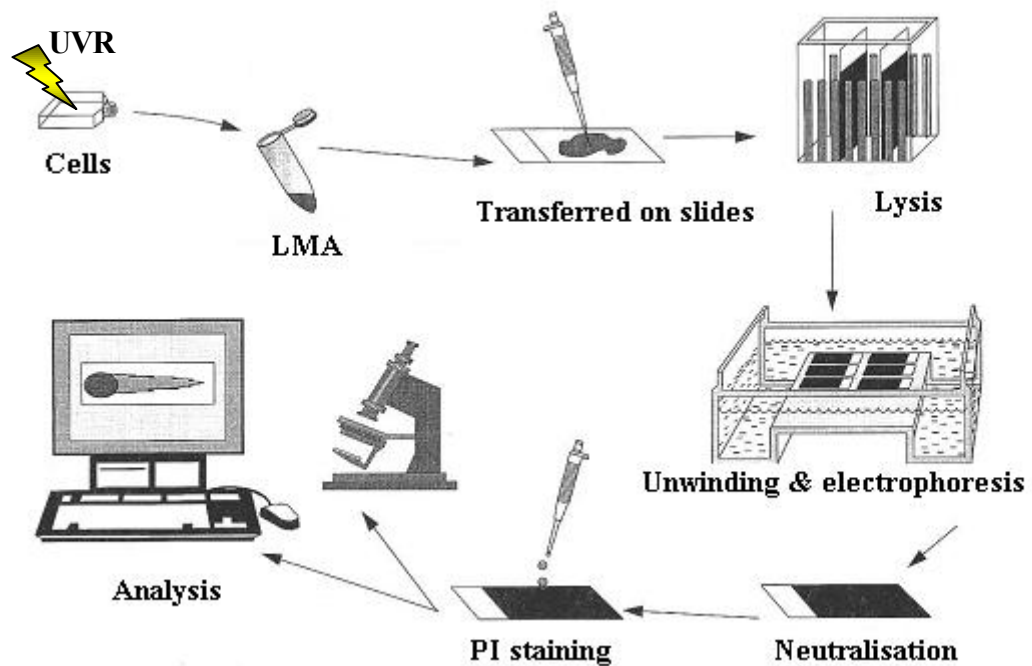
England Biolabs, UK) - diluted 1:500 in enzyme reaction buffer), or enzyme reaction buffer alone.

Coverslips were placed on top of the gels to ensure equal distribution of the enzymes, and slides were incubated at 37°C in a humid atmosphere for 45 min.

### **2.8.3 DNA unwinding and electrophoresis**

Slides were subsequently transferred into ice-cold electrophoresis buffer (NaOH 10 M, EDTA 200 mM, pH 13 in ddH<sub>2</sub>O) and incubated for 20 min in the dark. Electrophoresis was performed for 20 min at 25 V, 300 mA. Finally, slides were gently rinsed with neutralization solution (0.4 M TrisMABase, Sigma, pH 7.5) for 20 min and then washed with ddH<sub>2</sub>O for 10 minutes. Slides were allowed to dry at room temperature overnight. DNA was stained using 1 ml of propidium iodide (PI) solution at 2.5 µg/ml in PBS per slide, for 20 min. Slides were then washed with dd for 20 minutes. After drying in the oven (2-3h at 37°C), slides were ready for image analysis. Slides were examined at a magnification of 40×, using a Zeiss Axiophot epifluorescence microscope (Carl Zeiss, Germany) equipped with a green excitation filter. Pictures covering the whole area of the slides were taken with a Nikon camera linked to the microscope. Routinely, 50 randomly selected cells per slide and 3 slides per experimental condition were analysed (n=150) with the comet scoring software Comet Score (TriTek Corp., Summerduck, VA). The tail intensity, defined as the percentage of DNA migrated from the head into the tail of the comet, was measured for each nucleus scored

(I)



(II)

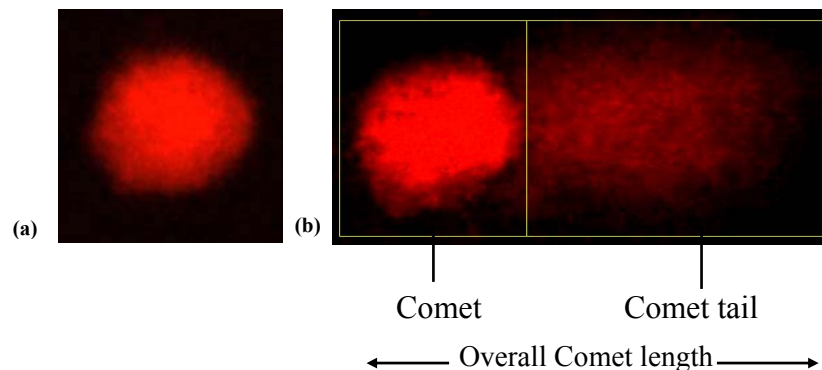


**Figure 2.8:** Schematic representation of the basic steps of the comet assay

**(I)** Cells are embedded in a thin agarose gel. All cellular proteins are removed by lysis. Following lysis, certain DNA repair enzymes may be employed for the specific detection of various types of DNA damage. DNA is then allowed to unwind under alkaline conditions. DNA undergoes electrophoresis, allowing the broken DNA fragments/damaged DNA to migrate away from the nucleus. After PI staining, the gel is “read” for amount of fluorescence in head and tail. *Image was adapted from the book DNA repair protocol (Günter Speit and Andreas Hartmann, 2005).* **(II)** Comets stained with PI; (a) Control: undamaged DNA remains trapped in nucleus; (b) Damaged DNA streams out of nucleus after UVR, forming a “comet” with a distinct head and tail.

## **2.9 A mechanistic approach to study UVA-induced DNA damage**

In order to have a better understanding of the UVA-induced photolesions studied above, we needed to obtain some mechanistic information. In order to distinguish between direct or indirect DNA damage, certain inhibitors of ROS-producing enzymes were employed. The aim of this approach was to target specific pathways of interest, to gain an insight on the role of free radicals in DNA damage.

The compounds used were the following:

- (a) Rotenone: it inhibits the mitochondrial respiratory chain complex I. Since the mitochondrial respiratory chain is one of the most important sites of ROS production under physiological conditions, inhibiting this pathway would help us test if ROS are involved in the formation of CPD. Rotenone was used at a concentration of 100  $\mu$ M in DMEM for 30 min treatment prior to UVR.
  
- (b) Diphenyleneiodonium (DPI): DPI reduces superoxide anion production and ROS generation by inhibition of NADPH oxidase and other flavine-containing enzymes. Several groups have highlighted the importance of NADPH oxidase in UVA-induced ROS; therefore, inhibiting this pathway can be crucial in understanding which radicals are involved in specific DNA damage. DPI was used at a concentration of 10  $\mu$ M in DMEM for 30 min prior to UVR.

## **2.10 Gene expression studies**

### **2.10.1 RNA isolation**

Total RNA for real-time RT-PCR was isolated using the Absolutely RNA Microprep kit (Agilent Technologies) according to the manufacturer's protocol. 0.7  $\mu$ l of  $\beta$ -mercaptoethanol ( $\beta$ -ME) was added to 100  $\mu$ l of lysis buffer for each sample of up to  $5 \times 10^5$  cells. A fresh mixture of lysis buffer and  $\beta$ -ME was prepared before each experiment. 100  $\mu$ l of the lysis buffer- $\beta$ -ME mixture was added to each cell sample. All tubes were mixed thoroughly (by vortexing and pipetting) to ensure samples were homogenized. An equal volume (usually 100  $\mu$ l) of 70% ethanol was added to each cell lysate and mixed thoroughly by vortexing for 5 sec.

The mixtures were then transferred to RNA-binding spin cups seated in 2 ml collection tubes. Samples were mixed in a microcentrifuge for 1 min at maximum speed. Filtrates were discarded, while spin cups were retained. Spin cups were attached to new tubes and the matrixes were washed with low-salt buffer (600  $\mu$ l). Samples were mixed by centrifugation for 1 min at maximum speed; the spin cup was retained and the filtrate was discarded. Spin cups were placed in new collection tubes and centrifuged for 2 min at maximum speed to dry the matrixes. DNase solution was added directly onto the matrix inside the spin cup of each sample, to remove DNases. Samples were then placed in a 37°C incubator for 15 min. After the incubation 500  $\mu$ l of high-salt wash buffer were added to each spin cup, and samples were mixed in a microcentrifuge at maximum speed for 1 min. Filtrates were discarded and the spin cups were returned to the collection tubes. Following a wash with 600  $\mu$ l of low-salt buffer, tubes were centrifuged at maximum speed for 1 min. Filtrates were discarded and spin cups were



washed with 300  $\mu$ l of low-salt wash buffer. Samples were then centrifuged at maximum speed for 2 min to dry the matrixes. Spin cups were finally transferred to 1.5 ml collection tubes and 30  $\mu$ l of Elution Buffer was added directly onto each matrix inside the spin cup. Samples were incubated at room temperature for 2 min and then centrifuged for 1 min. The RNA yield was determined by quantifying the samples on a Nanodrop ND1000 UV-vis Spectrophotometer (Labtech). RNA samples were stored at  $-20^{\circ}\text{C}$  for up to one month or at  $-80^{\circ}\text{C}$  for long-term storage, until PCR.

### **2.10.2 cDNA synthesis**

cDNA synthesis was carried out on 500 ng of total RNA using the QuantiTect reverse transcription kit (Qiagen) according to the manufacturer's instructions.

### **2.10.3 Real Time RT-PCR**

Gene expression was assessed by singleplex real-time quantitative RT-PCR using Taqman Gene Expression Assays according to the manufacturer's instructions. cDNA samples were diluted with distilled water to a final concentration of 500 ng/ $\mu$ l per sample. Probes labeled with 6-carboxyfluorescein (FAM) used for real-time RT-PCR were purchased as "Assay-on-Demand" from Applied Biosystems. The target genes were matrix metalloprotease 12 (MMP12) [Hs00899668\_m1] and heme oxygenase 1 (HO1) [Hs00157965\_m1]; HO1 is a well-studied gene, known to be induced by UVA irradiation (Tyrrell, 2004). MMP12 was chosen as it was strongly upregulated in a pilot human study, following microarray analysis. Human  $\beta$ 2-Macroglobulin (B2M) [Hs99999907\_m1] was used as a housekeeping gene as well as Human Glyceraldehyde 3-phosphate dehydrogenase (GAPDH), which was labeled with 4,7,2'-trichloro-7'-

phenyl-6-carboxyfluorescein (VIC). Reactions were performed using 10 µl of 1X TaqMan Universal PCR master mix (Applied Biosystems, Foster City, CA), 1 µl of the appropriate probe, and 2 µl cDNA (500 ng/µl), in a total volume of 20 µl. All PCR reactions were carried out in triplicates in 96 well plates covered by optical adhesive lids. Samples were amplified in an Applied Biosystems 7900HT Sequence Detection System, under the following conditions: 15 min 95°C; (15 s 95°C, 1 min 60°C) x 40. After amplification, relative expression levels for MMP12 and HO1 were analyzed using the  $\Delta\Delta C_t$  method as described in the following section.

#### **2.10.4 Analysis of real-time PCR data**

The expression of transcripts of interest was normalized to that of the  $\beta 2$ -Macroglobulin and GAPDH housekeeping genes. Data analysis was performed using the  $\Delta\Delta C_t$  threshold ( $C_t$ ) method, which does not require the use of a standard curve (Livak and Schmittgen 2001; Lopez-Albaitero, Mailliard et al. 2009). The  $\Delta\Delta C_t$  value was calculated using the formula:  $\Delta\Delta C_t = (C_{tGOI} - C_{tHK})$ , where  $C_{tGOI}$  and  $C_{tHK}$  are the averaged  $C_t$  values for the gene of interest and the housekeeping gene. Data were expressed as mRNA expression fold changes, relative to a calibrator sample. Assuming a doubling of material during each PCR cycle, this relative quantification (RQ) was estimated according to the formula:  $(RQ) = 2^{-\Delta\Delta C_t}$ .

## 2.11 Total glutathione (GSH) measurement

Intracellular concentrations of reduced glutathione (GSH) were measured using the GSH/GSSG kit (Calbiochem, cat. no. 371757). Reduced glutathione (GSH), a tripeptide ( $\gamma$ -glutamylcysteinylglycine) with a free thiol group, is a major antioxidant in human tissues that provides reducing equivalents for the glutathione peroxidase (GPx) catalyzed reduction of hydrogen peroxide and lipid hydroperoxides to water and the respective alcohol. During this process GSH becomes oxidized glutathione (GSSG). The GSSG is then recycled into GSH by glutathione reductase (GR) and  $\beta$ - nicotinamide adenine dinucleotide phosphate (NADPH). When mammalian cells are exposed to increased oxidative stress, the ratio of GSH/GSSG will decrease as a consequence of GSSG accumulation. Measurement of the GSSG level or determination of the GSH/GSSG ratio is a useful indicator of oxidative stress and can be used to monitor the effectiveness of antioxidant intervention strategies.

The technique employs a chromogen known as Ellman's reagent (5,5'-dithiobis-2-nitrobenzoic acid or DTNB), which reacts with GSH to form a spectrophotometrically detectable product at 412 nm. GSSG can be determined by the reduction of GSSG to GSH, which is then determined by the reaction with the chromogen. The change in color development during the reaction, and the reaction rate is proportional to the GSH and GSSG concentrations.

Cell pellets were homogenized in 50  $\mu$ l of cold metaphosphoric acid (5% w/v) and resuspended in a total volume of 500  $\mu$ l. The homogenate was centrifuged for 10 min (3,000  $\times$  g) at 4° C and 100  $\mu$ l of the resulting supernatant was analysed by spectrophotometry using a UV-Vis Spectrophotometer.

## **2.12 Immuno-Slot-Blot (ISB) for the detection of UVA-induced CPD**

UVB-irradiated calf-thymus DNA (CT-DNA) was used to establish the technique worked.

DNA from cells was isolated using the DNeasy Blood & Tissue Kit (Qiagen), according to the manufacturer's instructions.

3.5 µg of each DNA sample were sonicated in a water bath for 20 min to obtain approximately 100 base pair long fragments. DNA was then boiled for 5 min to produce single-stranded DNA, prior to being placed on ice for 10 min, and then mixed with an equal volume of 2 M ammonium acetate. Single-stranded DNA was then immobilised on nitrocellulose (NC) filters using a Minifold II, 72-well Slot-Blot microfiltration apparatus (Schleicher and Schuell, Keene, NH, USA). Prior to use, the NC filters were presoaked in 1 M ammonium acetate. After loading the DNA, the slots were rinsed with 200 µL of 1 M ammonium acetate. The NC filters were then removed from the filter support and baked at 80°C for 90 min.

The filters were then immersed in 100 mL of PBS-Tween (PBS with 0.1% Triton X-100 were added) plus 5% non-fat milk powder for 1h at room temperature. After extensive washing in PBS-Tween with several buffer changes, the NC filters were incubated with anti T<>T monoclonal antibody (Anti-Thymine Dimer mAb, clone KTM53; Kamiya Biomedical Company, Seattle, WA USA) diluted 1 in 4,000 in PBS-Tween plus 0.5% milk powder, for 1h at room temperature followed by two further 5 min washes with PBS-Tween. The filters were then incubated with the secondary antibody (goat anti mouse immunoglobulin horse radish peroxidase conjugated; Dako A/S, Glostrup,

Denmark). The secondary antibody was diluted 1 in 4,000 in PBS-Tween plus 0.5% milk powder. The filters were allowed to rock in plastic boxes for 2 h, at room temperature. The filters were then washed with PBS-Tween by gentle rocking in a tray for 15 min followed by two further 5 min washes. Care was taken not to let the filters dry out. Enzymatic activity was visualised by bathing the NC membrane with Super Signal West Dura Extended Duration Substrate for 5 min (Pierce, IL, USA). The substrate working solution was prepared immediately before use by mixing equal volumes of the ultra luminol/enhancer solution with the ultra stable peroxide solution. Care was taken not to touch the bands.

### **2.12.1 Densitometry**

Quantification of T<math>\alpha</math>T in each DNA sample was obtained by scanning the blots on a ChemiGenius2 image acquisition system (Syngene, Cambridge, UK) and obtaining a chemiluminescent image of the nitrocellulose filter. The frame width fitting the slot areas was drawn and stored, and chemiluminescence intensities (relative units) per slot area were quantified using the Gene tools software (Syngene, Cambridge, UK).

### **2.13 Statistical analysis**

All experiments were conducted in triplicates and values are presented as mean  $\pm$  standard error of the mean (SEM). Statistical analysis was conducted with GraphPad Prism version 4.0 (GraphPad software, San Diego, CA). Two-way ANOVA with Bonferroni multiple comparison post-test was chosen for the comet assay and one-way ANOVA with Bonferroni post-test was used for cell viability assay analyses. Student's unpaired t-test was chosen for all other analyses. Significance limits were set at \* $p < 0.05$ , \*\* $p < 0.001$ , and \*\*\* $p < 0.0001$ .

## **Chapter 3: Results**

## Structure

The chapter is divided into six studies, each of which is further subdivided in several sections, starting with the development of the comet technique and the optimisation experiments that established the parameters selected in the main experiments.

**Study 1:** UVB-induced DNA damage for technique development and optimisation of concentrations of DNA restriction enzymes and vitamin E.

**Study 2:** Time-course/repair kinetics experiments to establish DNA repair time-points for specific types of UVA-induced DNA damage.

**Study 3:** Pre- and post-UVR effect of vitamin E against UVA-induced DNA damage and oxidative stress.

**Study 4:** Assessment of NAC in the protection against UVA-induced DNA damage.

**Study 5:** Real time PCR for detection of HO-1 and MMP-12 induction by UVA.

**Study 6:** ROS pathways inhibitors study.

**Study 7:** Stiefel compound testing against UVA-induced DNA damage and oxidative stress.

### 3.1 Study of UVB-induced DNA damage for technique development

Due to some complications with the UVA source early in my PhD, a UVB source was employed to develop the comet assay, especially for CPD measurements, as UVB is known to readily induce CPD. Enzyme concentrations used for the UVB experiments were based on the experience of my second supervisor's laboratory, Dr Marcus Cooke, and on protocols supplied by Dr Tiago Duarte (Leicester University, Department of Cancer Studies and Molecular Medicine and Genetics). These experiments helped establish the routine use of the technique in the laboratory.

#### 3.1.1 UVB-induced DNA damage on HaCaT keratinocytes

The effect of increasing doses of UVB irradiation on cell viability is shown on Table 3.1. Representative images of comets produced by UVB irradiation are presented in Figure 3.1. No comet tails were observed on cells exposed to 50 mJ/cm<sup>2</sup>, without any enzyme (ALS/SB), or with hOGG1. Small comet tails were formed with 100 mJ/cm<sup>2</sup> in these two groups (Figures 3.1a and 3.1b). HaCat cells treated with T4endoV exhibited significantly increased comet tails compared to the rest (Figure 3.1c).

UVB dose (mJ/cm <sup>2</sup> )	Viable cells (%)
0	92.9 ± 2.6
50	84.2 ± 4.1
100	79.3 ± 3.9
200	73.8 ± 4.5
300	66.5 ± 5.2

**Table 3.1: HaCaT cell viability following UVB irradiation**

Cell viability was assessed immediately after UVB irradiation by the MTT assay. Data represent the mean of three independent experiments ± SEM. One-way ANOVA with Bonferroni correction showed significant differences between dose increments ( $p < 0.001$  in all cases).



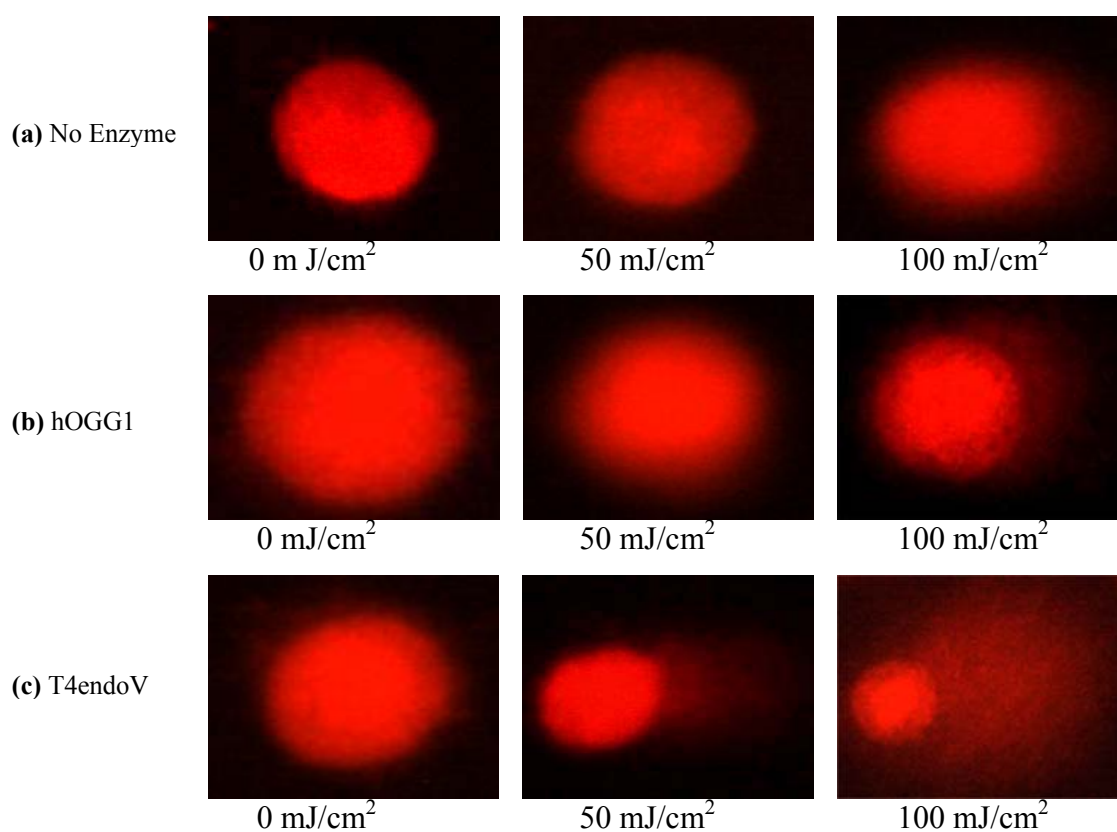


**Figure 3.1:** Comets formed due to UVB radiation with two doses (50 and 100 mJ/cm<sup>2</sup>)

A dose-dependent increase in the formation of CPD, 8-oxoGua and ALS/SB was observed following UVB irradiation of HaCat keratinocytes (Figure 3.2a). CPD levels were much greater than 8-oxoGua levels as expected, since UVB is directly absorbed by DNA. Figure 3.2b shows the frank CPD and 8-oxoGua levels (background correction was performed using the “no enzyme” values for each group; please see section 3.2 for further details).

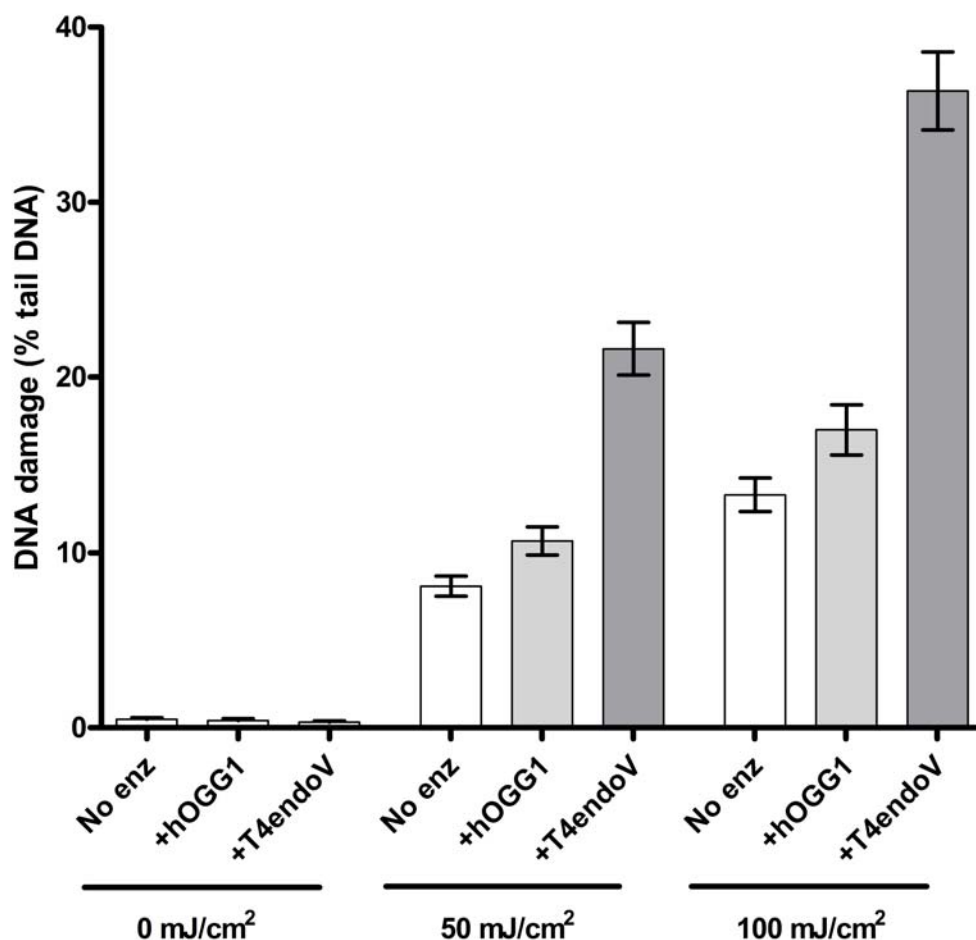


**Figure 3.2a:** Effect of UVB irradiation on the formation of 8-oxoGua, CPD and ALS/SB detected by the hOGG1- and the T4endoV-modified comet assay

The mean percentage of tail DNA in HaCaT cells exposed to UVA doses of 50 and 100 mJ/cm². Results are the mean  $\pm$ SEM of three independent experiments (50 comets scored per experiment);  $p < 0.0001$  in all cases when comparing irradiated samples to their corresponding non-irradiated samples;  $p < 0.05$  in all cases when comparing “No enz” to “+ enz” samples.

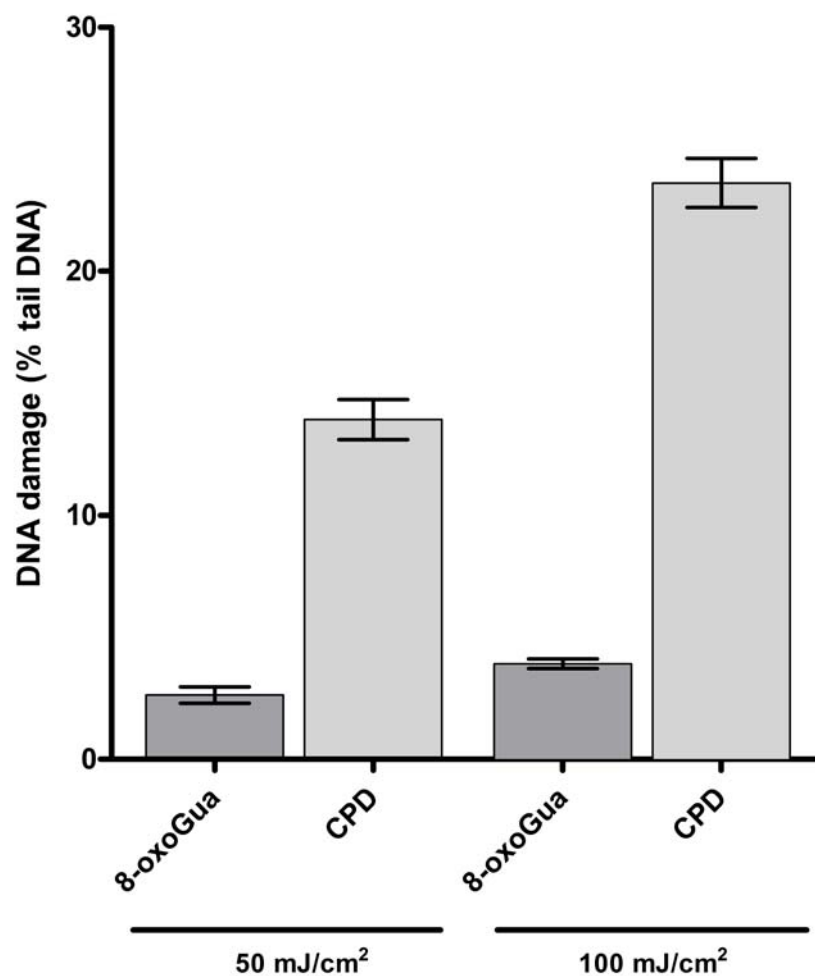


**Figure 3.2b:** Effect of UVB irradiation on the formation of 8-oxoGua and CPD formation as detected by the hOGG1- and the T4endoV-modified comet assay (background corrected)

Mean percentage of tail DNA HaCaT cells exposed to UVB doses of 50 and 100 mJ/cm². Background correction was performed using no enzyme values for each group. Results are the mean  $\pm$ SEM of three independent experiments.

### **3.2 Optimisation of hOGG1, T4endoV and vitamin E concentrations for the comet assay**

In order to determine the ideal concentrations of the DNA repair enzymes used in the UVA studies, various concentrations of hOGG1 and T4endoV were tested, based on the protocol provided by Dr Tiago Duarte. Based on that, optimal concentrations for the hOGG1-modified comet assay ranged between 3-4 U/mL, while for the T4endoV-modified comet assay ranged between 0.05-0.15 U/mL. Pilot studies confirmed these ranges and the final concentrations chosen for all the experiments were 3.2 U/mL for hOGG1 (Figure 3.3), and 0.1 U/mL for T4endoV (Figure 3.4), which is at the top of the dose responses, after which there is a plateau.

Vitamin E was originally chosen in this study as a potent antioxidant and an ideal compound for technique development and assessment. However, as the initial experiments produced some interesting data, vitamin E was further investigated. Concentration optimisation for vitamin E is presented in Figure 3.5.

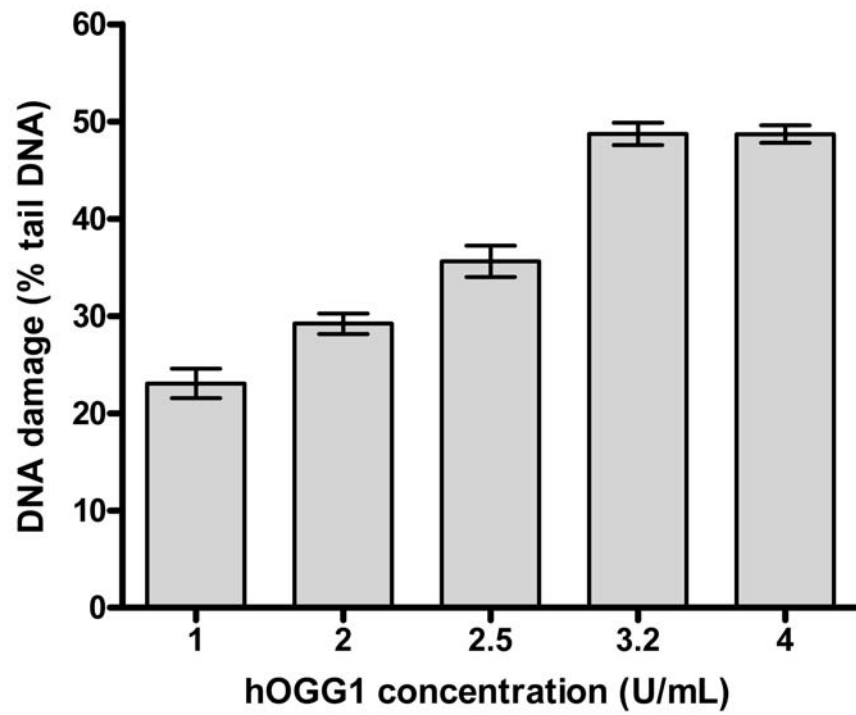


**Figure 3.3:** Optimisation of hOGG1 concentration by the comet assay

HaCaT keratinocytes were irradiated with 5 J/cm<sup>2</sup> UVA and were subsequently incubated with different concentrations of enzyme for 45 min. Results are the mean  $\pm$ SEM of three independent experiments.

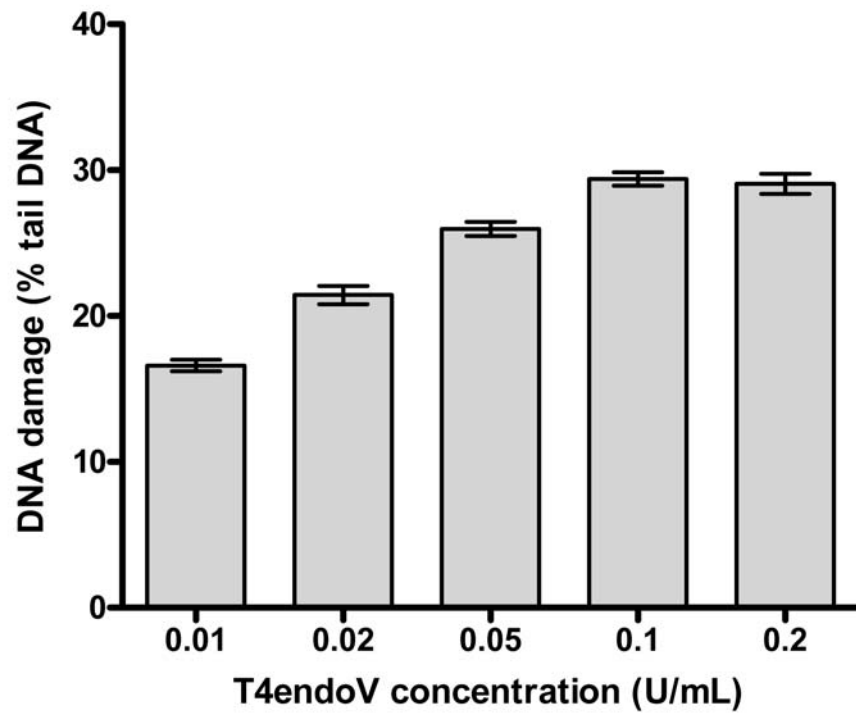


**Figure 3.4: Optimisation of T4endoV concentration by the comet assay**

HaCaT keratinocytes were irradiated with 5 J/cm<sup>2</sup> UVA and were subsequently incubated with different concentrations of enzyme for 45 min. Results are the mean  $\pm$ SEM of three independent experiments.

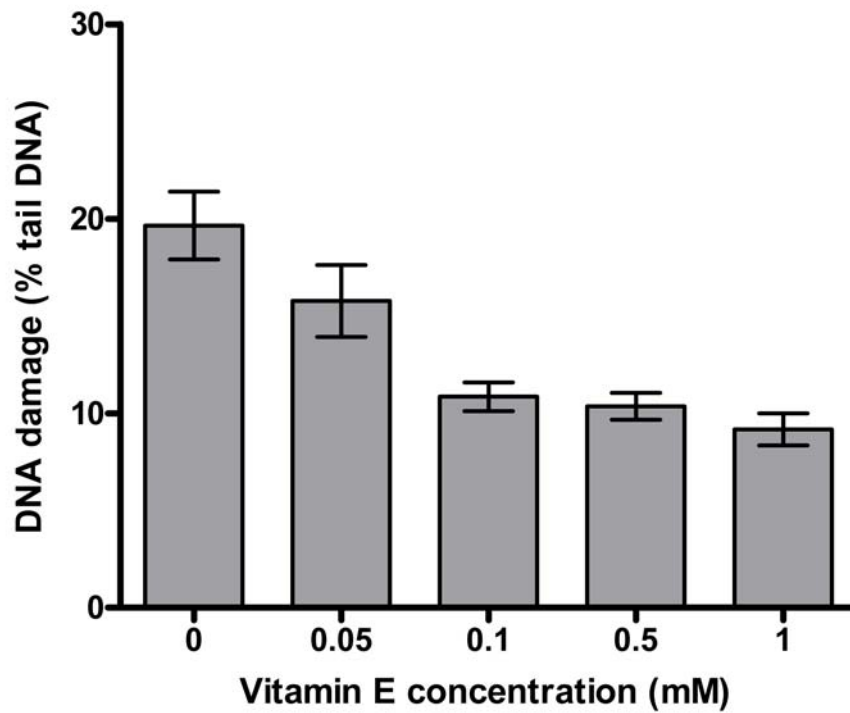


**Figure 3.5:** Optimisation of vitamin E concentration (without the use of any DNA repair enzymes)

HaCaT keratinocytes were incubated with different concentrations of vitamin E (diluted in EtOH) for 24 h, and then washed thoroughly with PBS; they were subsequently irradiated with 5 J/cm<sup>2</sup> UVA. Results are the mean  $\pm$ SEM of three independent experiments.

### 3.2.1 Cell viability

UVA exposure doses were chosen based on published literature, physiological relevance and cell viability assays (Table 3.2).

UVA dose (J/cm <sup>2</sup> )	Viable cells (%) TB	Viable cells (%) MTT
0	90.3 ± 4.2	89.9 ± 3.8
2.5	89.7 ± 5.1	88.7 ± 2.1
5	88.6 ± 3.3	88.0 ± 3.9
10	85.3 ± 4.6	84.4 ± 3.4
20	82.3 ± 2.9	81.2 ± 4.3
40	79.7 ± 5.0	80.1 ± 4.2
80	73.2 ± 4.6	71.1 ± 5.3

**Table 3.2: HaCaT cell viability following UVA irradiation**

Cell viability was assessed immediately after UVA irradiation by the trypan blue (TB) exclusion and the MTT assays. Data represent the mean of three independent experiments ± SEM. One-way ANOVA with Bonferroni correction showed significant differences between dose increments ( $p < 0.05$  in all cases).

Based on Table 3.2, the dose range of between 5-20 J/cm<sup>2</sup> was chosen, but in some cases a dose of 40 J/cm<sup>2</sup> was given. The average time to give a dose of 20 J/cm<sup>2</sup> was 11 min. Furthermore, cell viability was not significantly altered by UVA exposure or vitamin E supplementation for 24 h (Table 3.3), as demonstrated by both trypan blue exclusion assay and the MTT assay.

Treatment	Viable cells (%) TB	Viable cells (%) MTT
Control*	87.3 ± 3.2	88.7 ± 2.5
20 J/cm <sup>2</sup> UVA*	81.8 ± 4.3	80.1 ± 3.6
Vitamin E	88.6 ± 2.5	89.2 ± 2.0
20 J/cm <sup>2</sup> UVA + Vitamin E	85.9 ± 1.6	86.5 ± 2.5

**Table 3.3: HaCaT cell viability following UVA ± vit E**

Cell viability was assessed by the trypan blue (TB) exclusion and the MTT assays. Data represent the mean of three independent experiments ± SEM. One-way ANOVA with Bonferroni correction showed significant differences between all groups ( $p < 0.05$ ).

\*Cells incubated with EtOH for 24 h.



### **3.3 Time-course experiments to establish DNA repair time-points for specific types of UVA-induced DNA damage**

The comet assay was employed to measure the repair kinetics of 8-oxoGua, CPD and non-enzyme specific lesions (ALS/SB) after 5 J/cm<sup>2</sup> UVA, over a period of 10 h. Following UVR, samples were left to repair in their conditioned media, at 37°C in a humidified incubator with 95% air/5% CO<sub>2</sub>.

Both photolesions increased over a period of 30 min; however, formation of 8-oxoGua continued to increase up to 1 h after UVR, while CPD levels started to decline after 30 min. 8-oxoGua reached control levels at 10 h whereas the level of CPDs decreased at a slower rate (Figure 3.6). Slide incubation in the absence of hOGG1 and T4endoV measured alkali labile sites (ALS) and frank strand breaks (SB). Repair kinetics for these lesions was also plotted, with a half-life of approximately 4 h.

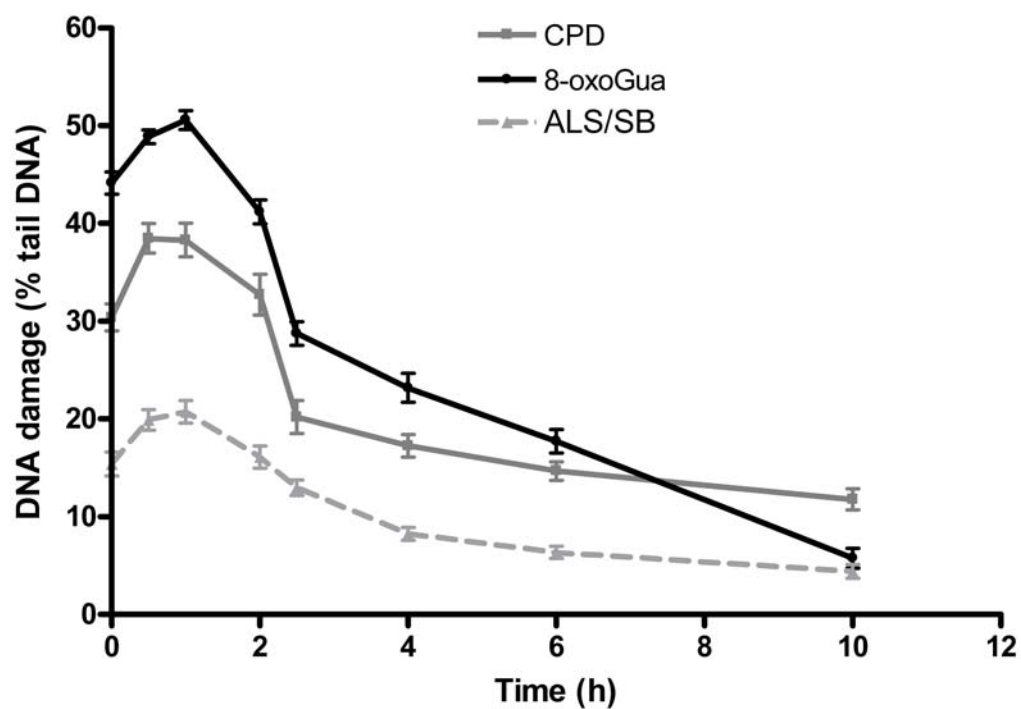


**Figure 3.6: Induction and repair of UVA-induced 8-oxoGua and CPDs, over 10 h**

HaCaT keratinocytes were irradiated with 5 J/cm<sup>2</sup> UVA and were left to repair for different time periods. Results are the mean  $\pm$ SEM of three independent experiments.

It should be noted in Figure 3.6, that the ALS/SB values measured by the assay without any enzymes, have not been subtracted from the values obtained by the hOGG1 and the T4endoV comet assay. This approach was taken in order to follow the formation of ALS and SB due to UVA irradiation. The same principle was followed in the sections presenting comet data below. In most cases, the difference between enzyme-treated (specific DNA damage) and the non-treated (ALS/SB) was big enough to obtain a clear indication of the effects of the compounds used in each study. However, in order to have a more accurate observation of each compound tested by the comet assay, graphs presenting the frank 8-oxoGua and CPD values were also plotted, in which the corresponding background values (ALS/SB) were subtracted from the hOGG1 and T4endoV-obtained values.

Figures showing all types of damage were produced by plotting the mean of 150 comets (obtained from three different experiments) for each group studied ( $\pm$  enzyme and  $\pm$  compound). For background-corrected graphs the mean from each non-enzyme treated group (n=3, 50 comets per experiment) was subtracted from the corresponding (same UVA dose and compound treatment) enzyme-treated group.

### **3.4 Pre- and post-UVR effect of vitamin E against UVA-induced DNA damage and oxidative stress**

#### **3.4.1 Vitamin E pre-treatment protects against UVA-induced ROS formation and DNA damage**

##### **ROS**

ROS generation was quantified by carboxy-H<sub>2</sub>DCFDA staining, in which the outcome is measured as fluorescence. An increase in ROS was observed with increasing UVA doses (10, 20 and 40 J/cm<sup>2</sup>), as shown in Figure 3.7; cells pre-treated with vitamin E for 24 h prior to UVR exhibited a lower fluorescence. Vitamin E offered significant protection at all UVA doses. This was highly significant at 40 J/cm<sup>2</sup> with a 33% reduction of ROS compared to the control. Vitamin E did not alter the level of intracellular ROS in unirradiated cells (data not shown).

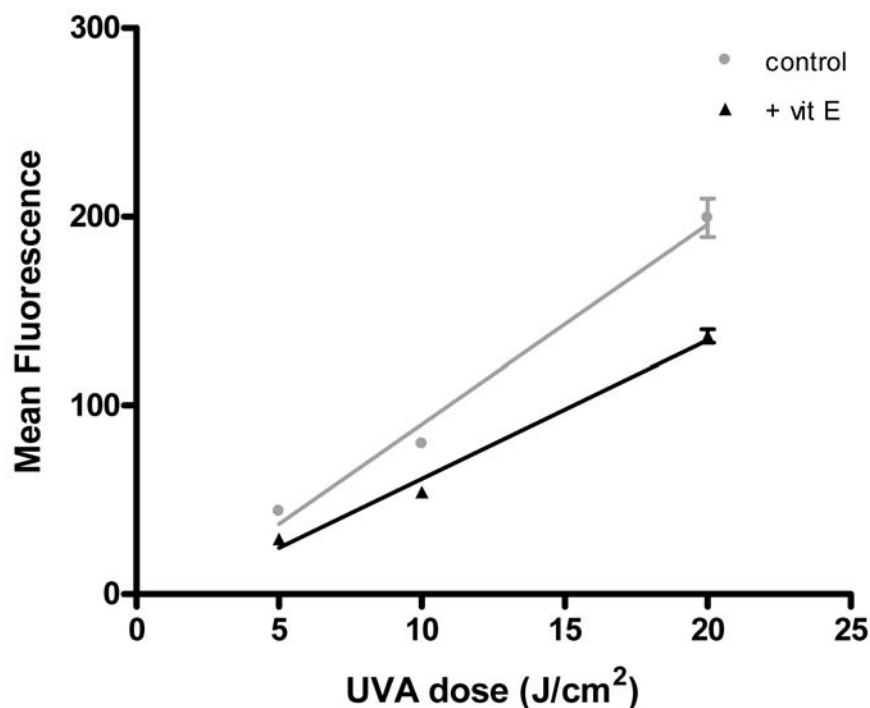


**Figure 3.7:** Comparison of ROS production between control (EtOH) and pre-UVR treated (+ vit E) groups

Fluorescence intensity of H<sub>2</sub>DCFDA was excited at 488 nm. Results are the mean of three independent experiments  $\pm$ SEM. The UVR dose-responses were determined by linear regression analyses. The R<sup>2</sup> values for both test conditions were >0.97 and both slopes were very significantly different from zero ( $p < 0.0001$ ), which demonstrates a strong dose-response. The control slope was significantly steeper than the vitamin E-treated slope ( $p < 0.001$ ), demonstrating a clear protection, which is more marked with higher UVR doses.

## **DNA photolesions**

A clear dose-dependent increase in both 8-oxoGua and CPD formation immediately after irradiation was demonstrated (Figures 3.8a and 3.8b). DNA damage in the absence of lesion-specific enzymes, representing ALS/SB levels, was also observed (Figure 3.8a). This possibly includes apurinic/apyrimidinic sites and some forms of alkali-labile modified nucleobases, as well as single strand breaks (Cadet et al., 2000).

HaCaT keratinocytes pretreated with vitamin E exhibited a decrease in 8-oxoGua levels at both UVA doses. The effect was greater at 5 J/cm<sup>2</sup> (approximately 61% decrease;  $p < 0.0001$ ). A significant decrease in CPD levels was also observed, present at both UVA doses (52% and 33 % decrease at 5 and 10 J/cm<sup>2</sup> respectively). DNA damage levels induced by UVR were statistically significant ( $p < 0.0001$ ) compared to the corresponding controls (unirradiated cells).

Comet analysis in the absence of any enzyme treatment suggests that a large percentage of the damage was ALS/SB sites. Comparisons between enzyme-treated and non-treated samples, in the absence of vitamin E, were statistically significant ( $p < 0.0001$ ) in all cases. This demonstrates the presence of a high level of enzyme-specific damage i.e. damage to nucleobases. Vitamin E also offered significant ( $p < 0.0001$ ) protection against non-specific (ALS/SB) DNA damage. Figure 3.8b shows vitamin E's effect on frank 8-oxoGua and CPD formation, following background correction (subtraction of ALS/SB levels from each group studied).

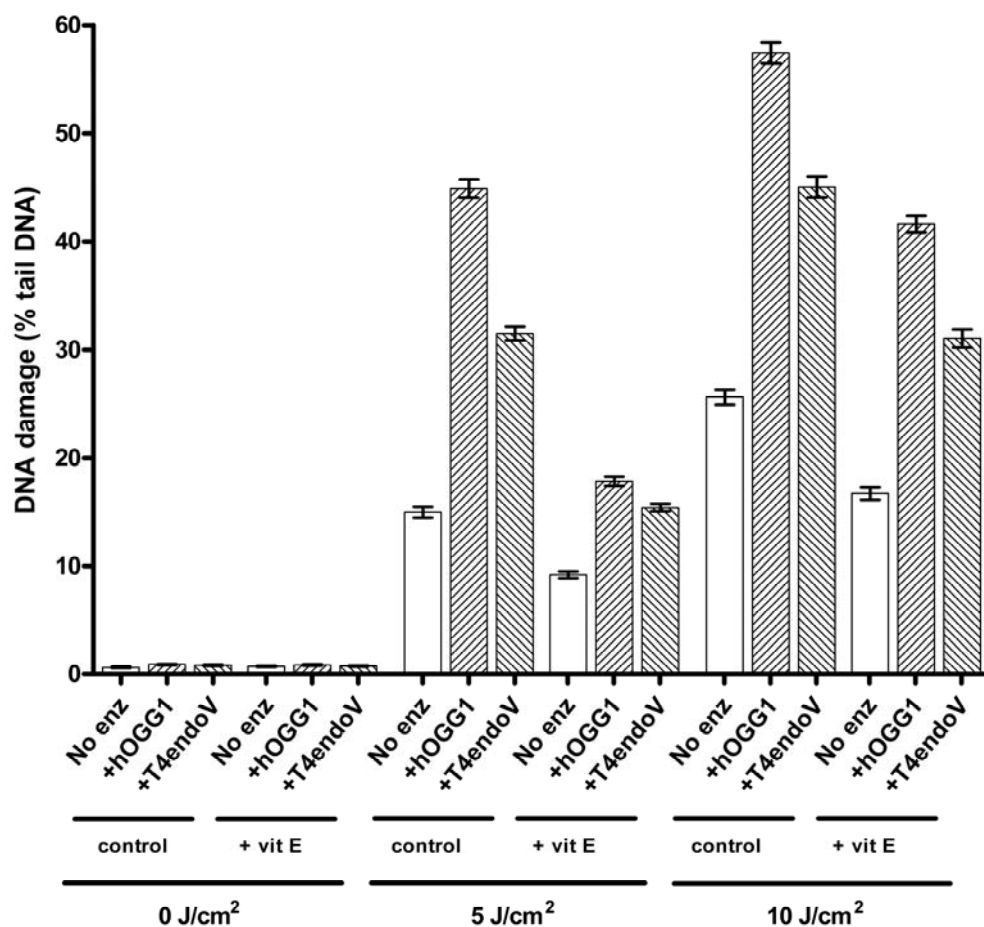


**Figure 3.8a:** Effect of pre-UVR incubation with vitamin E on 8-oxoGua, CPD and ALS/SB formation detected by the hOGG1- and the T4endoV-modified comet assay

The mean percentage of tail DNA in HaCaT cells exposed to UVA doses of 5 and 10 J/cm<sup>2</sup>. Results are the mean  $\pm$ SEM of three independent experiments (50 comets scored per experiment);  $p < 0.0001$  in all cases when comparing irradiated samples to their corresponding non-irradiated samples;  $p < 0.001$  in all cases when comparing “No enz” to “+ enz” samples.

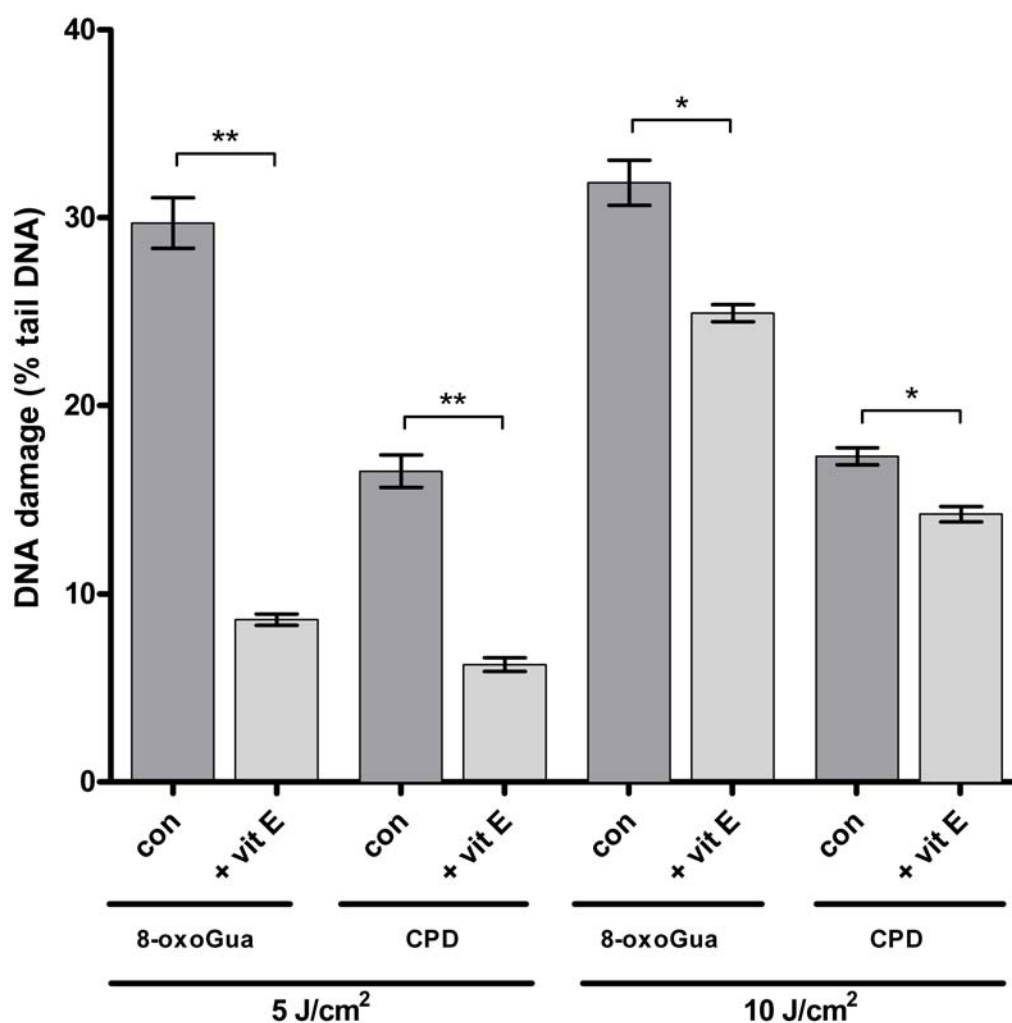


**Figure 3.8b:** Effect of pre-UVR incubation with vitamin E on 8-oxoGua and CPD formation as detected by the hOGG1- and the T4endoV-modified comet assay (background corrected)

Mean percentage of tail DNA HaCaT cells exposed to UVA doses of 5 and 10 J/cm<sup>2</sup>. Background correction was performed using no enzyme values for each group. Results are the mean  $\pm$ SEM of three independent experiments; \*\*p<0.001, \*p< 0.05 for selected comparisons, based on two-way ANOVA with Bonferroni correction



### **3.4.2 Post-UVR treatment with vitamin E also offers significant protection against ROS formation and DNA damage**

As shown in the spectral distribution of the UVASPOT (*see Materials and Methods, Table 2.7*), the very small UVB content (0.1-0.2%, depending on definition) of the source used contributes 10.4-12.7% of the EEE. Given the similarity of the action spectra for erythema and CPD in human skin *in vivo* (Young et al., 1998), it may be assumed that UVB makes a comparable contribution to CPD formation. Figure 2.1 (*see Materials and Methods*) shows that vitamin E has some UVB absorption, which overlaps with the emission spectrum of the source. In order to examine a possible sunscreening effect of vitamin E, the experiments were repeated with post-UVR treatment with vitamin E. Various post-UVR incubation times were tested in pilot studies and an incubation of 2.5 h was selected as the shortest period with a significant effect on both lesion types.

## **ROS**

A similar effect on ROS to that after pre-UVR treatment with vitamin E was observed (Figure 3.9). Cells treated with vitamin E for 2.5 h after UVR exposure, again exhibited lower fluorescence levels. However, mean fluorescence values were greater in general, compared to those found in the pre-UVR treatment experiment. As with pre-incubation, the maximal inhibition of ROS generation (31%) was observed at 40 J/cm<sup>2</sup>.

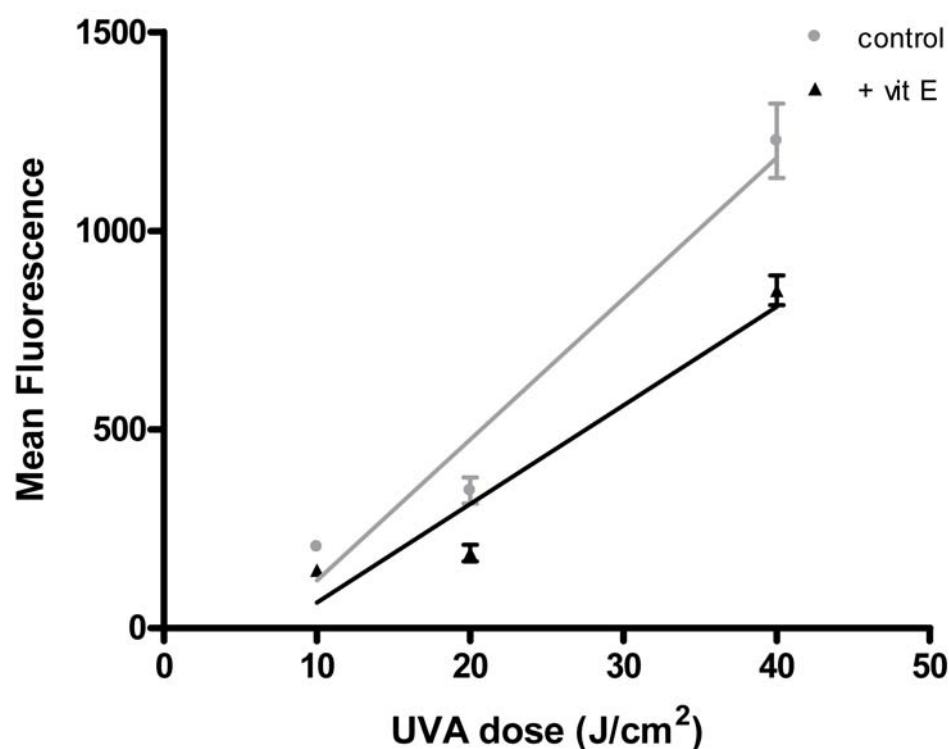


**Figure 3.9:** Comparison of ROS production between control (EtOH) and post-UVR treated (+ vit E) groups

Fluorescence intensity of H<sub>2</sub>DCFDA was excited at 488 nm. Results are the mean of three independent experiments  $\pm$ SEM. The UVR dose-responses were determined by linear regression analyses. The R<sup>2</sup> values for both test conditions were >0.91 and both slopes were very significantly different from zero ( $P < 0.0001$ ), which demonstrates a strong dose-response. The control slope was significantly steeper than the vitamin E-treated slope ( $p < 0.05$ ), demonstrating a clear protection, which is more marked with higher UVR doses.

## **DNA photolesions**

Figures 3.10a and 3.10b demonstrate the effect of post-UVR treatment with vitamin E on DNA damage. Similarly to the pre-UVR treatment experiment, a clear dose-dependent response in 8-oxoGua, CPD and ALS/SB formation was observed (Figure 3.10a). DNA damage levels in general were lower in the post-UVA exposure vitamin E treatment experiment, compared to the pre-UVA exposure vitamin E treatment experiment results. Vitamin E treatment after UVR reduced levels of hOGG1-detected sites at both doses tested. The strongest effect of vitamin E (0.1 mM) was again observed at 5 J/cm<sup>2</sup> at which 8-oxoGua and CPD levels exhibited a 67% and 65% reduction, respectively. Figure 3.10b shows the background-corrected data for the same experiment.

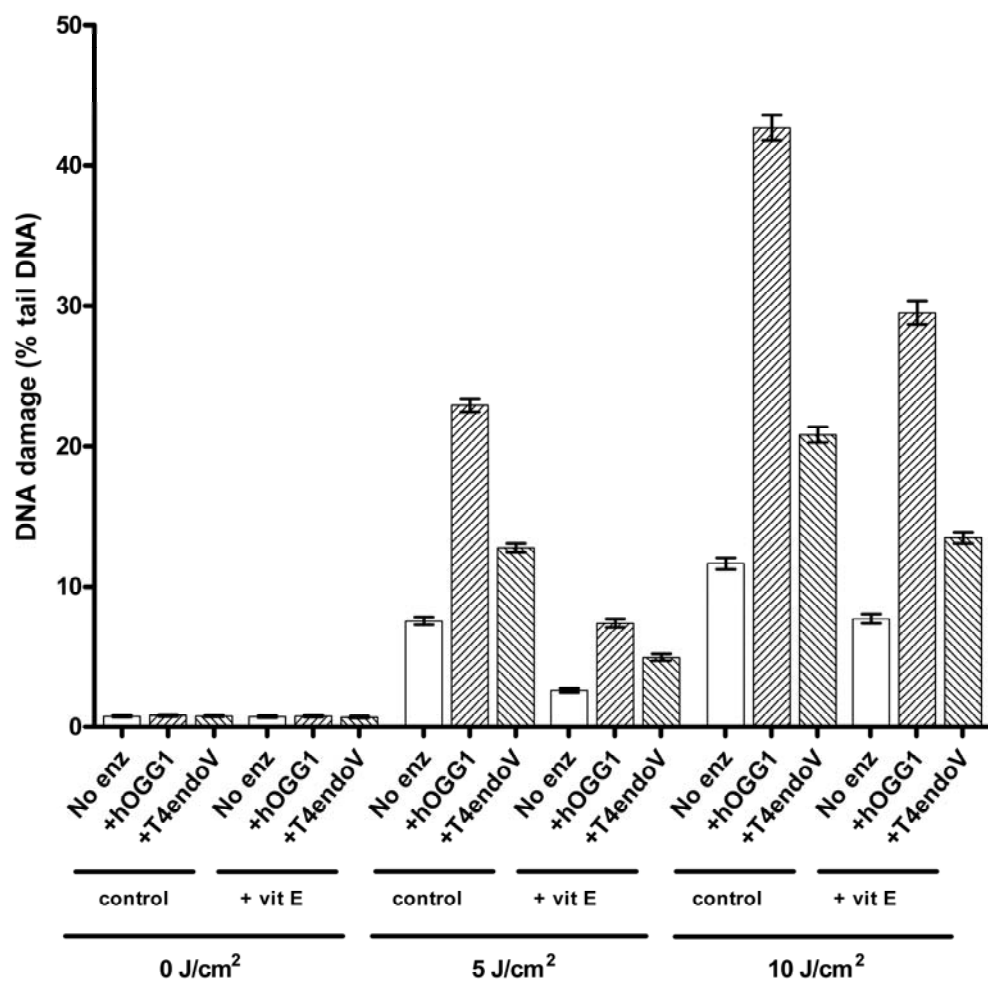


**Figure 3.10a:** Effect of post-UVR incubation with vitamin E on 8-oxoGua, CPD and ALS/SB formation as detected by the hOGG1- and the T4endoV-modified comet assay

Mean percentage of tail DNA HaCaT cells exposed to UVA doses of 5 and 10 J/cm<sup>2</sup>.

Results are the mean ±SEM of three independent experiments;  $p < 0.0001$  in all cases when comparing irradiated samples to their corresponding non-irradiated samples;  $p < 0.001$  in all cases when comparing “No enz” to “+ enz” samples.

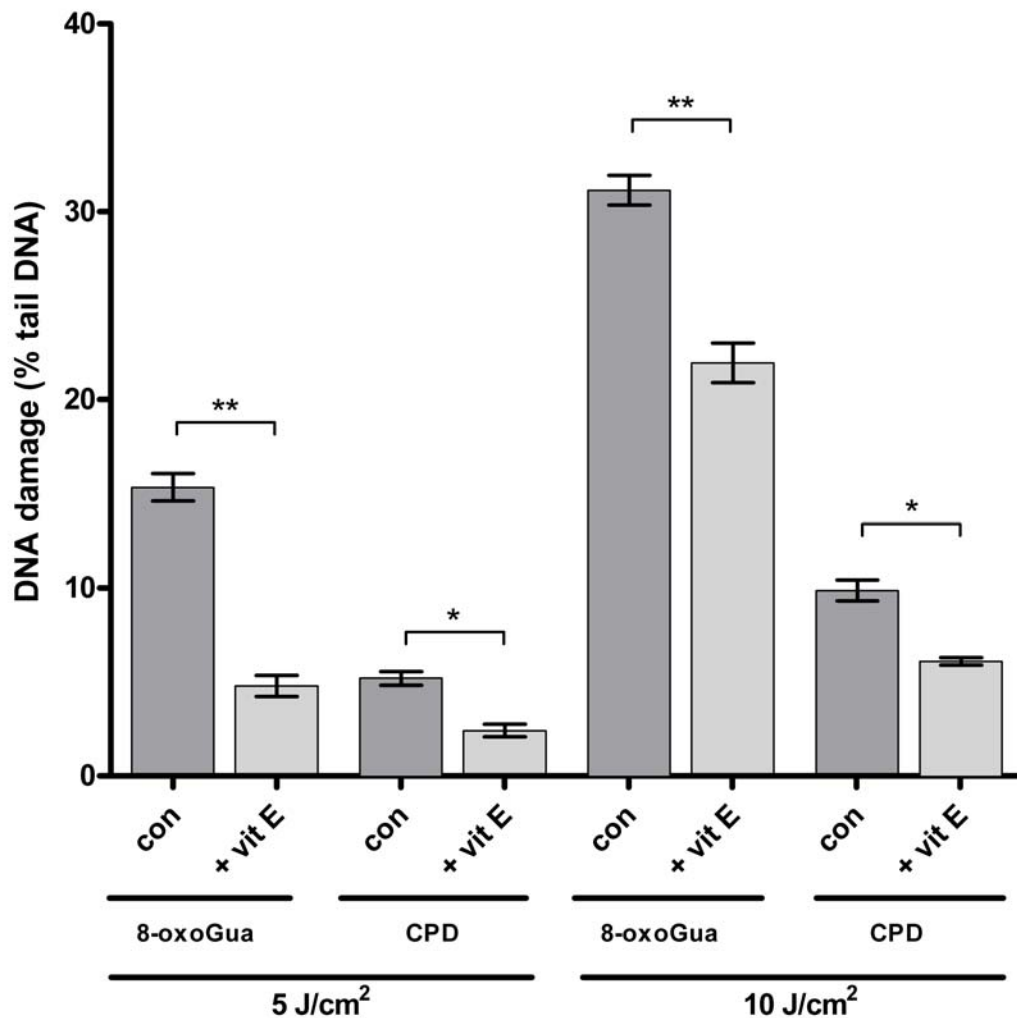


**Figure 3.10b:** Effect of post-UVR incubation with vitamin E on 8-oxoGua and CPD formation as detected by the hOGG1- and the T4endoV-modified comet assay (background corrected)

Mean percentage of tail DNA HaCaT cells exposed to UVA doses of 5 and 10 J/cm<sup>2</sup>. Background correction was performed using no enzyme values for each group. Results are the mean  $\pm$ SEM of three independent experiments; \*\*p<0.001, \*p< 0.05 for selected comparisons, based on two-way ANOVA with Bonferroni correction

### **3.4.3 Vitamin E does not protect against UVC-induced formation of CPD but does protect against the formation of 8-oxoGua and ALS/SB**

Some experiments were also performed with UVC (254 nm) because it is a potent inducer of CPD. As expected, there was a very large difference ( $p < 0.0001$ ) between non-specific damage (ALS/SB) and that observed with T4endoV (Figure 3.11a). UVC also induced the formation of 8-oxoGua. Pre-incubation with vitamin E reduced non-specific damage and 8-oxoGua levels, but had no effect on CPD formation. This was even more obvious in the background-corrected graph (Figure 3.11b).

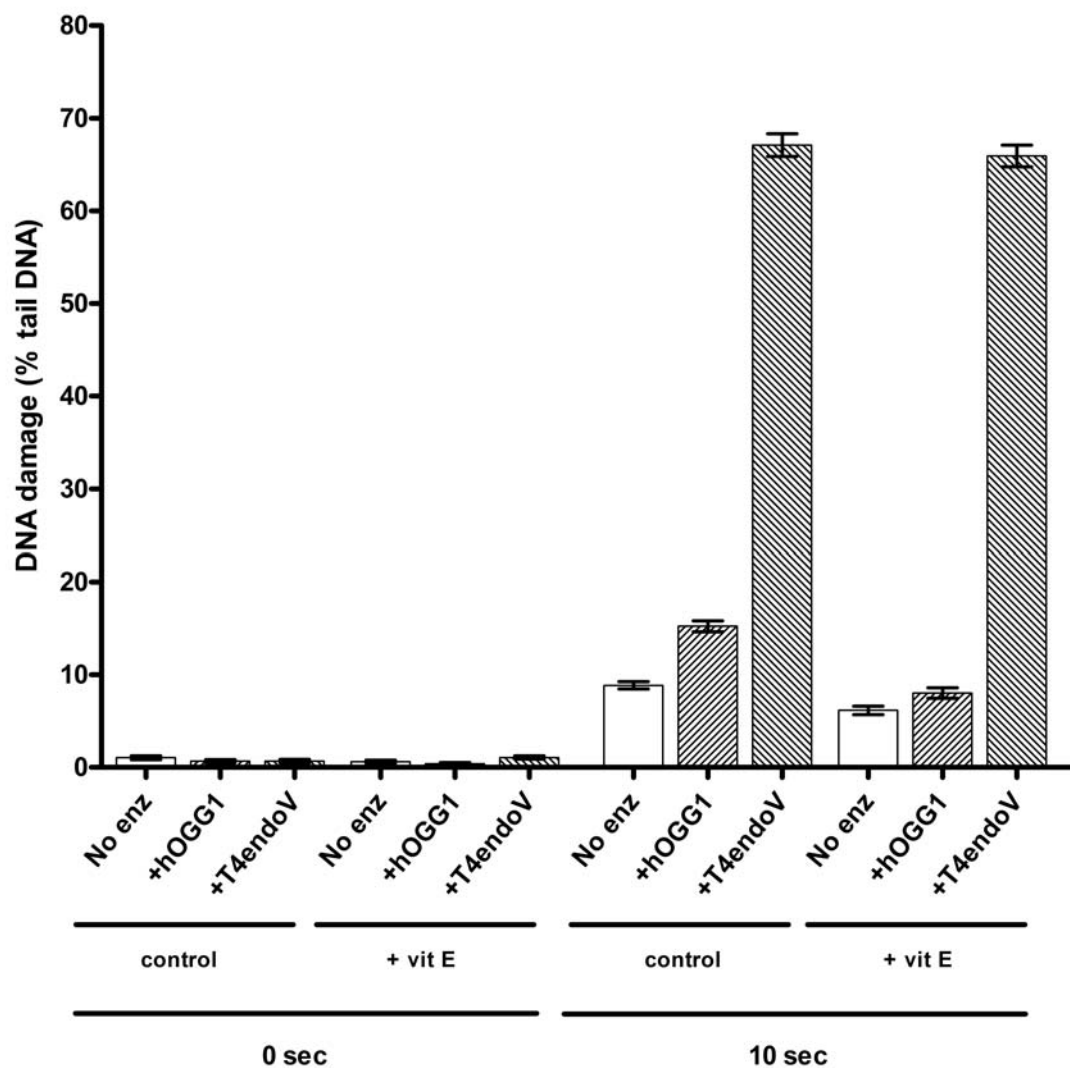


**Figure 3.11a:** Effect of pre-incubation with vitamin E on UVC-induced formation of CPD, 8-oxoGua and ALS/SB. Mean percentage of tail DNA HaCaT cells exposed to UVC for 10 sec

Results are the mean  $\pm$ SEM of three independent experiments;  $p < 0.0001$  in all cases when comparing irradiated samples to their corresponding non-irradiated samples;  $p < 0.05$  in all cases when comparing “No enz” to “+ enz” samples.

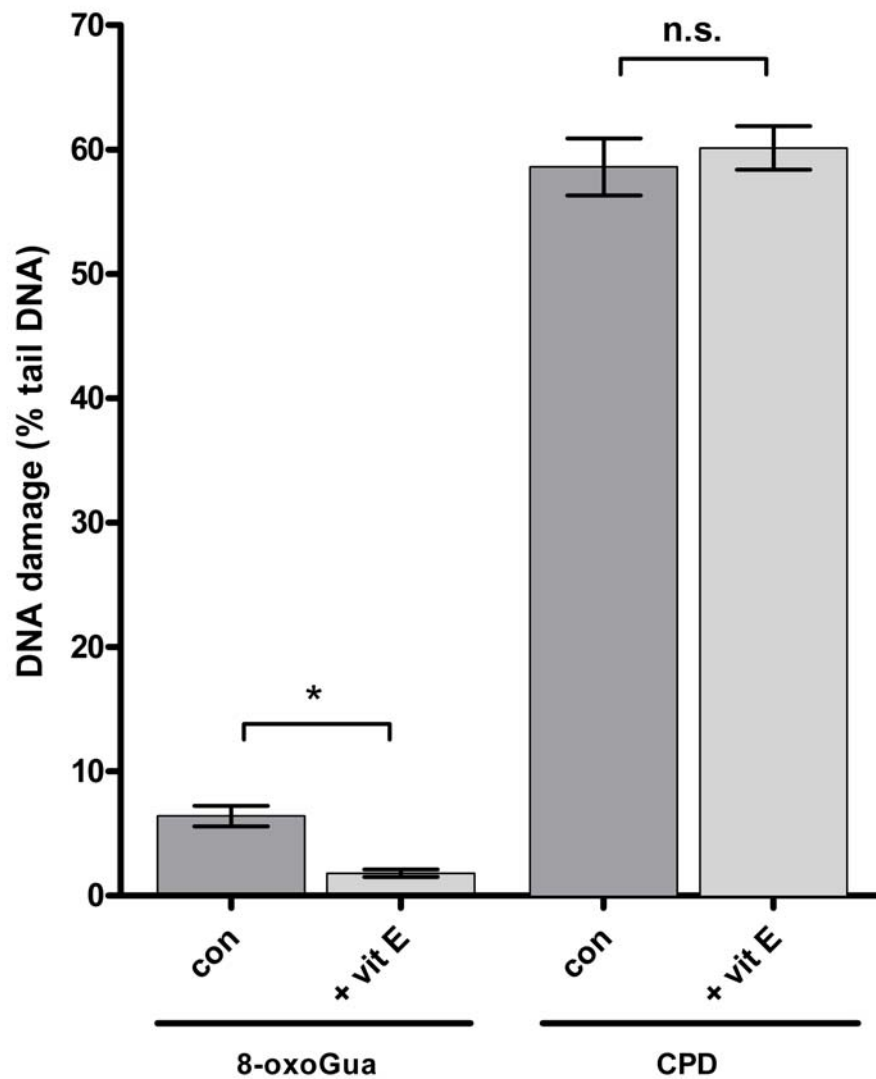


**Figure 3.11b:** Effect of pre-incubation with vitamin E on UVC-induced formation of CPD and 8-oxoGua. Mean percentage of tail DNA HaCaT cells exposed to UVC for 10 sec (background corrected)

Background correction was performed using no enzyme values for each group. Results are the mean  $\pm$ SEM of three independent experiments; \* $p < 0.05$  for selected comparisons, based on two-way ANOVA with Bonferroni correction



#### **3.4.4 Vitamin E treatment prior to UVA significantly protects against T $\diamond$ T formation**

It was decided to validate the T4endoV comet data with a different assay to measure CPD. UVB irradiation (doses ranging from 0 to 1 J/cm<sup>2</sup>) was used for the induction of CPD in order to develop the immuno-slot blot technique (Figure 3.12). This shows a dose-response with a plateau starting at 0.5 J/cm<sup>2</sup>.

Pre-UVA treatment with vitamin E reduced the formation of UVA-induced (20 J/cm<sup>2</sup>) T $\diamond$ T by 37%, as observed from the immuno-slot blot (Figure 3.13). On the other hand, post-UVA treatment did not have a significant effect. It is worth noting that CPD levels were lower in the post-UVA treatment experiment, indicating DNA repair during the 2.5 h incubation period with vitamin E (samples were kept at 37°C during post-UVA treatment with vitamin E).

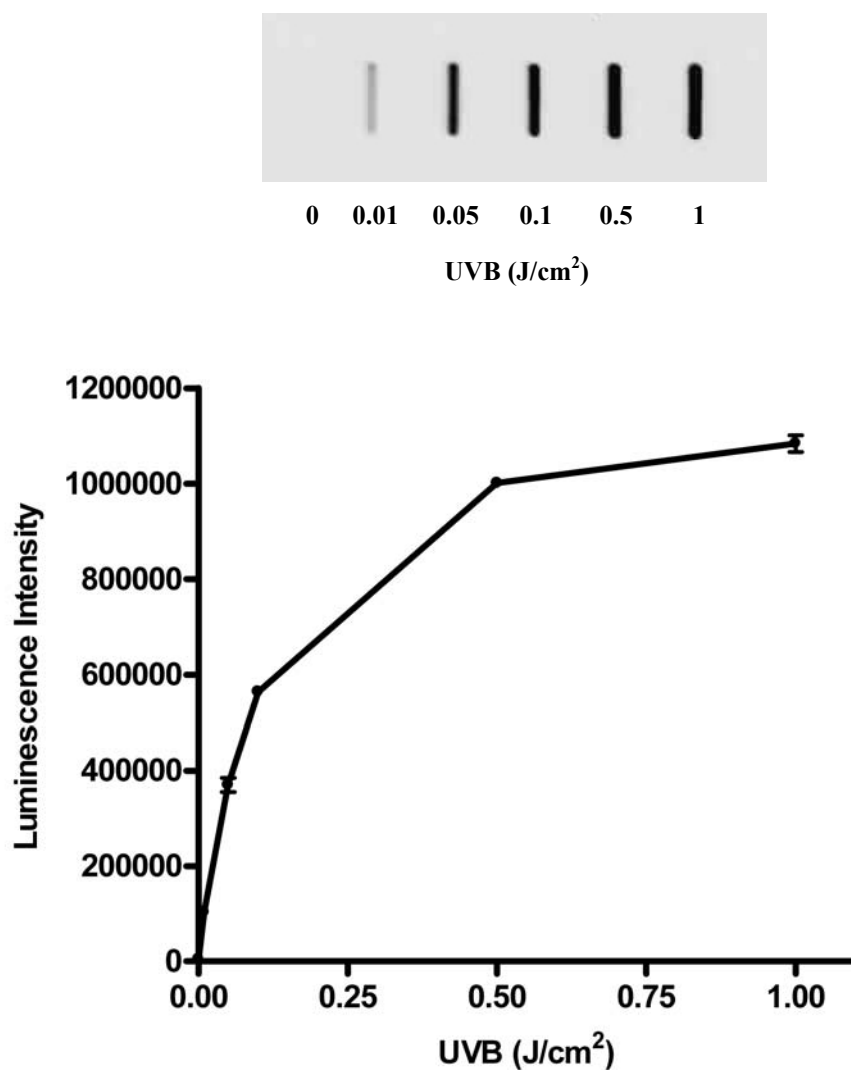


**Figure 3.12:** UVB-irradiated (0-1 J/cm<sup>2</sup>) CT-DNA was analyzed with the immuno-slot blot assay by using a T $\hookrightarrow$ T-specific mAb

See *Materials and Methods section 2.12*; Results are the mean  $\pm$ SEM of three independent experiments, with each experiment run in triplicate. Image is representative of data.

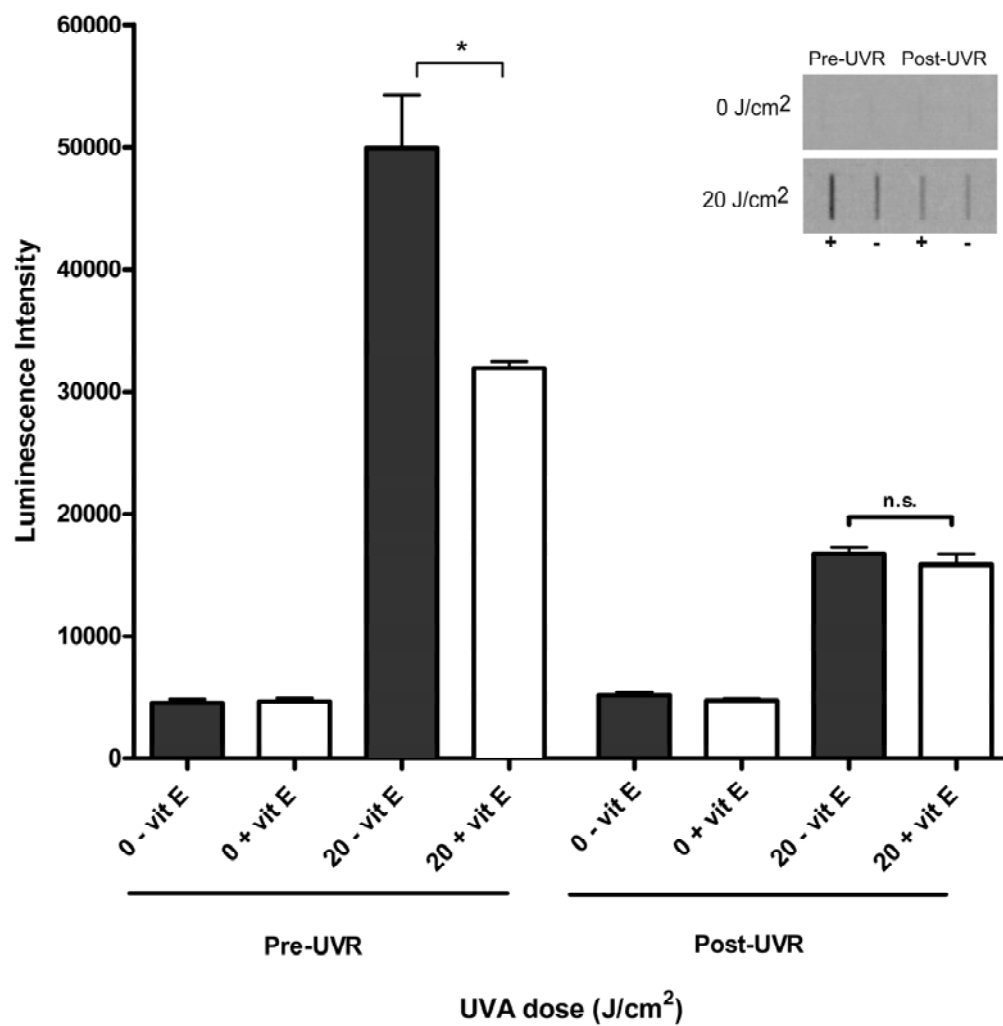


**Figure 3.13:** Genomic DNA of UVA-irradiated (20 J/cm<sup>2</sup>) HaCaT keratinocytes was analyzed with immuno-slot blot assay by using a T to T-specific mAb

Results are the mean  $\pm$ SEM of three independent experiments, with each experiment run in triplicate. Images are representative of data. \*p<0.05

#### **3.4.5 Vitamin E increases total GSH levels in HaCaT keratinocytes and protects against UVA-induced GSH depletion**

24h incubation with vit E increased total intracellular GSH levels by 2.3-fold ( $p=0.002$ ) in HaCaT keratinocytes. Furthermore, vitamin E also protected against UVA-induced depletion, maintaining GSH levels in control levels (Figure 3.14). While UVA ( $20 \text{ J/cm}^2$ ) caused a 73% decrease of GSH levels in the untreated group, the decrease observed in the vitamin E-treated group was approximately 53%. This effect has been shown in the past (Masaki et al., 2002) and along with the results presented in this study, it is clearly demonstrated that vitamin E has numerous advantages in photoprotection, which will be discussed in Chapter 4.

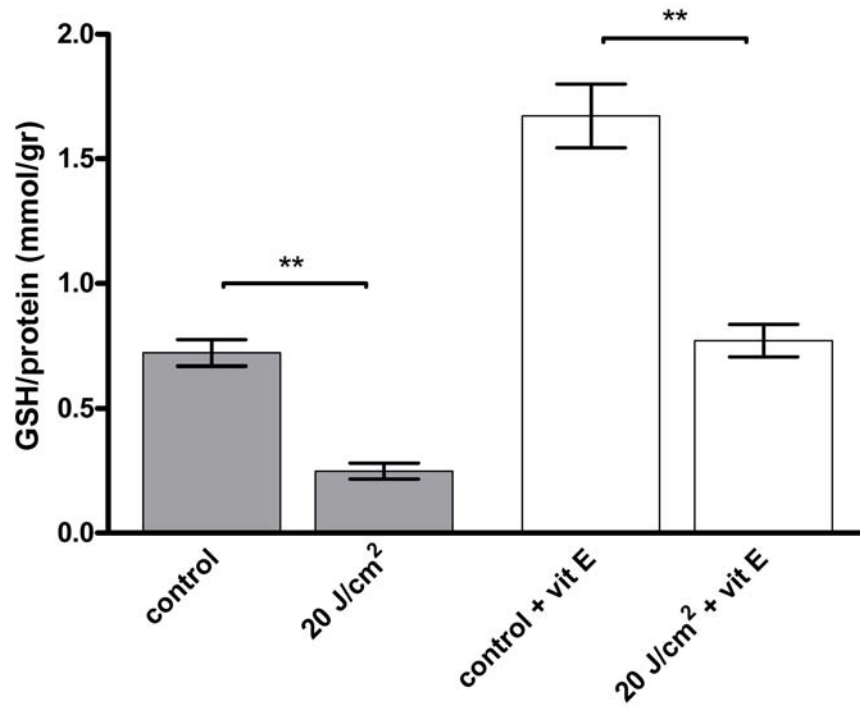


**Figure 3.14:** Effect of UVA ( $\pm$ vit E) on total GSH levels in HaCaT keratinocytes

HaCaT keratinocytes were supplemented with vit E for 24h prior to UVA irradiation.

Data are expressed as means  $\pm$ SEM of three independent experiments. \*\*p<0.01

### 3.5 Assessment of NAC in the protection against UVA-induced DNA damage

N-acetylcysteine (NAC) is a thiol with antioxidant properties. It is a cell permeable GSH pro-drug. NAC protects against oxidatively induced DNA damage and UVR-induced melanoma in mice (Cotter et al., 2007). Topical application of NAC reduces UVR-mediated depletion of GSH and H<sub>2</sub>O<sub>2</sub> in human skin (Kang et al., 2003). Additionally, NAC has been found to reduce UVR-induced tumour formation in mice (D'Agostini et al., 2005).

As shown in Figure 2.2 in *Materials and Methods*, NAC does not absorb in the UVR waveband (van den Broeke and van Henegouwen, 1995). Therefore, NAC was an ideal compound because it has no sunscreen properties, and any protective effects could only be attributed to its antioxidant properties. Incubation with NAC had no significant effect on cell viability, as shown in Table 3.4.

NAC concentration (mM)	Cell viability (%)
0*	91.9 ± 2.7
2	90.8 ± 3.3
5	90.5 ± 2.9
10	92.3 ± 2.5
20	91.1 ± 3.5

**Table 3.4:** HaCaT cell viability following incubation (4 h) with various concentrations of NAC

Cell viability was assessed by the trypan blue exclusion assay. Data represent the mean of three independent experiments ± SEM. One-way ANOVA with Bonferroni correction showed significant differences between NAC concentration increments ( $p < 0.05$  in all cases). \*Cells incubated with PBS for 4h.

### **3.5.1 NAC protects against UVA-induced ROS and GSH depletion**

Treatment with 10 mM NAC for 4 h prior to irradiation significantly protected against UVA-induced ROS formation (Figure 3.15). The effect was stronger at 20 J/cm<sup>2</sup>, where a 30% reduction of ROS levels was observed in the NAC-treated group.

Incubation with NAC also increased total intracellular GSH levels by 2.7-fold (p=0.007) in HaCaT keratinocytes. It also offered protection against UVA-induced depletion of total GSH, as observed in Figure 3.16. UVA (20 J/cm<sup>2</sup>) caused a 79% decrease of GSH levels in the untreated group, while the decrease observed in the NAC-treated group was 73%.

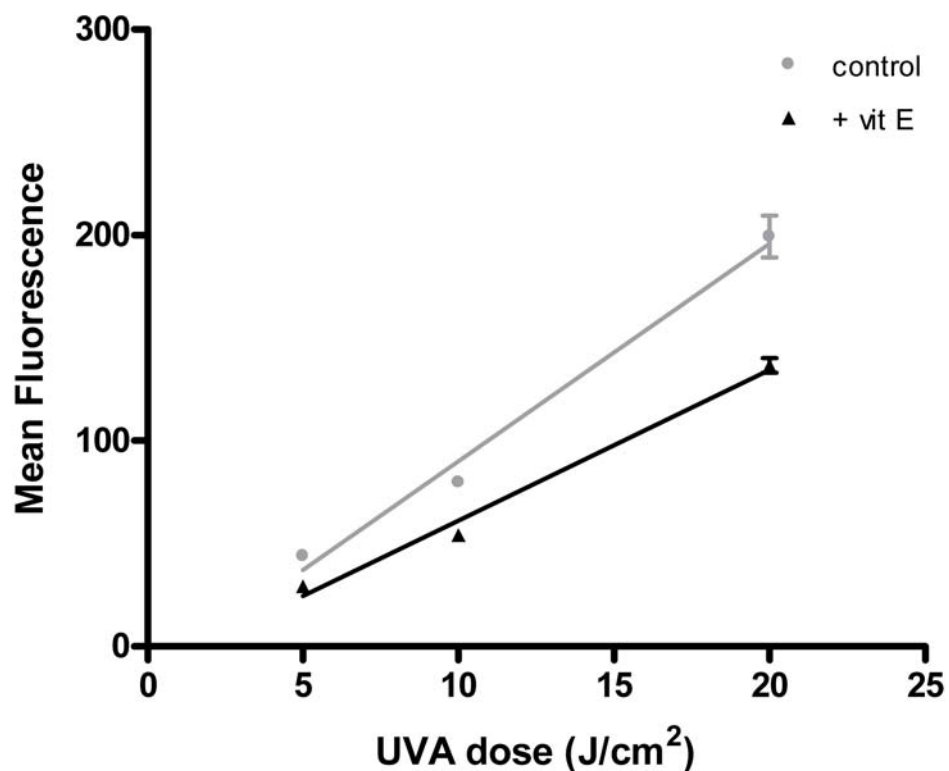


**Figure 3.15: Comparison of ROS production between control and NAC-treated groups**

Fluorescence intensity of H<sub>2</sub>DCFDA was excited at 488 nm. Results are the mean of three independent experiments  $\pm$ SEM. The UVR dose-responses were determined by linear regression analyses. The  $R^2$  values for both test conditions were  $>0.96$  and both slopes were very significantly different from zero ( $p<0.0001$ ), which demonstrates a strong dose-response. The control slope was significantly steeper than the NAC-treated slope ( $p<0.05$ ), demonstrating a clear protection, which is more marked with higher UVR doses.



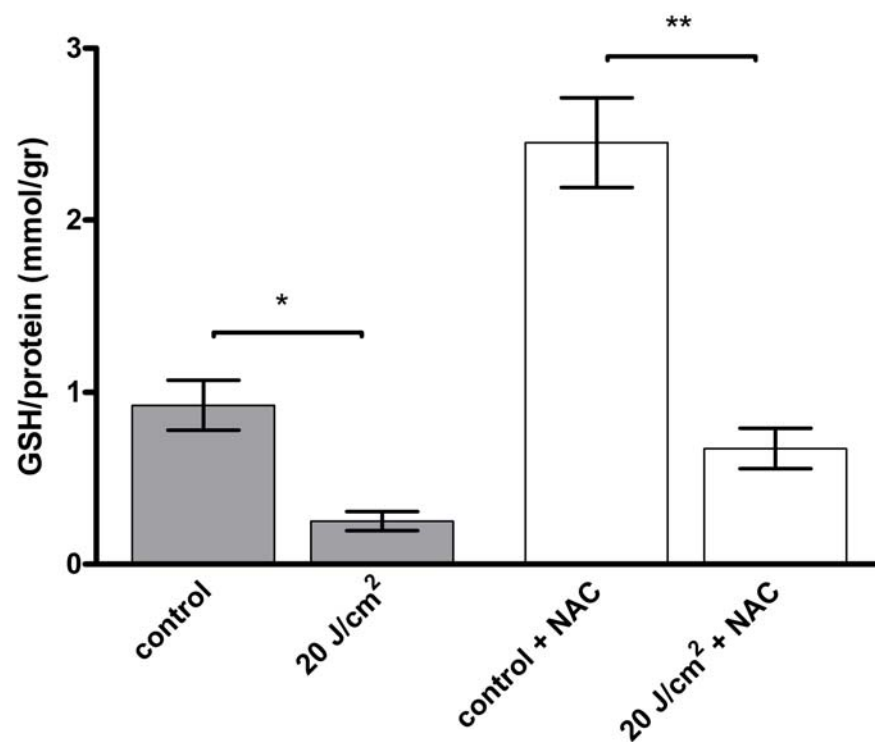


**Figure 3.16:** Effect of NAC on total GSH levels in HaCaT keratinocytes

HaCaT keratinocytes were supplemented with 20 mM NAC for 4h prior to UVA irradiation. Data are expressed as means  $\pm$ SEM of three independent experiments;

\* $p < 0.05$ ; \*\* $p < 0.01$

### **3.5.2 NAC protects against UVA-induced 8-oxoGua formation but not against CPD**

Treatment of HaCaT keratinocytes with NAC (10 mM, 4 h prior to 5 J/cm<sup>2</sup> of UVA) offered significant protection against the formation of 8-oxoGua. This effect was clear in Figure 3.17a (29% reduction). However, although a small decrease was observed in CPD levels in Figure 3.17a, background correction by the removal of the appropriate no-enzyme treatment values (measuring ALS/SB levels) showed that NAC had no effect on the formation of UVA-induced CPD (Figure 3.17b).

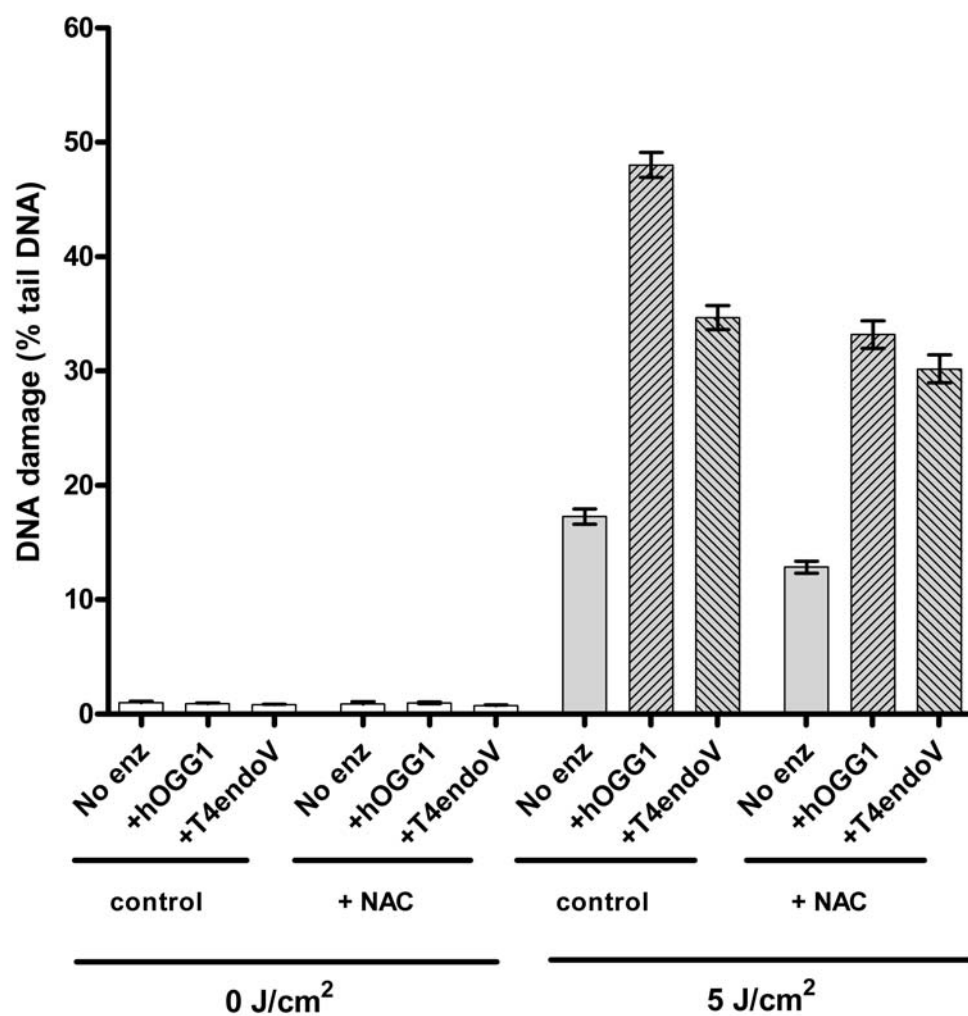


**Figure 3.17a:** Effect of pre-UVR incubation with NAC on 8-oxoGua, CPD and ALS/SB formation as detected by the hOGG1- and T4endoV-modified comet assay

The mean percentage of tail DNA in HaCaT cells exposed to UVA (5 J/cm²). Results are the mean  $\pm$ SEM of three independent experiments;  $p < 0.0001$  in all cases when comparing irradiated samples to their corresponding non-irradiated samples;  $p < 0.0001$  in all cases when comparing “No enz” to “+ enz” samples.

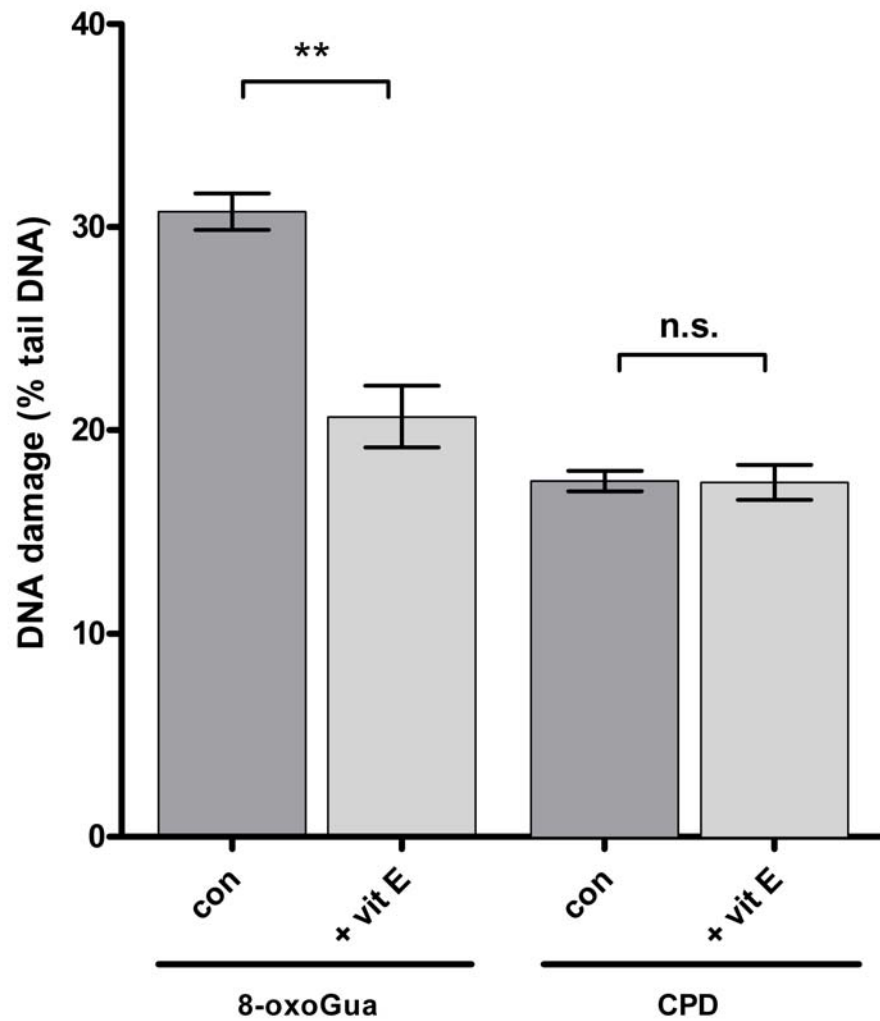


**Figure 3.17b: Effect of pre-UVR incubation with NAC on 8-oxoGua and CPD levels (background corrected)**

The mean percentage of tail DNA in HaCaT cells exposed to UVA (5 J/cm<sup>2</sup>). Background correction was performed using no enzyme values for each group. Results are the mean  $\pm$ SEM of three independent experiments; \*\*p<0.001 for the selected comparison, based on two-way ANOVA with Bonferroni correction

### **3.6 Real time PCR for detection of HO-1 and MMP-12 induction by UVA**

All PCR experiments presented in this study were repeated using two different housekeeping genes, GAPDH and B2M. In all occasions results were very similar; Primarily, GAPDH was selected as the gene to which data were normalized, while some B2M data are also presented in this section to show data integrity.

Induction of HO1 by UVA irradiation was measured by quantitative real-time Taqman PCR, using specific probes for HO1 and MMP12 mRNA. HO1 was selected as an established marker of oxidative stress (Vile et al., 1994), while MMP12 was selected because it was highly upregulated by UVA in an *in vivo* microarray pilot study conducted by our group. Time-course studies showed that the highest HO1 levels were reached 3 h following UVA irradiation (Figure 3.18), while MMP12 levels reached their peak 12 h after irradiation (Figure 3.22).

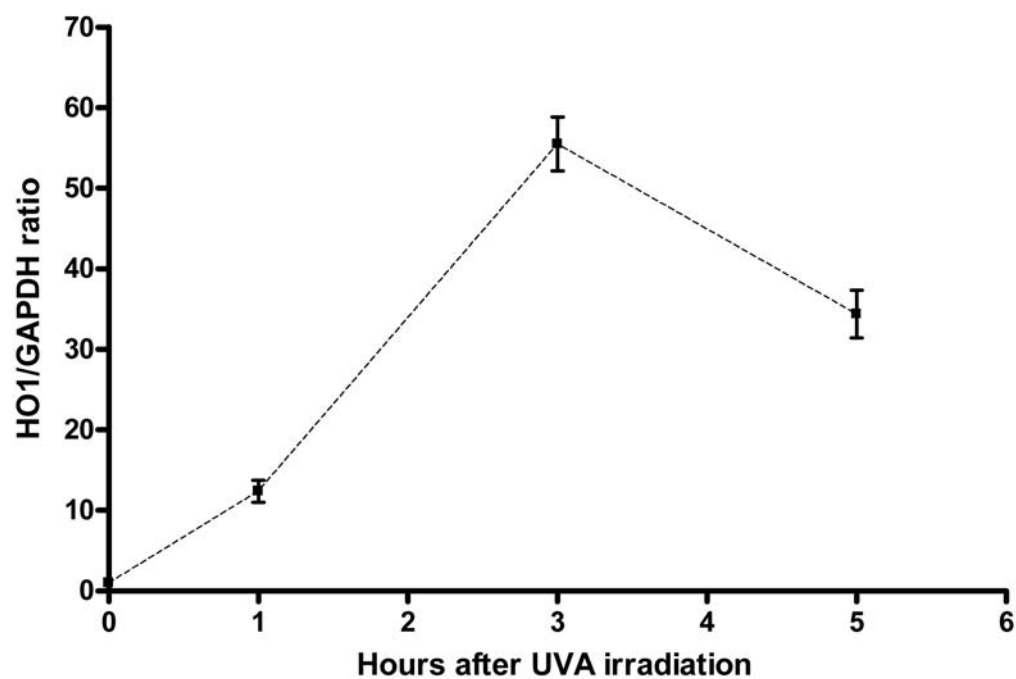


**Figure 3.18:** Time-course assay for HO1 induction following UVA irradiation (20 J/cm<sup>2</sup>)

Transcript levels were quantified in HaCaT keratinocytes. Results are expressed as the mean  $\pm$ SEM of the HO1/GAPDH ratio observed in three independent experiments, with the HO1/GAPDH ratio for the untreated sample set as the baseline value.

UVA-induced HO1 expression was similar in all cell lines used, with both housekeeping genes tested (Figures 3.19a and 3.19b). The effect of vitamin E pre-treatment in HO1 induction was assessed in HaCaT keratinocytes and the immortalised fibroblast cell line MRC5V1.

Treatment of HaCaT keratinocytes with vitamin E offered a significant protection (~28% decrease) against UVA-induced expression of HO1 (Figure 3.20). A similar, statistically significant, decrease (~13%) was also observed with MRC5V1 cells (Figure 3.21).

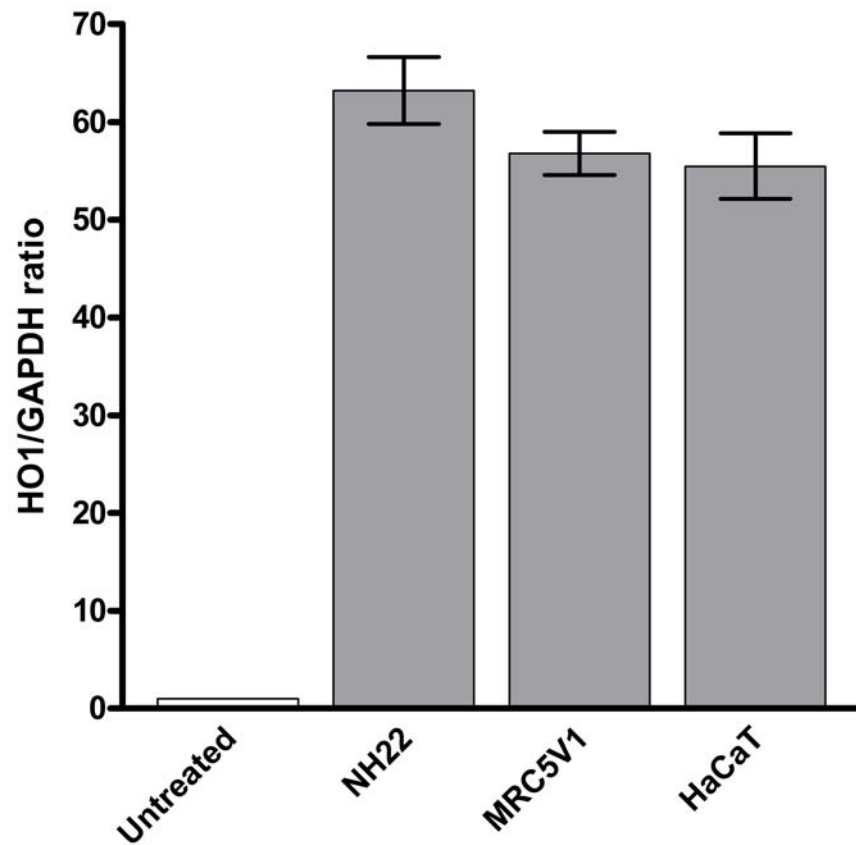


**Figure 3.19a: Real-time PCR analysis of HO1 expression in three different cell lines, 3 h after UVA irradiation**

Transcript levels were quantified using the GAPDH housekeeping gene as an endogenous control. The HO1/GAPDH ratio was set as a baseline value to which transcript levels were normalized. Results are the mean of three independent experiments  $\pm$ SEM.



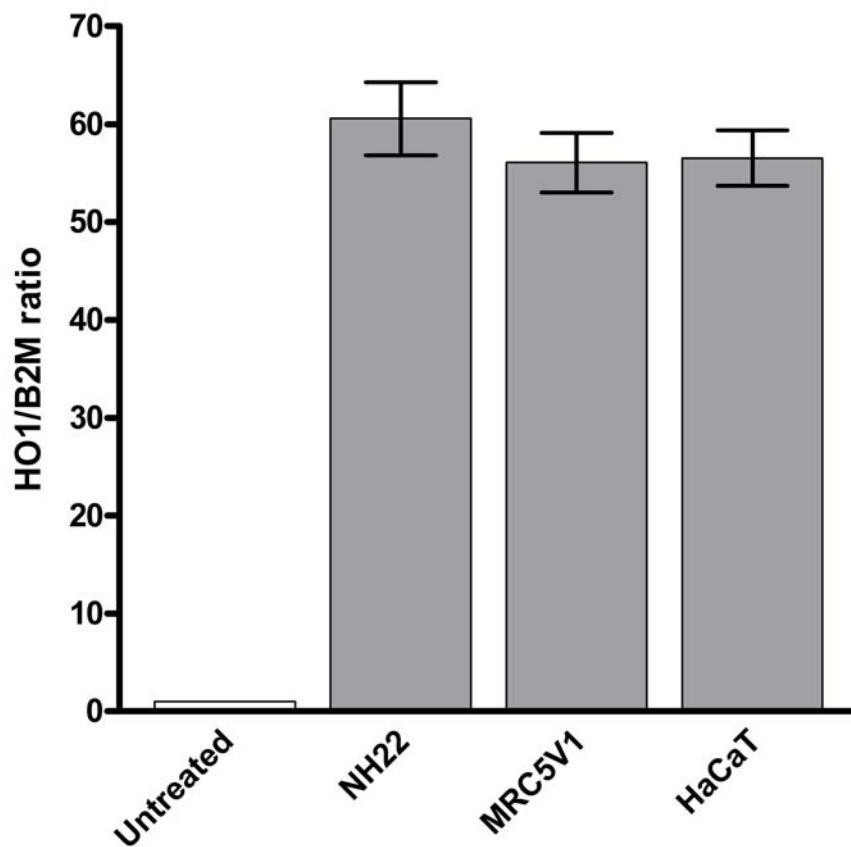


**Figure 3.19b: Real-time PCR analysis of HO1 expression in three different cell lines, 3 h after UVA irradiation**

Transcript levels were quantified using the B2M housekeeping gene as an endogenous control. The HO1/B2M ratio was set as a baseline value to which transcript levels were normalized. Results are the mean of three independent experiments  $\pm$ SEM.

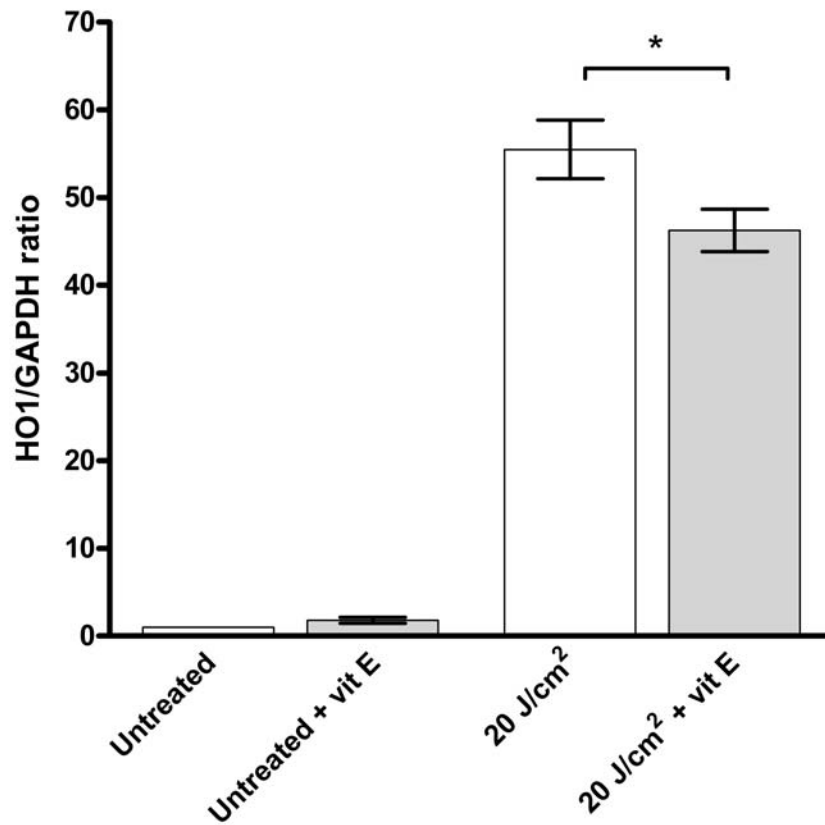


**Figure 3.20: Real-time PCR analysis HO1 expression in HaCaT keratinocytes ( $\pm$  vit E pretreatment) 3 h after UVA irradiation**

Transcript levels were quantified using the GAPDH housekeeping gene as an endogenous control. The HO1/GAPDH ratio was set as a baseline value to which transcript levels were normalized. Results are the mean of three independent experiments  $\pm$ SEM; \* $p$ <0.05

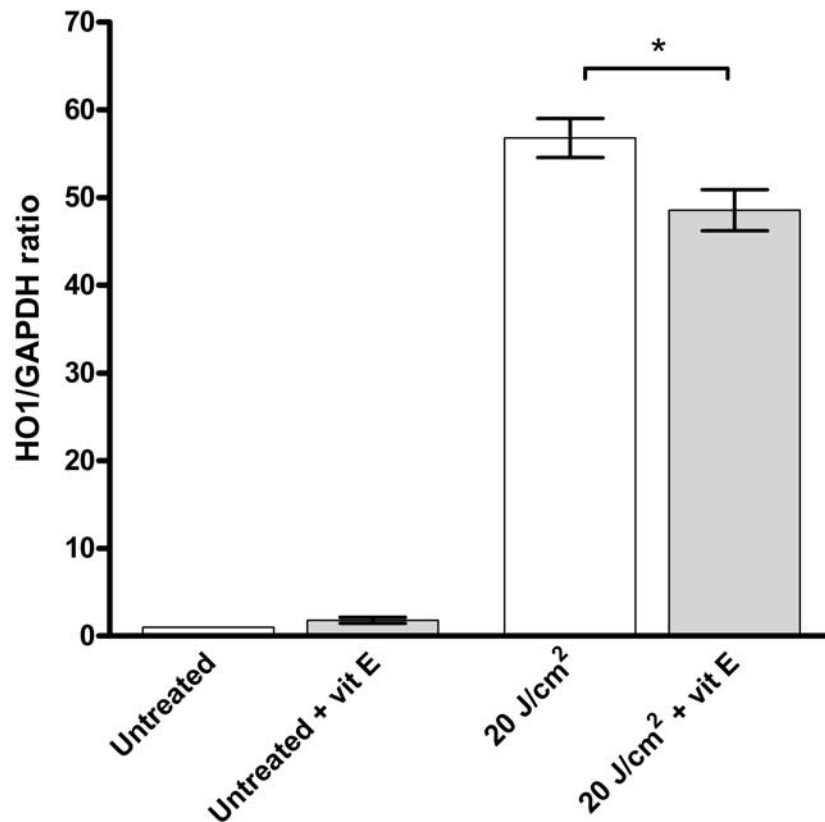


**Figure 3.21: Real-time PCR analysis of HO1 expression in MRC5V1 fibroblasts ( $\pm$  vit E pretreatment), 3 h after UVA irradiation**

Transcript levels were quantified using the GAPDH housekeeping gene as an endogenous control. The HO1/GAPDH ratio was set as a baseline value to which transcript levels were normalized. Results are the mean of three independent experiments  $\pm$ SEM. \* $p < 0.05$

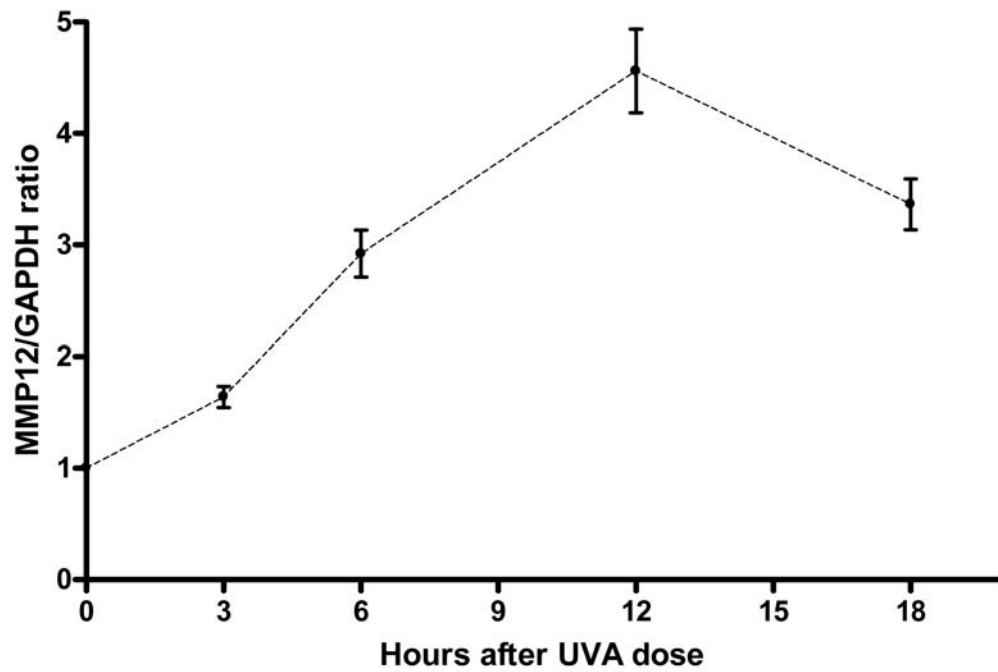


**Figure 3.22: Time-course assay for MMP12 induction following UVA irradiation (20 J/cm<sup>2</sup>)**

Transcript levels were quantified in HaCaT keratinocytes. Results are expressed as the mean  $\pm$ SEM of the MMP12/GAPDH ratio observed in three independent experiments, with the MMP12/GAPDH ratio for the untreated sample set as the baseline value.

UVA-induced MMP12 expression was similar in all cell lines used, with both housekeeping genes tested (Figures 3.23a and 3.23b). Vitamin E pre-treatment had no significant effect in UVA-induced MMP12 expression in HaCaT keratinocytes and MRC5V1 fibroblasts as seen in Figures 3.24 and 3.25, respectively (small reduction in both cases, but not statistically significant).

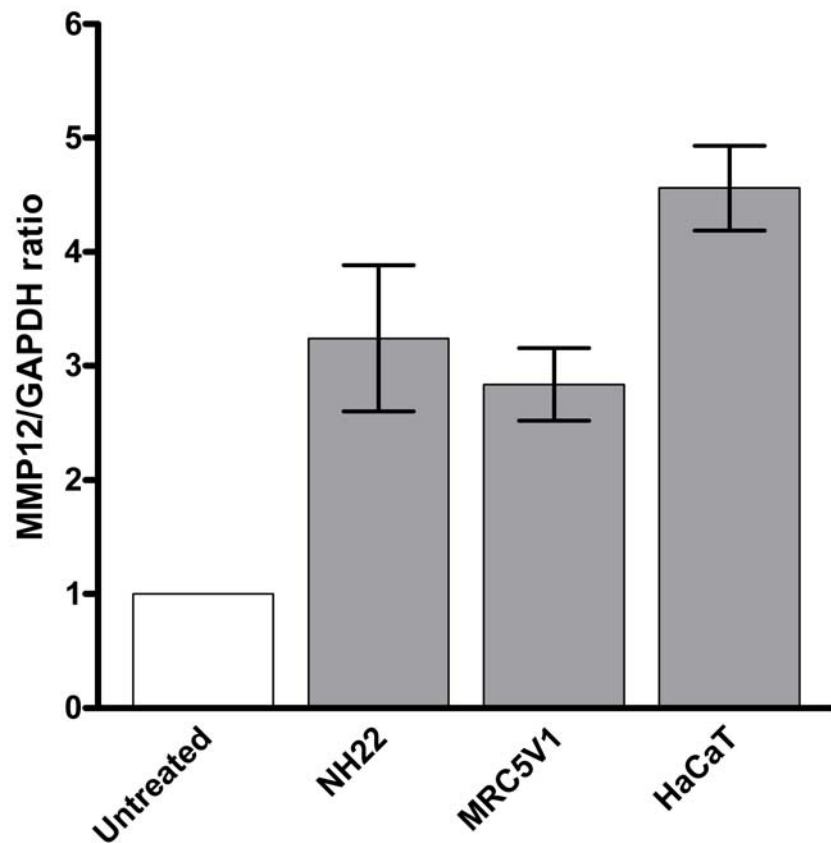


**Figure 3.23a:** Real-time PCR analysis of MMP12 expression in three different cell lines, 12 h after UVA irradiation (20J/cm<sup>2</sup>)

Transcript levels were quantified using the GAPDH housekeeping gene as an endogenous control. The MMP12/GAPDH ratio was set as a baseline value to which transcript levels were normalized. Results are the mean of three independent experiments  $\pm$ SEM. Expression of MMP12 in HaCaT keratinocytes was significantly higher than NH22 and MRC5V1 fibroblasts ( $p < 0.05$ ).

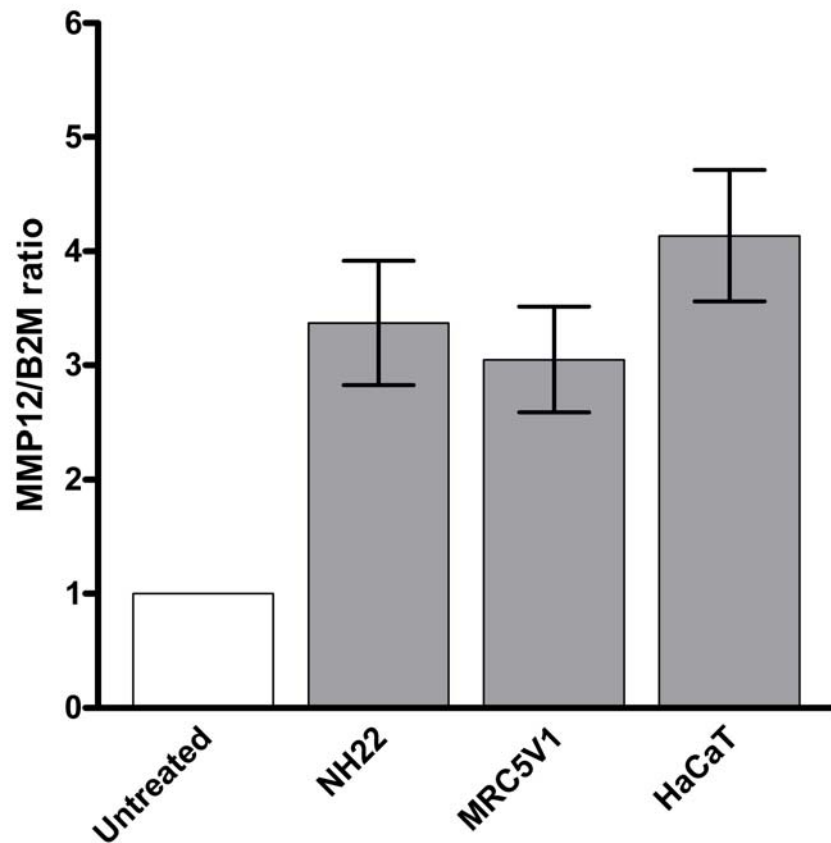


**Figure 3.23b: Real-time PCR analysis of MMP12 expression in three different cell lines, 12 h after UVA irradiation (20J/cm<sup>2</sup>)**

Transcript levels were quantified using the B2M housekeeping gene as an endogenous control. The MMP12/B2M ratio was set as a baseline value to which transcript levels were normalized. Results are the mean of three independent experiments  $\pm$ SEM. Expression of MMP12 in HaCaT keratinocytes was significantly higher than MRC5V1 fibroblasts ( $p < 0.05$ ).

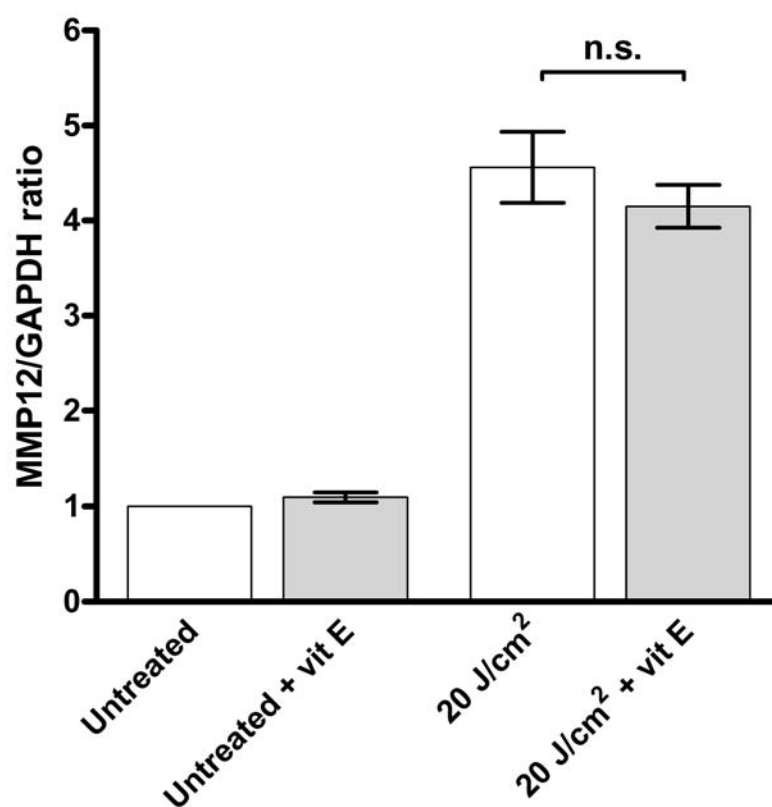


**Figure 3.24:** Real-time PCR analysis of MMP12 expression in HaCaT keratinocytes ( $\pm$  vit E pretreatment) 12 h after UVA irradiation

Transcript levels were quantified in HaCaT keratinocytes. Results are expressed as the mean  $\pm$ SEM of the MMP12/GAPDH ratio observed in three independent experiments, with the MMP12/GAPDH ratio for the untreated sample set as the baseline value.



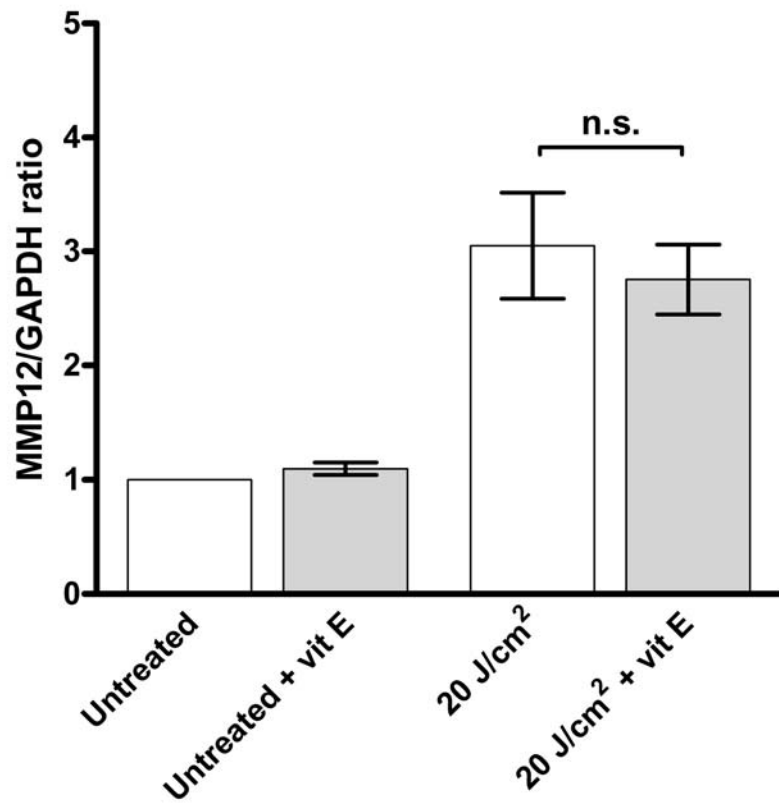


**Figure 3.25:** Real-time PCR analysis of MMP12 expression in MRC5V1 fibroblasts, 12 h after UVA irradiation

Transcript levels were quantified using the GAPDH housekeeping gene as an endogenous control. The MMP12/GAPDH ratio was set as a baseline value to which transcript levels were normalized. Results are the mean of three independent experiments  $\pm$ SEM.

### 3.6.1 *In vivo* study for the UVA1-induced expression of HO1 and MMP12

HO1 and MMP12 data obtained in the study above were subsequently compared with results obtained in an *in vivo* study conducted by my colleague, Dr Angela Tewari. The UVA1 source used for the irradiation of previously unexposed buttock skin of five volunteers (skin types 1 and 2; age: 18-40) was a Sellamed 3000 Dr Sellmeier (Sellas, Gevelsberg, Germany).

In contrast with the *in vitro* results on UVA-induced expression of HO1, the *in vivo* study conducted by Dr Tewari showed almost no upregulation of HO1 (Figure 3.26). The only significant increase (about 1.8-fold) observed was with a dose of 50 J/cm<sup>2</sup>, 6 h after UVA1 irradiation, which was still extremely low compared to the approximately 55-fold increase found *in vitro*.

On the other hand, MMP12 was significantly upregulated *in vivo* with a dose of 50 J/cm<sup>2</sup>, both 6 and 24 h after irradiation (Figure 3.27; 13-fold and 30-fold increase, respectively). At 6 h after UVA *in vitro* only a 3-fold increase was observed (Figure 3.22), which shows a significant difference between UVA-induced MMP12 expression *in vitro* and *in vivo*.

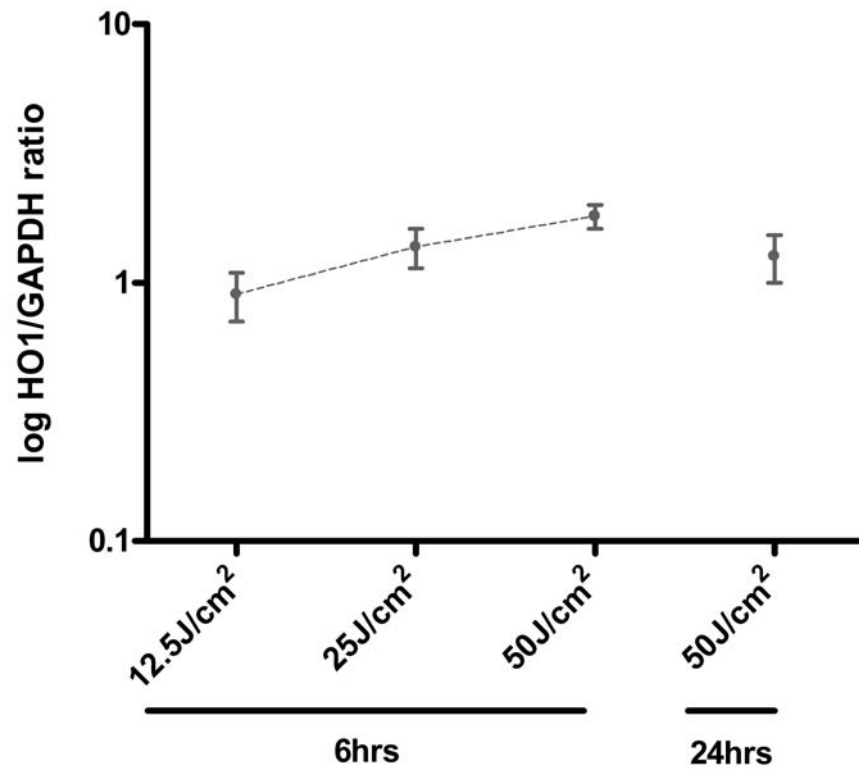


**Figure 3.26:** Real-time PCR analysis of HO1 expression *in vivo*, 6 and 24 h following UVAI irradiation (relevant to untreated)

Transcript levels were quantified using the GAPDH housekeeping gene as an endogenous control. The HO1/GAPDH ratio was set as a baseline value to which transcript levels were normalized. Results are the mean expression levels of 5 volunteers  $\pm$ SEM.

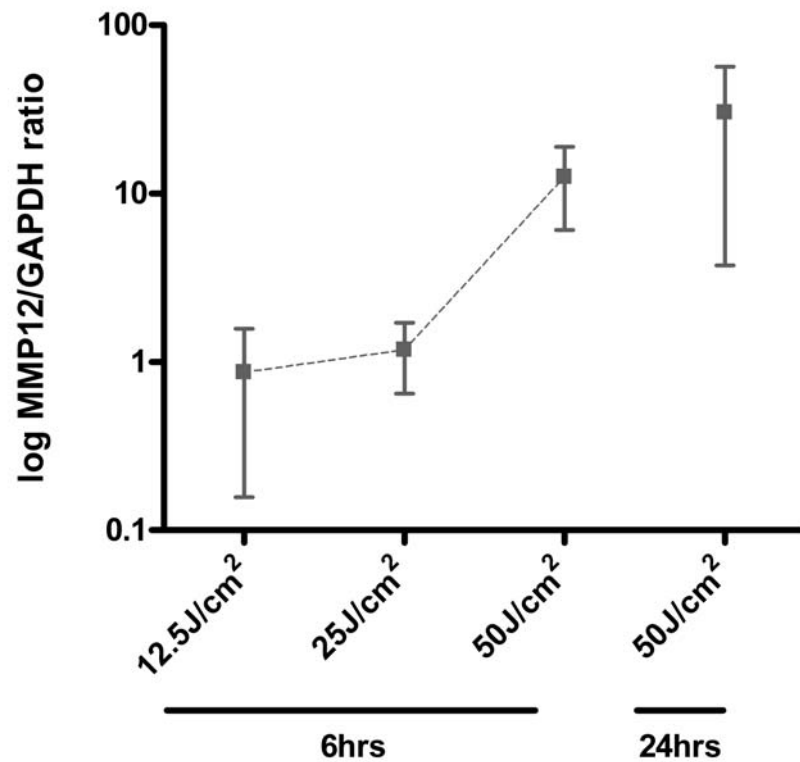


**Figure 3.27: Real-time PCR analysis of MMP12 expression *in vivo*, 6 and 24 h following UVAI irradiation (relevant to untreated)**

Transcript levels were quantified using the GAPDH housekeeping gene as an endogenous control. The MMP12/GAPDH ratio was set as a baseline value to which transcript levels were normalized. Results are the mean expression levels of 5 volunteers  $\pm$ SEM.

### **3.7 ROS pathways inhibitors study**

In order to have a better understanding about the induction of 8-oxoGua and CPD following UVA irradiation, a mechanistic study was carried out, employing two inhibitors of ROS-producing enzymes. The compounds used were rotenone, a specific inhibitor of the mitochondrial respiratory chain complex I, and DPI, an inhibitor of NADPH oxidase. Therefore, targeting specific pathways of interest, an insight on the mechanisms by which UVA induces the formation of free radicals could be gained.

Tables 3.5 and 3.6 present the effect of various concentrations (based on published literature) of the two inhibitors used on HaCaT cell viability.

After UVA irradiation, the production of ROS was measured by FACS analysis and presented in Figure 3.28. Rotenone incubation (10  $\mu$ M for 30 min) resulted in an elevation of intracellular ROS by 1.7-fold, indicating that the mitochondrial respiratory chain complex I plays a role in UVA-induced ROS formation. Pretreatment with DPI (10  $\mu$ M for 30 min) significantly reduced ROS production (more than 2-fold), also suggesting a role of NADPH oxidase in UVA-induced oxidative stress.

<b>Rotenone concentration (μM)</b>	<b>Cell viability (%)</b>
0	92.5 ± 3.1
10	79.4 ± 4.2
50	71.8 ± 2.3
100	65.2 ± 3.8
200	60.5 ± 2.6

**Table 3.5: HaCaT cell viability following incubation (2 h) with various concentrations of rotenone**

Cell viability was assessed by the MTT assay. Data represent the mean of three independent experiments ± SEM. One-way ANOVA with Bonferroni correction showed significant differences between increasing rotenone concentrations ( $p < 0.05$  in all cases).

<b>DPI concentration (μM)</b>	<b>Cell viability (%)</b>
0	93.2 ± 2.8
5	91.7 ± 3.3
10	92.8 ± 2.7
20	89.7 ± 3.9

**Table 3.6: HaCaT cell viability following incubation (2 h) with various concentrations of DPI**

Cell viability was assessed by the MTT assay. Data represent the mean of three independent experiments ± SEM. One-way ANOVA with Bonferroni correction showed no significant differences between increasing doses ( $p > 0.05$  in all cases).

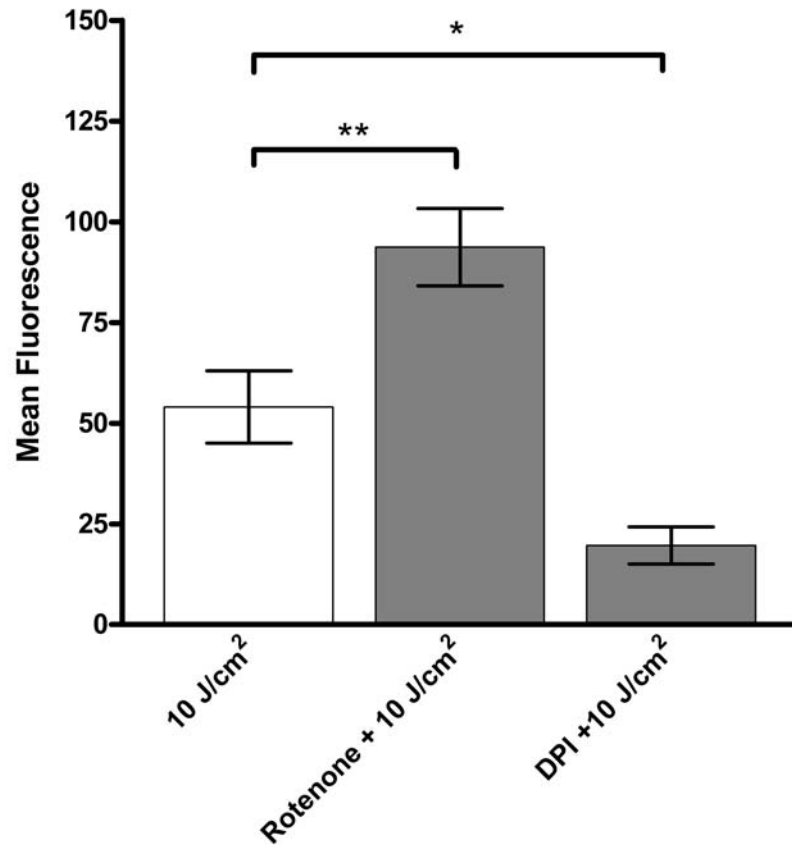


**Figure 3.28: Effect of rotenone and DPI in intracellular UVA-induced ROS production**

Fluorescence intensity of H<sub>2</sub>DCFDA was excited at 488 nm. Results are the mean of three independent experiments  $\pm$ SEM (values for endogenous ROS, *i.e.* cells not exposed to UVR, for both with and without inhibitors were subtracted from treatment values); \* $p < 0.05$ , \*\* $p < 0.001$

Pre-treatment of cells with rotenone (100  $\mu$ M for 30 min; Figure 3.29) significantly (2-fold,  $p < 0.0001$ ) increased the UVA-induced DNA damage as measured by the alkaline comet assay (“no enz” groups). Rotenone also caused a significant upregulation (1.6-fold,  $p < 0.0001$ ) of 8-oxoGua levels as measured by the hOGG1-specific comet assay, compared to the untreated group (control). Interestingly, a small but significant ( $p = 0.01$ ), increase was also observed in CPD formation in the + rotenone group, measured by the T4endoV-specific comet assay.

DPI pre-treatment (10  $\mu$ M for 30 min, Figure 3.30) significantly (approximately 1.9-fold,  $p = 0.006$ ) reduced the UVA-induced DNA damage as measured by the alkaline comet assay (“no enz” groups). DPI significantly reduced 8-oxoGua levels (approximately 1.2-fold,  $p = 0.04$ ), compared to the untreated group (control). Furthermore, a small decrease was observed in CPD formation, but this effect did not reach a significant level.

The background-corrected versions for these experiments are presented in Figure 3.31.



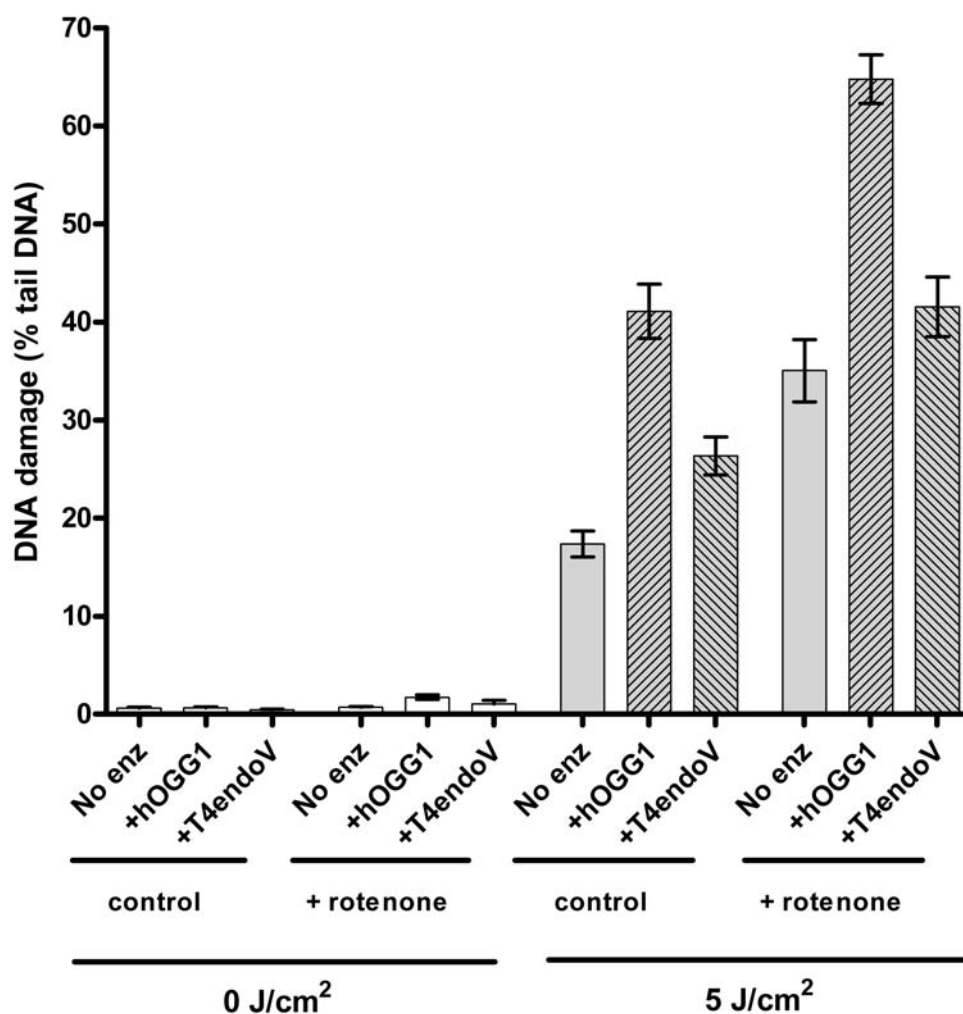


**Figure 3.29:** Effect of rotenone on UVA-induced DNA damage detected by the T4endoV- and hOGG1-modified comet assay

The mean percentage of tail DNA in HaCaT cells exposed to UVA (5 J/cm<sup>2</sup>). Results are the mean  $\pm$ SEM of three independent experiments;  $p < 0.0001$  in all cases when comparing irradiated samples to their corresponding non-irradiated samples;  $p < 0.05$  in all cases when comparing “No enz” to “+ enz” samples, with the exception of the “+ rotenone” irradiated group, where the difference between “No enz” and “+T4endoV” was not significant.

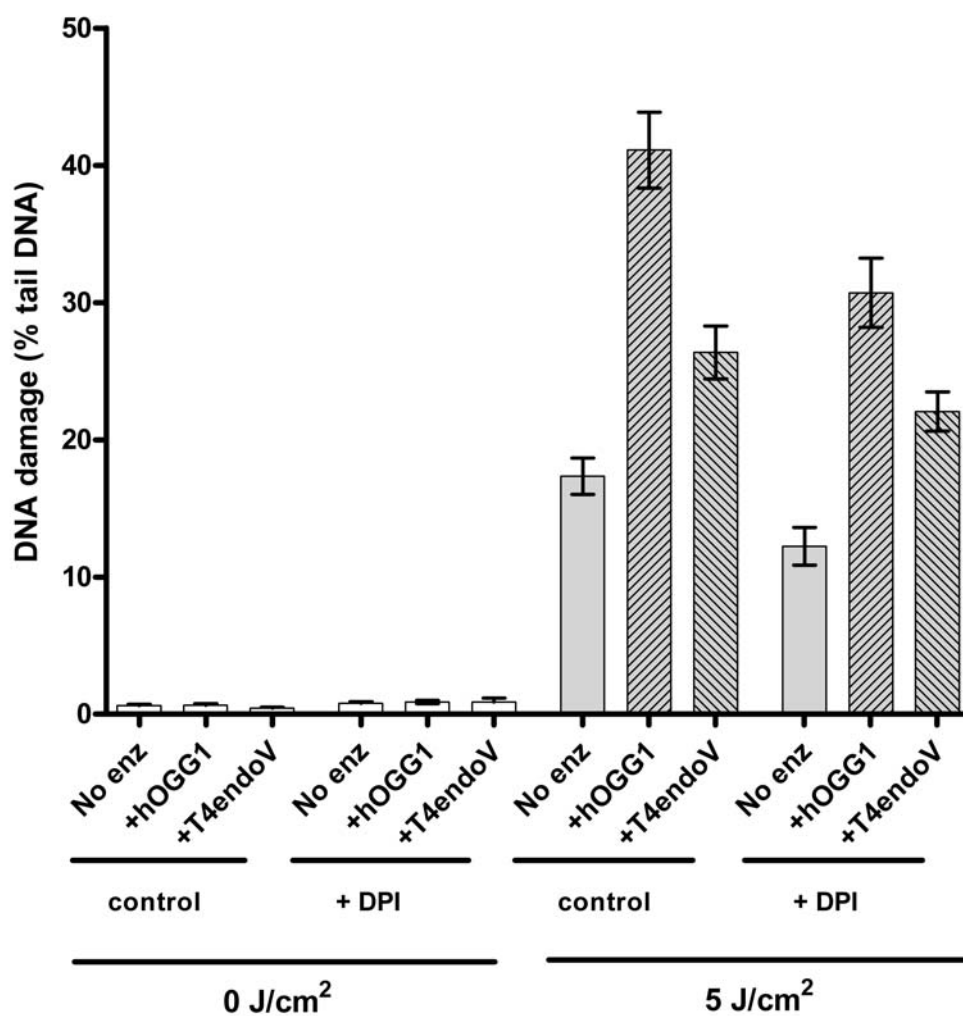


**Figure 3.30:** Effect of DPI on UVA-induced DNA damage detected by T4endoV- and hOGG1-modified comet assay

The mean percentage of tail DNA in HaCaT cells exposed to UVA (5 J/cm<sup>2</sup>). Results are the mean  $\pm$ SEM of three independent experiments;  $p < 0.0001$  in all cases when comparing irradiated samples to their corresponding non-irradiated samples.

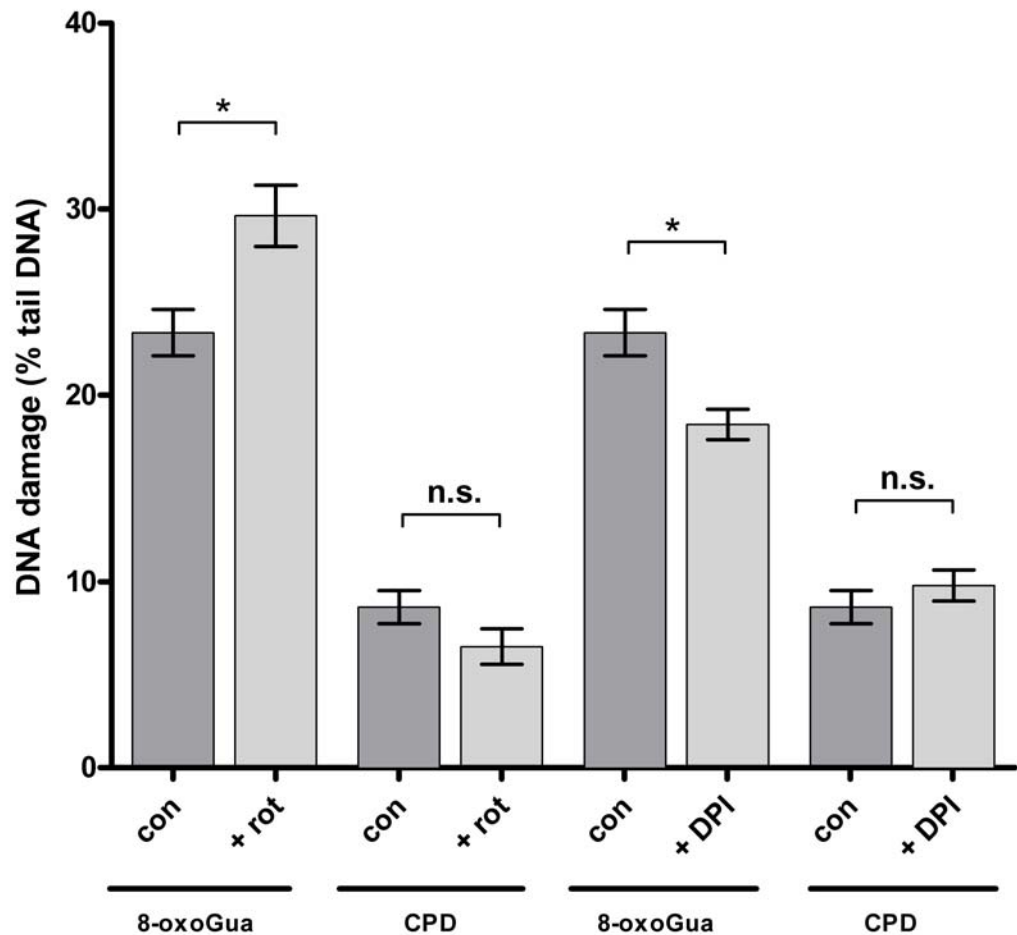


**Figure 3.31:** Effect of pre-incubation with rotenone (rot) and DPI on UVA-induced DNA damage detected by the T4endoV- and hOGG1-modified comet assay (background corrected)

The mean percentage of tail DNA in HaCaT cells exposed to UVA (5 J/cm<sup>2</sup>). Background correction was performed using no enzyme values for each group. Results are the mean  $\pm$ SEM of three independent experiments; \* $p$ <0.05 for selected comparisons, based on two-way ANOVA with Bonferroni correction

### 3.8 Stiefel compounds testing against UVA-induced DNA damage and oxidative stress

The compounds supplied by Stiefel laboratories for screening for antioxidant properties were initially tested for their effect on cell viability on HaCaT keratinocytes (Table 3.7). Based on suggestions by Stiefel, the compounds were tested at concentrations ranging from 5 to 80  $\mu$ M. It should be noted at this point that going for concentrations higher than 80  $\mu$ M, was extremely difficult due to the high viscosity of the compounds, especially lanosterol.

Compound/Concentration	0 $\mu$ M*	5 $\mu$ M	10 $\mu$ M	20 $\mu$ M	40 $\mu$ M	80 $\mu$ M
<b>Lanosterol</b>	92.1 $\pm$ 3.3	91.6 $\pm$ 3.6	92.3 $\pm$ 4.2	90.5 $\pm$ 3.9	87.5 $\pm$ 3.9	83.7 $\pm$ 4.3
<b>Guggulsterone</b>	89.7 $\pm$ 4.3	86.4 $\pm$ 3.7	87.4 $\pm$ 3.4	86.2 $\pm$ 4.5	82.3 $\pm$ 3.8	79.4 $\pm$ 4.2
<b>Farnesol</b>	90.8 $\pm$ 3.9	66.8 $\pm$ 5.5	60.2 $\pm$ 6.3	50.1 $\pm$ 4.8	35.8 $\pm$ 6.3	23.8 $\pm$ 5.2

**Table 3.7: HaCaT cell viability following incubation with various concentrations of the Stiefel compounds**

Cell viability was assessed by the MTT assay. Data represent the mean of three independent experiments  $\pm$  SEM. \*Cells were incubated with the appropriate dilutant for each compound (EtOH for lanosterol, DMSO for guggulsterone and ddH<sub>2</sub>O for farnesol). One-way ANOVA with Bonferroni correction showed no significant differences between lanosterol and guggulsterone concentration increments ( $p > 0.05$  in all cases), but significant differences between farnesol concentration increments ( $p < 0.05$  in all cases).

Farnesol was found to be toxic to HaCaT keratinocytes in a dose dependent manner, even at the lowest suggested dose (similar toxicity was observed in other cell lines as well) therefore it was dropped from the study. Following a series of investigations using various concentrations of lanosterol and guggulsterone, their effect on UVA-induced ROS production is presented in Figures 3.32 and 3.33, respectively. Treatment with lanosterol (for 24 h prior to UVA irradiation) reduced ROS production (approximately 2-fold), an effect that was highly significant at a concentration of 10  $\mu$ M. Guggulsterone treatment (for 24 h prior to UVA irradiation) on the other hand had no effect against UVA-induced ROS formation.

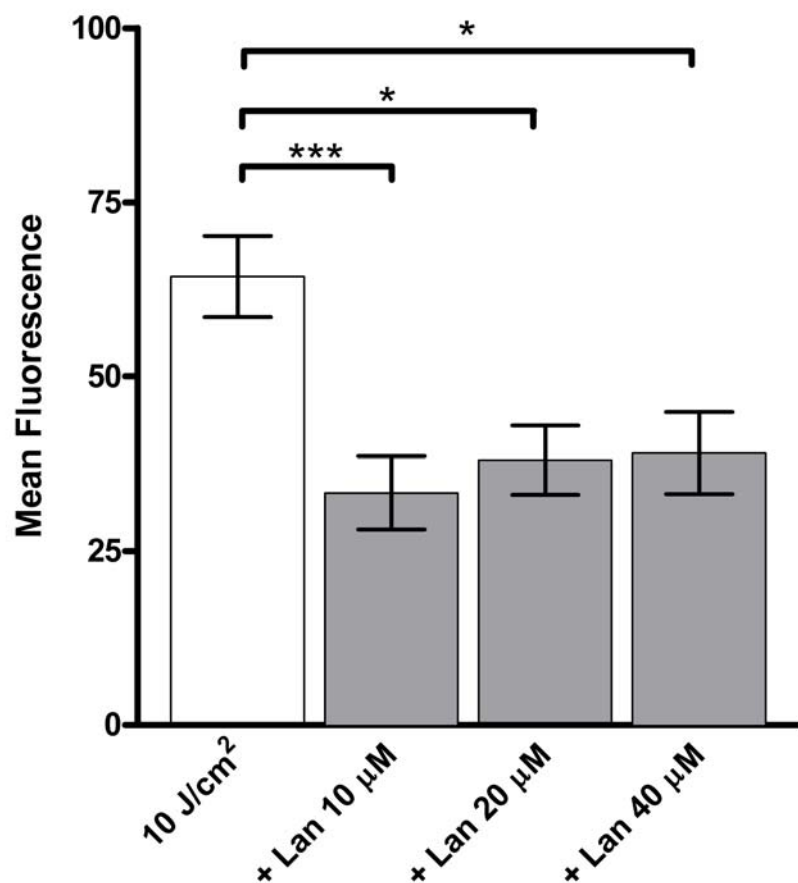


**Figure 3.32:** Effect of lanosterol (10, 20 and 40 µM) in intracellular UVA-induced ROS production

Fluorescence intensity of H<sub>2</sub>DCFDA was excited at 488 nm. Results are the mean of three independent experiments ±SEM (values for endogenous ROS, *i.e.* cells not exposed to UVR, for both with and without compound were subtracted from treatment values); \**p*<0.05, \*\*\**p*< 0.0001.

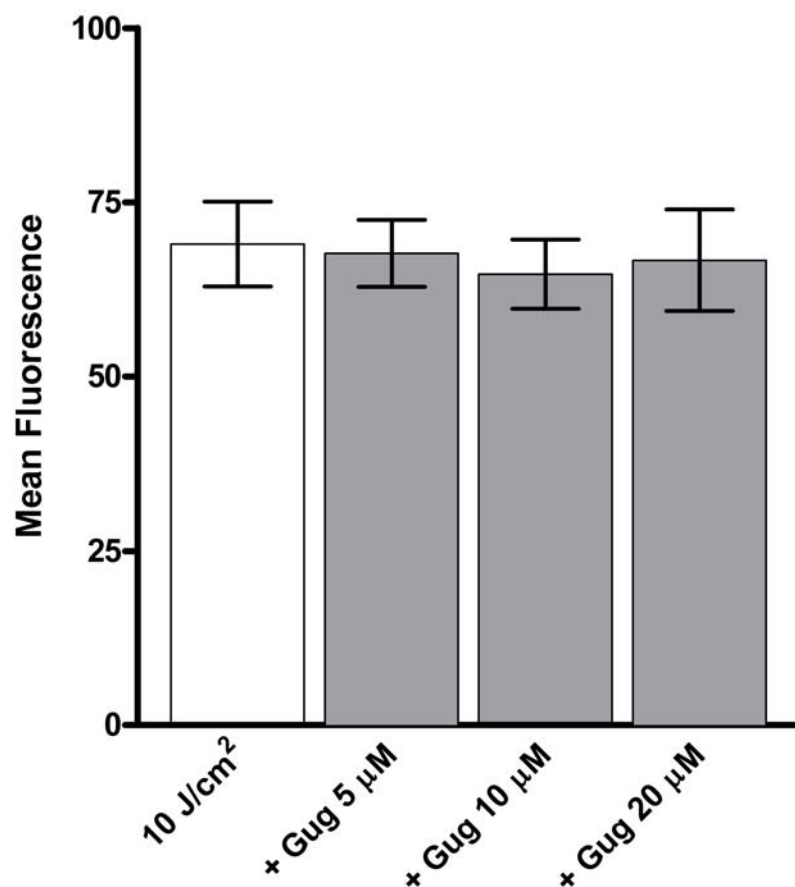


**Figure 3.33:** Effect of guggulsterone (5, 10 and 20 µM) in intracellular UVA-induced ROS production

Fluorescence intensity of H<sub>2</sub>DCFDA was excited at 488 nm. Results are the mean of three independent experiments  $\pm$ SEM (values for endogenous ROS, *i.e.* cells not exposed to UVR, for both with and without compound were subtracted from treatment values); no significance levels were reached.

Pretreatment with lanosterol (10 $\mu$ M for 24 h) slightly reduced UVA-induced DNA damage as measured by the alkaline comet assay (“no enz” groups), but the change was not statistically significant. That was also the case for 8-oxoGua and CPD formation (Figure 3.34). Guggulsterone treatment (10 $\mu$ M for 24 h) had no effect in UVA-induced DNA damage as measured by the lesion-specific comet assay (Figure 3.35). Combined data for the background-corrected version of this experiment are presented in Figure 3.36.



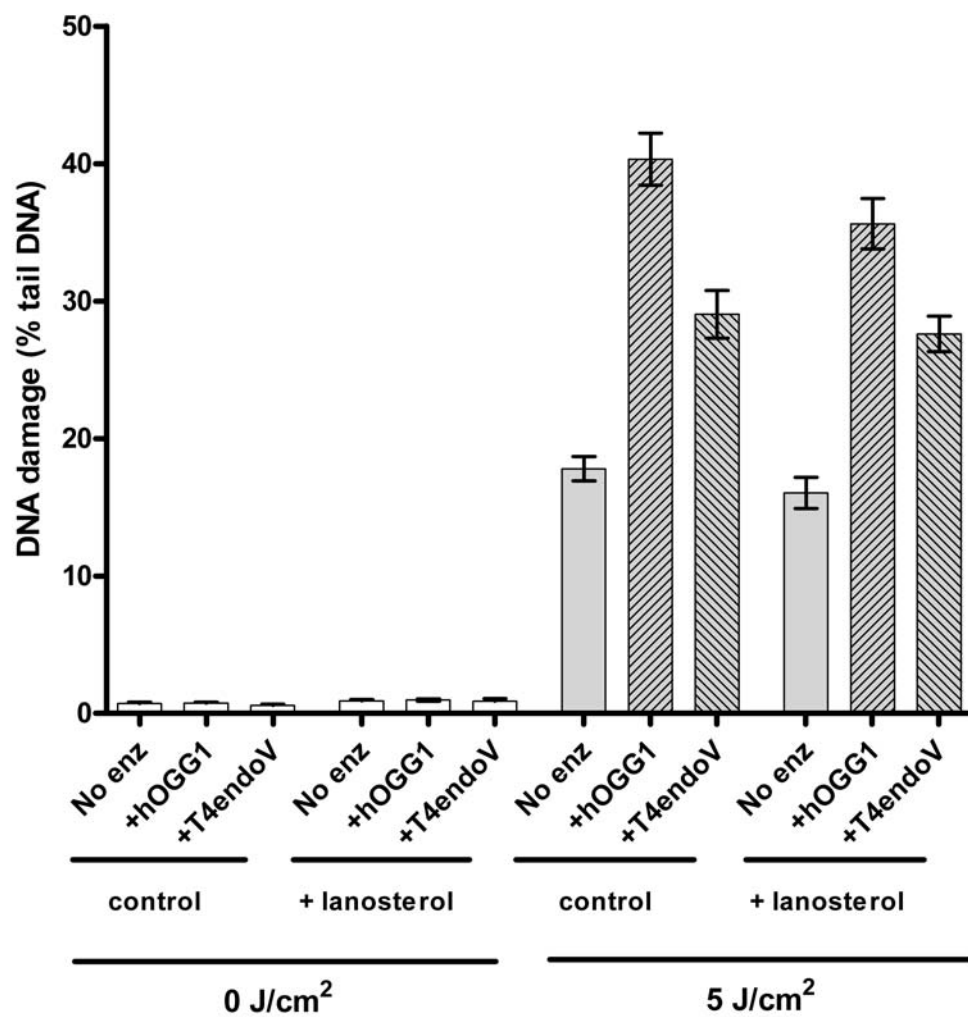


**Figure 3.34:** Effect of lanosterol on UVA-induced DNA damage detected by T4endoV- and hOGG1-modified comet assay

The mean percentage of tail DNA in HaCaT cells exposed to UVA (5 J/cm<sup>2</sup>). Results are the mean  $\pm$ SEM of three independent experiments;  $p < 0.0001$  in all cases when comparing irradiated samples to their corresponding non-irradiated samples;  $p < 0.0001$  in all cases when comparing “No enz” to “+ enz” samples.

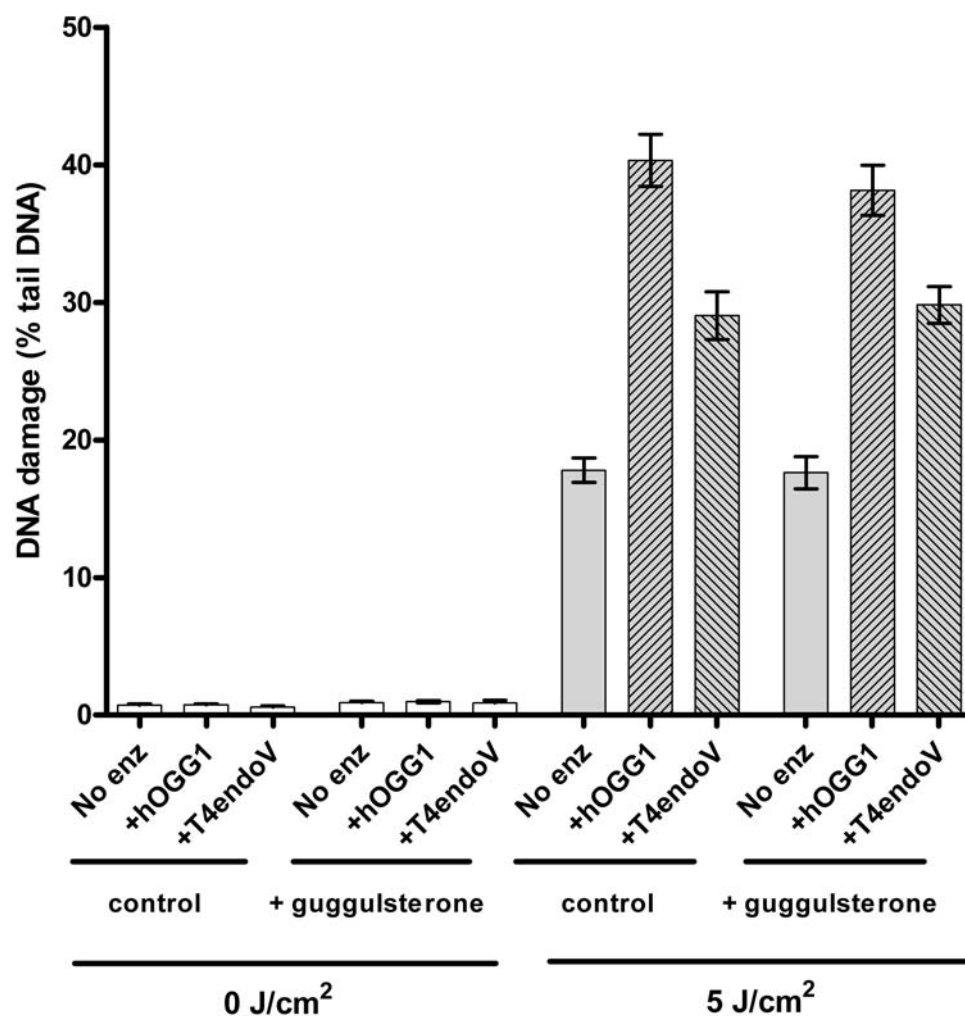


**Figure 3.35:** Effect of guggulsterone on UVA-induced DNA damage detected by T4endoV- and hOGG1-modified comet assay

The mean percentage of tail DNA in HaCaT cells exposed to UVA (5 J/cm<sup>2</sup>). Results are the mean  $\pm$ SEM of three independent experiments;  $p < 0.0001$  in all cases when comparing irradiated samples to their corresponding non-irradiated samples;  $p < 0.05$  in all cases when comparing “No enz” to “+ enz” samples.

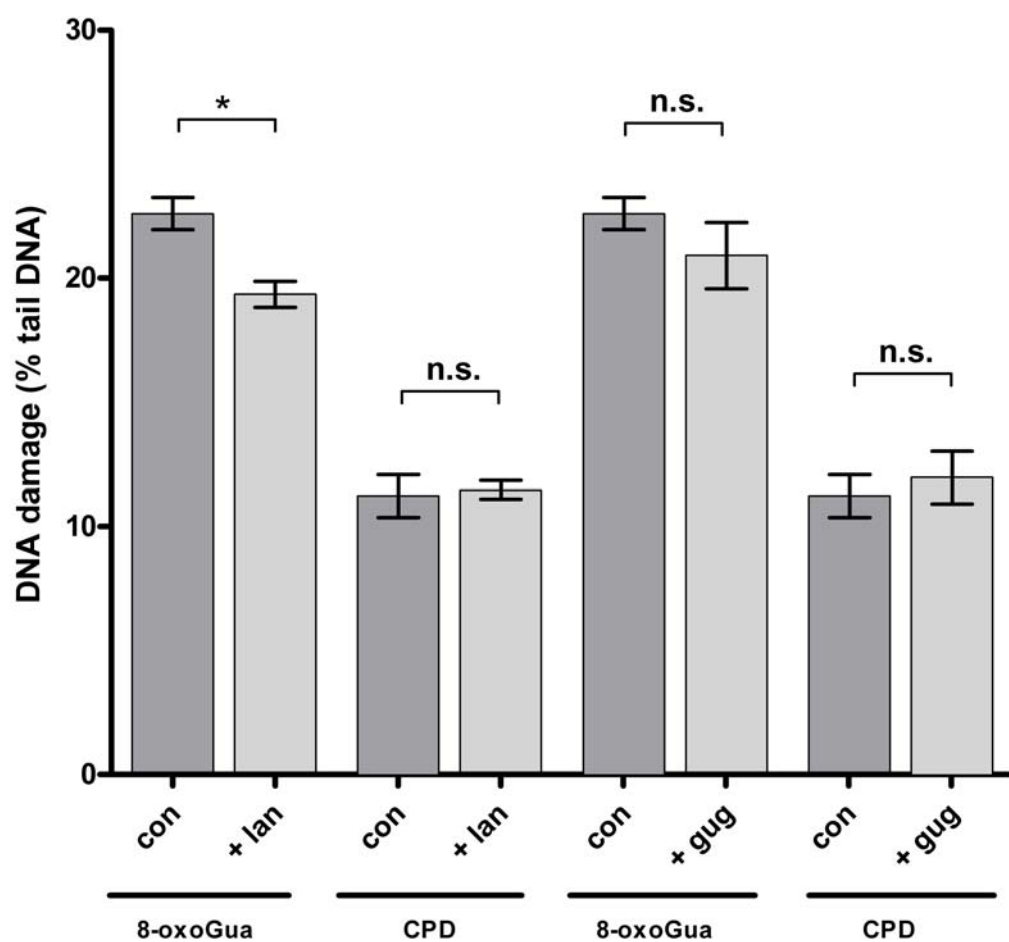


**Figure 3.36:** Effect of pre-incubation with lanosterol (lan) and guggulsterone (gug) on UVA-induced DNA damage detected by the T4endoV- and hOGG1-modified comet assay (background corrected)

The mean percentage of tail DNA in HaCaT cells exposed to UVA (5 J/cm<sup>2</sup>). Background correction was performed using no enzyme values for each group. Results are the mean  $\pm$ SEM of three independent experiments; \*p<0.05 for the selected comparison, based on two-way ANOVA with Bonferroni correction

## **Chapter 4: Discussion**

## 4.1 UVR-induced DNA damage

Although UVB irradiation was only used at the beginning of my studies to develop the comet assay and slot-blot protocols, comparison of DNA damage induced with later experiments involving UVA, gave some interesting outcomes. As might be expected, the different spectra gave different distributions of damage with the comet assay; UVB was found to induce considerably more CPD than 8-oxoGua whilst the reverse was seen with UVA.

### 4.1.1 UVA vs UVB-induced CPD formation

UVB has been known for decades to cause DNA damage through direct absorption by DNA, however, UVA was thought to cause DNA damage mainly through indirect mechanisms. Although UVA-induced CPD formation had been reported in the past, most measures of CPD detection have not been base-specific, or they were primarily detected with T&ltgtT specific antibodies. However, more recent work from the laboratory of Thierry Douki and his colleagues in Grenoble, provided a more detailed analysis of CPD production and showed (both *in vitro* and *ex vivo*) that UVAI primarily induces T&ltgtT, but very few C&ltgtC, C&ltgtT and no 6-4PPs or Dewar isomers (Douki et al., 2003; Mouret et al., 2006). These findings had led to the theory of a triplet energy transfer from an endogenous photosensitiser to a thymine. However, a hypothetical UVA chromophore that absorbs UVA has not yet been definitively identified. Most recent research has turned the photobiology community towards the belief that CPD formation occurs as a result of direct absorption of UVA by DNA. This had been suggested as early as 1999 (Kuluncsics et al., 1999) but the latest findings showed that UVA-induced DNA damage is similar in isolated or plasmid DNA and cells. The absence of any

photosensitisers in the purified irradiation mixture used in these studies indicated that UVA-induced CPD formation could occur by direct absorption (Jiang et al., 2009; Mouret et al., 2010). This was supported by findings that UVA induced the formation of CPD in a DNA duplex composed of thymine oligos (dA20:dT20), which could not have been contaminated by cellular components (Mouret et al., 2010).

The present study measured UVB- and UVA-induced CPD levels in a cellular environment. The *in vitro* action spectrum for CPD, and in specific T<>T, has a peak at 260 nm (Matsunaga et al., 1991), and high doses (and high fluence rates as well) of UVA are needed for significant CPD production, which is actually the case in recent UVA studies (Girard et al, 2011; Mouret et al., 2010) measuring CPD levels (in the range of 100-300 J/cm<sup>2</sup>, which is much higher compared to the doses used in the present study).

Comparing DNA damage induction between the two sources used, a 50 mJ/cm<sup>2</sup> UVB dose (estimated to be about 0.8 MED) was found to cause approximately the same amount of CPD production with a 100-fold higher UVA dose of 5 J/ cm<sup>2</sup> (a very low dose in terms of erythema). A higher dose of UVB (100 mJ/cm<sup>2</sup>) induced 39% more CPD damage than 10 J/ cm<sup>2</sup> and 22% more than 5 J/ cm<sup>2</sup> UVA. Based on *in vitro* keratinocyte data (T4endoV comet assay) with different cut-off filters (Woollons et al., 1999), it can be estimated that between ~10-25% CPD were induced by the 0.02% UVB content of the source in the current studies. Thus UVA was responsible for the majority of CPD production.

The 8-oxoGua:CPD ratio was approximately 1:6 for UVB and approximately 2:1 for UVA. Although some studies have shown a higher yield of CPD than 8-oxoGua levels following UVA irradiation in various cell lines or naked DNA (Girard et al, 2011; Douki et al., 2003), this was not the case in the present study. However, these ratios depend greatly on the spectral distribution of the source, as well as the doses used (Perdiz et al., 2000). Woollons et al also reported different ratios for T4endoV and endonuclease III (which detects oxidised pyrimidines) sites with different spectra (Woollons et al., 1999).

#### **4.2 Time-course assay for UVA-induced 8-oxoGua, CPD and ALS/SB**

The time-course comet assay data (Figure 3.6) showed similar curves for 8-oxoGua, CPD and ALS/SB kinetics, possibly suggesting a similarity in the repair mechanism of these lesions. One study on human fibroblasts showed that the half-life for 8-oxoGua (Fpg-sensitive sites) was about 7 h (Eiberger et al., 2008) which is similar to my findings (~5 h). Also it has been shown that 8-oxoGua repair differs between various epidermal cell types. Specifically, 8-oxoGua repair is slower in the basal layer of the epidermis than in the suprabasal cells (Javeri et al., 2008). Another study (personal communication with my colleague M. Karbaschi from Leicester University) showed that the half-lives of UVA-induced CPD and ALS/SB in HaCaT keratinocytes, were also very similar to ours, at approximately 5 and 4 h, respectively (compared to findings of this study, of about 6 and 4 h, respectively). The same study also showed that UVA-induced CPD is repaired with a much slower rate than UVB-induced CPD. This has also been reported by Mouret et al *ex vivo* (Mouret et al., 2006), but was not confirmed by Tewari et al who showed similar repair kinetics for UVB (300 nm) and UVAI-induced T<>T (Tewari et al., 2012a). It should also be noted that repair of T<>T in keratinocytes

*in vivo* is much slower (Bykov et al., 1999; Young et al., 1996) with half-lives of greater than 24 h.

Although the comet assay also detects endogenous endonuclease activity directed at 6-4PP as well as CPD, very few 6-4PPs would be expected from the spectra used in this study (Tewari et al., 2012a; Douki et al., 2003). Furthermore, 6-4PPs are known to be repaired with a much quicker rate than CPD (Bykov et al., 1999; Young et al., 1996).

CPD are known to be removed by nucleotide excision repair (NER) (Freyer et al., 1995), while 8-oxoGua is repaired by the base excision repair pathway (BER). Briefly, the NER pathway acts by cutting out damaged bases and replacing them as directed by the undamaged template strand. On the other hand, the BER system differs from NER in the types of substrates that it recognises, as well as the initial cleavage event, which occurs at the glycosilic bond, as opposed to phosphodiester bond for NER (Fleck and Nielsen, 2004). In contrast with NER, BER detects damaged bases that do not cause a major distortion to the DNA helix. However, there is also evidence implicating NER in the repair of UVA-induced 8-oxoGua (Reardon et al., 1997), which is supported by my time-course data. Another possible explanation for the similarity in the repair kinetics may be related to the fact that the HaCaT cell line possesses mutations in both alleles of the p53 gene (Lehman et al., 1993). p53 is important for base excision repair (BER) (Offer et al., 2001) both *in vitro* and *in vivo*, and if BER is impaired, repair can be carried out instead by NER (Dianov et al., 1998). This argument is strengthened by a study in 2006 that demonstrated that loss of p53 function leads to lowered hOGG1 repair activity (Chatterjee et al., 2006). Overall, my data provides evidence for a role for NER in the repair of 8-oxoGua. Whether this is specific to HaCaT keratinocytes, or is a



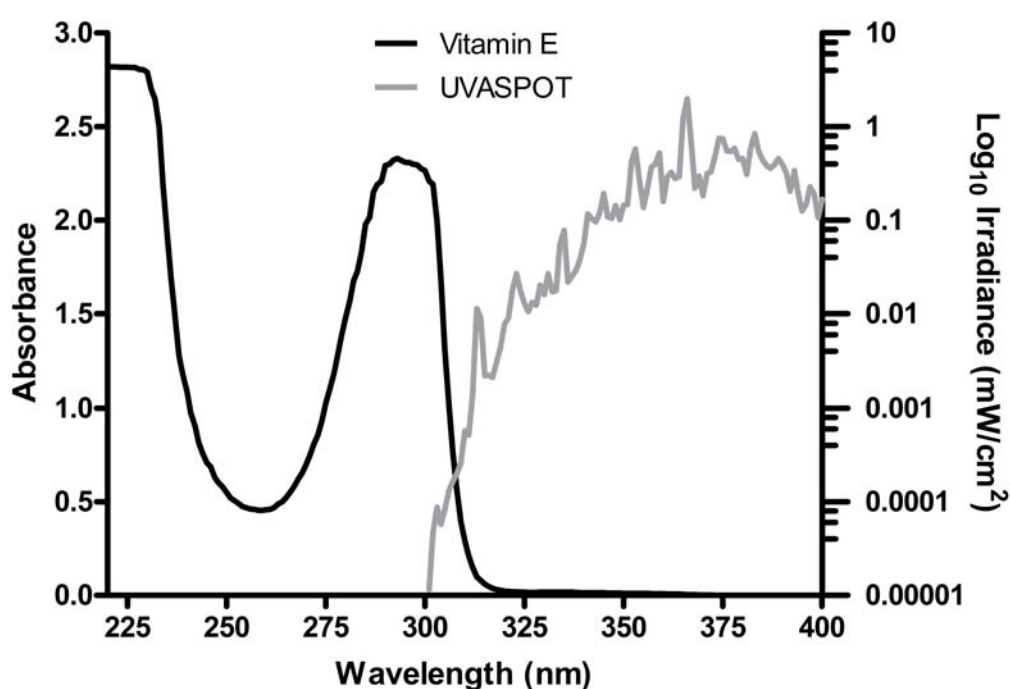
general phenomenon, remains to be elucidated.

Figure 3.6 also shows an increase in the formation of both 8-oxoGua and CPD until 30 min after UVR exposure. 8-oxoGua levels continued to increase up to 1 h after irradiation, while CPD levels started to decline 30 min after irradiation. This observation has also been reported by others for ROS *in vitro* (Valencia and Kochevar, 2008) and may provide an explanation for the increase in 8-oxoGua. CPD and 8-oxoGua levels have also been found to increase for up to 1 h following UVA irradiation *in vitro* (Javeri et al., 2011). An increase in CPD formation *in vivo* has also been shown by our group (Tewari et al., 2012a), as observed shortly after UVR exposure using antibody techniques. One possible explanation for this could be the unfolding of DNA prior to repair, that allows greater enzyme/antibody access (Duan and Smerdon, 2010).

### **4.3 Vitamin E photoprotection**

Results section 3.3 showed that pre-incubation with vitamin E can offer significant protection against UVR-induced formation of ROS, CPD and 8-oxoGua, as well as ALS/SB in human keratinocytes. Vitamin E shows some absorption in the terrestrial UVB range (an overlap between the emission spectrum of the UVASPOT and vitamin E is presented in Figure 4.1) and one of the problems with some previous studies with vitamin E (and other antioxidants), is that it is possible that its protective effects could partly be attributed to optical filtering, although it is not considered to have sunscreen properties (Eberlein-Konig and Ring, 2005). This possibility was addressed by also incubating the cells post-irradiation, and similar results were observed with the lesion-specific comet assay. The time-course assay (Figure 3.6) shows significant repair of

both lesions examined during the 2.5 h period of post-UVR incubation with vitamin E. Nevertheless, compared to the corresponding controls, the comet assay showed a decrease in both types of DNA damage, as well as non-specific DNA damage. However, one of the reasons that post-UVR incubation is effective in the comet assay is the increase of damage during the first half of the incubation period.



**Figure 4.1:** Emission spectrum of the UVASPOT, together with the absorption spectrum of a vit E solution (0.1 mg/ml in *n*-hexane)

Some studies were performed with UVC (254 nm) radiation, which is about the peak wavelength in the action spectrum for CPD induction *in vitro* (Matsunaga et al., 1991). Efficacy at 300-310 nm is three orders of magnitude lower. As can be seen in Figure 4.1, the absorption of 254 nm by vitamin E is similar to that at about 310 nm, and greater than that at wavelengths longer than 310 nm. The data in Figure 3.11 show that monochromatic UVC induced high levels of CPDs as well as 8-oxoGua. Vitamin E protected against the latter but not the former, which strongly suggests that the protection against 8-oxoGua was not a sunscreensing effect.

Although induction of 8-oxoGua by UVC radiation has been reported in the past (Evans et al., 1999; Bruge et al., 2003), there is not much literature on UVC-induced oxidative stress. However, a study in 1997 demonstrated that UVC-induced 8-oxoGua is due to increased singlet oxygen ( $^1\text{O}_2$ ) formation following UVC irradiation (Zhang et al., 1997). It is often stated that UVA is the main cause of oxidative stress, however, it should not be forgotten that this can also be caused by other wavebands, including UVB (Perluigi et al., 2010).

Since UVA-induced 8-oxoGua is formed indirectly, predominantly via  $^1\text{O}_2$  (Cooke et al., 2003; Zhang et al., 1997), the antioxidant properties of vitamin E were not surprising. This protective effect has not previously been demonstrated for this lesion by the comet assay. However, a 2004 study showed a protective effect of vitamin E against oxidatively-induced 8-oxoGua in ovarian epithelial cells (Murdoch and Martinchick, 2004), while an older report illustrated an inhibitory effect of vitamin E against ozone-induced 8-oxoGua (Cheng et al., 2003). In general, vitamin E has been established as a UVR-induced ROS scavenger (Jin et al., 2007). A very recent study by a former

colleague also showed a protective effect of vitamin E against cis-UCA-induced ROS formation, indicating a role of the antioxidant in indirect photoprotection (Kaneko et al., 2011).

In contrast, the formation of CPD is thought to occur mainly *via* direct photon absorption, especially in the UVC and UVB regions. However, the sensitized formation of T<>T in naked DNA in this spectral region has been reported (Kaneko et al., 1979). The photochemical mechanism by which UVA (and more specifically UVAI) selectively induces CPD formation is still not completely clear. It is known that UVA activation of certain photosensitizers can induce CPD *in vitro*, as was also recently shown with carprofen (Robinson et al., 2010). Therefore, unidentified endogenous photosensitizers might play a role in UVA-induced CPD, especially in the more complex *in vivo* system. However, DNA absorbs weakly in the whole UVA region (Sutherland and Griffin, 1981), so CPD formation by direct absorption can occur and has been recently reported, as mentioned above (Jiang et al., 2009; Mouret et al., 2010).

Post-UVA treatment with vitamin E was also found to offer significant protection against ROS production, with a similar trend to the pre-UVA experiment. Greater mean fluorescence values in the post-UVA treatment experiment (Figure 3.9) might either indicate an enhanced post-UVA ROS, which has been reported by others in keratinocytes (Valencia and Kochevar, 2008), or an increase in stress caused to cells due to harsher protocol conditions compared to the pre-UVR experiment. Figure 3.6 shows an increase of enzyme-specific DNA damage up to an hour post-UVA, which may also implicate post-UVA ROS release, especially with 8-oxoGua.

In contrast, DNA damage levels measured by the comet assay were lower in the post-UVR treatment experiment, in both hOGG1 and T4endoV groups (Figure 3.10). This decrease possibly indicates that the 2.5 h incubation period was enough for some repair (especially of ALS, considering the timeframe) as shown in Figure 3.6. Post-UVA incubation with vitamin E resulted in a significant reduction of non-specific (ALS/SB) and T4endoV and hOGG1-specific DNA damage. Levels for both lesions were found to be slightly lower (both approximately 5%) compared to the same time point (2.5 h) of the time-course assay (Figure 3.6), which indicates that data between different experiments are consistent. This small change could be attributed to different experimental conditions that involved the addition of EtOH (control) or vitamin E in fresh DMEM for the post-UVA vitamin E experiment, as opposed to the transfer of cells back to their conditioned DMEM for the 2.5 h period of incubation following UVR, for the time-course assay.

The immuno-slot blot experiment (Figure 3.13) supported the pre-UVR incubation data of the T4endoV comet assay; this was not the case with the post-UVR incubation results, where no significant effect of vitamin E was observed. A possible explanation for this may be the lack of CPD specificity of the T4endoV comet assay, which has also been shown to detect FapyAde sites (Dizdaroglu et al., 1996). Furthermore, T4endoV has an apurinic/apyrimidinic site endonuclease activity (Epe et al., 1993), which might lead to an overestimation of CPD.

It should also be noted that the T4endoV enzyme recognizes all types of CPD, T<>T, T<>C and C<>C, which based on findings by Douki et al in UVA-irradiated CHO cells, are produced with a ratio of 89:9:4, respectively (Douki et al., 2003). In contrast, the

immuno slot-blot assay is primarily specific for T<math>\searrow\swarrow</math>T, which is the most frequent type of UVA-induced CPD (Mitchell et al., 1992; Rochette et al., 2003). Although the mechanisms are not yet understood, UVA, especially UVAI, readily induces the formation of T<math>\searrow\swarrow</math>T but not the other CPD (Mouret et al., 2006; Rochette et al., 2003) that are also induced primarily with UVB sources (You et al., 2001). Thus, it is possible that T<math>\searrow\swarrow</math>T are not formed post-UVA, whereas other CPD are, as indicated in Figure 3.6. This could also relate to the fact that CPD have different repair kinetics, with T<math>\searrow\swarrow</math>C being repaired faster (Bykov et al., 1999).

Another possible explanation for the effects of vitamin E on DNA damage is the upregulation of DNA repair through reduction of ROS (Rassool et al., 2007). ROS as well as reactive nitrogen species (RNS) can decrease the efficiency of DNA repair enzymes and DNA polymerase (for both NER and BER) through oxidative protein damage (Wiseman and Halliwell, 1996). This theory has also been suggested recently and was based on suppression of UVA-induced nitric oxide (NO) products through post-UVR treatment with 1 $\alpha$ ,25-dihydroxyvitamin D3 (1,25D). The authors proposed a mechanism by which 1,25D suppresses NO products, thus enhancing DNA repair; this resulted in less DNA damage, with reduced CPD formation, reduced immunosuppression and reduced photocarcinogenesis (Mason et al., 2010). Therefore, it would be interesting to assess the effect of vitamin E on CPD and 8-oxoGua repair kinetics (*see Future perspectives*; section 4.9).

Overall, present data suggest that photoprotection by vitamin E should not be attributed to its UVR absorbing properties. There is literature to suggest that vitamin E protects against UVB-induced CPD formation (Chen et al., 1997; McVean and Liebler, 1997).

Some studies have also shown that vitamin E is capable of protecting against UVB-induced erythema, even if applied 8 h after UVR (Trevithick et al., 1993), and UVB-induced skin cancer in hairless mice (Berton et al., 1998). This effect has been observed both *in vitro* and *in vivo*, in mouse skin and has been attributed to the inhibition of CPD formation (Cario-Andr  et al., 2002; McVean and Liebler, 1999). However, results have varied, depending on the method of vitamin E application (topical or systemic), as well as the chemical form used in each study. This clearly illustrates why it is important to understand how this potent antioxidant is also able to protect against types of damage other than that induced by free radicals.

Endogenous vitamin E can prevent UVR-induced lipid peroxidation by acting as a chain-breaking antioxidant in the skin. Vitamin E ( $\alpha$ -tocopherol), used in the present study, appears to be more effective than other commercially available forms such as tocopherol acetate or  $\alpha$ -tocopheryl succinate (Werninghaus et al., 1994). The ability of Vitamin E to protect against UVR-induced cytotoxicity correlates with its level of uptake into cells and the level of its incorporation into the cell membranes has been correlated with its protection (Sakagami et al., 1997). Furthermore, photooxidation of vitamin E forms certain photoproducts with photoprotective properties (Krol et al., 2000). Finally, it has been reported that vitamin E interacts with endogenous antioxidant enzymes, playing a central role in recycling the antioxidant defence system in human cells (Wu et al., 2008; Petersen et al., 2000). Combinational studies of vitamins C and E have proven the protective effect of these antioxidants against sunburn (Eberlein-Konig and Ring, 2005) and UVB-induced T<>T (Placzek et al., 2005).

In summary, vitamin E is able to protect against different types of photodamage induced by solar range UVR and this is not related to its optical properties. Vitamin E is also

able to protect against oxidatively induced damage post-UVR. Our findings, as well as recent literature, suggest that UVA-induced ROS may play a role in the production of CPD at the cellular level (Petersen et al., 2000; Hochberg et al., 2006). This could be attributed to the interaction of ROS with histones, which can affect the nucleosome, opening the chromatin structure, which would lead to increased thymidine accessibility to UVR (Hawkins et al., 2002). Strong evidence supporting this argument has been the inability of vitamin E to protect against CPD formation on naked DNA (Hochberg et al., 2006). Another possible explanation mentioned earlier in the discussion, would be the ROS-induced downregulation of DNA repair through protein oxidation by UVA-induced radicals. In favour of this hypothesis was the finding that UVA induces oxidative crosslinking (through  $^1\text{O}_2$  production) between the subunits of the replication and repair protein, proliferating cell nuclear antigen (PCNA) (Montaner et al., 2007). As discussed earlier, UVA-induced ROS are also known to activate several MAPKs (Silvers et al., 2003; Son et al., 2011), therefore, by affecting various downstream effectors (such as AP-1 and NF $\kappa$ B) they may alter DNA repair responses, cell cycle arrest or apoptosis (Ridley et al., 2009). Furthermore, a study by Berton et al in 1998 showed that vitamin E treatment post-UVB irradiation increased CPD repair and this result was correlated with decreased p53 protein levels (Berton et al., 1998).

An ideal sunscreen would be able to protect against DNA damage and oxidative stress, as well as erythema. Our data, as well as those from other groups (Greul et al., 2002; Oresajo et al., 2010; Jiang et al., 2009; Matsui et al., 2009; Mouret et al., 2010), support the role of antioxidants in sunscreens, and possibly after-sun preparations. However, several questions remain to be addressed regarding the chemistry behind the protection offered by vitamin E, and it is important to establish if similar protection levels could be exhibited for the human skin.



#### **4.4 NAC photoprotection**

Figure 2.2 shows that NAC does not absorb in the spectral range of the UVR source used in this study. NAC protected against UVA-induced ROS formation (Figure 3.15) and UVA-induced GSH depletion (Figure 3.16). It also reduced 8-oxoGua levels but did not significantly alter CPD formation (Figure 3.17). An older study had demonstrated a protective effect of NAC against UVA-induced DNA damage using the comet assay, but this was done without the use of any lesion-specific enzymes (Morley et al., 2003). A recent study showed that NAC treatment on HaCaT keratinocytes strongly inhibited ROS and NO production induced by nano-titanium dioxide and UVA (Xue et al., 2011). NAC has been used in several antioxidant studies as its major function is to act as a cysteine donor, maintaining or even increasing intracellular GSH levels, thus protecting cells against free radicals. This effect was also shown in the present study, where NAC increased GSH levels in HaCaT keratinocytes (control group) by 2.7-fold, and offered a significant protection against UVA-induced depletion of total GSH as well (Figure 3.16).

#### **4.5 UVA-induced HO1 and MMP12 gene expression**

HO1, a redox-regulated enzyme that catalyses the degradation of heme to release biliverdin and carbon monoxide (CO), is a reliable indicator of cellular oxidative stress (Allanson and Reeve, 2004). HO1 gene and protein levels are hugely upregulated in skin fibroblasts due to UVA irradiation (Keyse and Tyrrell, 1989), but that effect has not always been observed in various keratinocyte cell lines (Applegate et al., 1995). A 2006 study also found that UVA-induced HO1 expression may offer immunoprotection against UVB irradiation in mouse skin (Reeve et al., 2006).

In the present study, HO1 gene expression was significantly upregulated following UVA irradiation of HaCaT keratinocytes, with a peak at 3 h (Figure 3.18). HO1 levels were slightly but significantly decreased following 24 h pretreatment with vitamin E in both HaCaT keratinocytes and MRCV1 fibroblasts (Figures 3.20 and 3.21). This effect had only been shown as a secondary result of a 1999 study, in which  $\beta$ -carotene had failed to protect against UVA-induced HO-1 gene expression, in contrast with vitamin E (Obermuller-Jevic et al., 1999).

Interestingly, HO1 was not found to be significantly induced in whole skin (epidermis and dermis) *in vivo* following pure UVAI irradiation (Figure 3.26), in a study conducted by my colleague Dr Tewari (which was based on a former pilot study partially done by me). This may highlight the variation of HO1 expression between *in vitro* and *in vivo* circumstances, since UVA doses used were comparable ( $20 \text{ J/cm}^2$  *in vitro* and  $12.5\text{-}50 \text{ J/cm}^2$  for the *in vivo* study). However, there was a difference in the time-points tested, as the *in vitro* work had shown a maximum upregulation of HO1 3 h after UVR and a significant decline 5 h after UVR (Figure 3.18). The *in vivo* experiment studied HO1 expression only at 6 and 24 h after UVR, but expression was also higher at 6 h.

There is no literature on UVA-induced MMP12, which was chosen for analysis as a highly upregulated gene in an *in vivo* UVA pilot study. MMP12 is a member of the MMP family, and the most active MMP against elastin (Chen et al., 2004). MMP12 is involved in the degradation of elastic fibres in various skin disorders (Vaalamo et al., 1999; Saarialho-Kere et al., 1999).

MMP12 mRNA and protein has been shown to be induced by UVB irradiation in human skin *in vivo* and it was demonstrated that it is increased in photoaged skin and

has a significant role in the development of solar elastosis (Chung et al., 2002). The same study showed that NAC and vitamin E were both able to inhibit UVB-induced MMP12 gene expression in human skin *in vivo*, while a more recent study showed that UVB-induced MMP12 protein production could be prevented by an antioxidant-derived product (Afaq et al., 2009).

MMP12 was only 4-fold upregulated by UVA irradiation *in vitro* (Figure 3.23). However, it was more upregulated *in vivo* (Figure 3.27), making it a possible new marker of oxidatively-induced DNA damage. However, vitamin E had no significant effect on MMP12 expression *in vitro* (Figures 3.24 and 3.25). The *in vitro* time-course experiment for MMP12 expression showed a maximum 12 h after UVR, with a decline at 18 h (Figure 3.22). In contrast, the *in vivo* study showed a maximum expression at 24 h following UVR, indicating a difference between *in vitro* and *in vivo* environments.

Based on the *in vivo* data with a pure UVAI source, MMP12 presents an appealing possible new marker for UVA-induced oxidative stress and photoageing and it would be interesting to be studied in more detail *in vivo*, and possibly in older subjects. In the more complex *in vivo* environment, antioxidants, and in specific vitamin E, might be able to exhibit a protective effect over time. The mechanism of induction of MMP12 in the human skin is also an interesting field of study, since MMPs have been shown to be triggered through different pathways. For example, MMP1 (the major enzyme responsible for collagen 1 digestion) protein expression has been linked with increased oxidative stress (Fisher et al., 2009), but also with direct, UVB-induced DNA damage (Dong et al., 2008). The involvement of ROS in UVAI-induced erythema, as well as evidence by MMP1 studies have suggested that DNA along with an unknown UVAI

absorbing molecule that probably generates ROS, are shared chromophores for erythema and MMP-1 induction (Dong et al., 2008; Scharffetter-Kochanek et al., 1993; Auletta et al., 1986). This hypothesis is also supported by recent findings of our group (Tewari et al., 2012b). Therefore, vitamin E could be a promising agent against photoageing, as it is implicated in both oxidative stress and direct DNA damage, as discussed earlier.

#### **4.6 Role of mitochondrial respiratory chain complex I and NADPH in UVA-induced DNA damage**

The results with the hOGG1-modified comet assay showed a decrease of 8-oxoGua when keratinocytes were pretreated with vitamin E for 24 h, but also when they were treated with the compound after UVR, for 2.5 h. This might indicate a cascade of events taking place after the initial photoreaction, which prolongs the existence of ROS, through  $^1\text{O}_2$  production (Ouedraogo and Redmond, 2003; Valencia and Kochevar, 2008).

A possible mechanism for the generation of such ROS would involve UVA-induced enzyme activity. An enzyme proposed to play an important role is NADPH oxidase (Valencia and Kochevar, 2008). NADPH oxidase has been shown to cause increased superoxide ( $\text{O}_2^{\cdot-}$ ) generation in response to UVA in mouse, monkey and human cell lines (Hockberger et al., 1999). The resulting  $\text{O}_2^{\cdot-}$  increase and its subsequent conversion to other ROS causes increased cellular and DNA damage. Prolonged generation of free radicals by such mechanisms in the initially exposed cells and their progeny therefore have the potential to cause severe genome instability (Ridley et al., 2009).

The probe used for ROS detection in this project was H<sub>2</sub>DCFDA, which is not specific for one type of ROS but reacts with several species in cells, including H<sub>2</sub>O<sub>2</sub>, NO and peroxides (Possel et al., 1997; Afri et al., 2004). Therefore, all types of free radicals produced immediately after, but also much later than the UVA irradiation (as seen in the post-UVA vitamin E ROS experiment; Figure 3.9) were detected by the assay.

Since recent literature has highlighted the production of CPD, especially T<math>\rightarrow</math>T, due to UVA irradiation, it has been debated recently whether this takes place through a direct or an indirect mechanism (Girard et al, 2011). The comet assay results exhibited a protective effect of vitamin E against CPD formation, both after 24 h pre-treatment and after 2.5 h post-UVR treatment. This could indicate an involvement of ROS in the production of CPD, a mechanism also suggested by Hochberg and colleagues (Hochberg et al., 2006), as discussed in detail in section 4.3.

Since the mitochondrial respiratory chain is a major source of ROS generation in the cells, it was decided to assess its role in UVA-induced oxidative stress. The use of rotenone -an inhibitor of the mitochondrial respiratory complex I- led to an increase in ROS formation as measured by the ROS assay, but also increased 8-oxoGua formation as measured by the hOGG1-modified comet assay (Figures 3.28 and 3.29). This upregulation of ROS and oxidatively-generated DNA damage by rotenone highlights the role of mitochondria in UVA-induced damage. It is now well established that the vast majority of cellular ROS are produced in mitochondria, “leaking” from the respiratory chain (Birch-Machin and Swalwell, 2010). Furthermore, the mitochondrial inner membrane contains several potential chromophores that can absorb UVA (such as flavoproteins, nicotinamide dinucleotides, ubiquinone, and cytochrome c1) and are capable of initiating photodynamic reactions (Schauen et al., 2007). Since UVA may

cause severe mitochondrial DNA damage, which persists longer than nuclear DNA damage (Yakes and Van Houten, 1997), it could generate sufficient ROS that reach the nucleus and cause further DNA damage. However, a 2004 study suggested that although visible light-induced mitochondrial ROS are responsible for most ROS present in the cells, they were not responsible for a significant 8-oxoGua formation, as measured by the Fpg-comet assay (Hoffmann et al., 2004), a finding that contradicts what was observed in the present study. This might relate to the use of Fpg, which has been shown to be less accurate than hOGG1 in 8-oxoGua detection (Smith et al., 2006). Treatment of cells with rotenone caused a small but not significant reduction in CPD formation (Figure 3.31), indicating it had no effect on this endpoint.

Data of rotenone-induced mitochondrial ROS measured at the cellular level have been inconsistent between studies. Rotenone has been shown to elevate cellular ROS production in some cases (Deng et al., 2010; Barrientos and Moraes, 1999) while inhibiting cellular ROS production in others (Vrablic et al., 2001; Schuchmann and Heinemann, 2000). Overall, findings of this study clearly show a role of the mitochondrial respiratory complex I in the production of UVA-induced ROS and oxidatively-induced DNA damage, but do not suggest a significant role of mitochondrial ROS in CPD formation.

The other inhibitor used was DPI, which is a specific inhibitor of NADPH oxidase, a major “player” in UVA-induced damage. NADPH oxidase inhibition by DPI has been shown to significantly attenuate UVA-induced ROS (He et al., 2005). Pretreatment of cells with DPI resulted in reduced ROS formation following UVA irradiation (Figure 3.28) and also a significant decrease of 8-oxoGua levels (Figure 3.31). Combined with

the observation of increased ROS levels 2.5 h after irradiation (Figure 3.9 compared to Figure 3.7), these results come in agreement with recent literature implicating NADPH oxidase in UVA-induced ROS production in HaCaT keratinocytes (Henri et al., 2011). Other studies found increased levels of ROS, detected up to at least 2 h following irradiation, suggesting that continued production of ROS is activated by UVA, possibly through a “feed forward” mechanism by  $H_2O_2$ , which further activates NADPH oxidase (Valencia et al., 2006; Li et al., 2001). Since NADPH oxidase and mitochondria are the major cellular sources of the ROS detected shortly after UVA exposure (Valencia and Kochevar, 2008) they are key “players” in UVA-induced DNA damage. In general, this “secondary ROS” production that can be a result of lipid peroxidation (which can be prevented by vitamin E) might initiate further oxidative DNA damage (such as 8-oxoGua, lipid and protein oxidation) in the nucleus (Ouedraogo and Redmond, 2003), as discussed above.

In summary, DPI reduced ROS and 8-oxoGua formation through inhibition of NADPH oxidase activity, indicating a major role of this signalling pathway in UVA-induced damage. On the other hand, DPI had no significant effect in UVA-induced CPD production, ruling out an involvement of NADPH oxidase in the formation of CPDs.

Using the two specific inhibitors rotenone and DPI, this study revealed a role of the mitochondrial respiratory chain, as well as NADPH oxidase in UVA-induced ROS production. Overall, this seems to be important for 8-oxoGua, but not CPD formation.

#### 4.7 Stiefel compounds with antioxidant potential

Of the three compounds supplied by Stiefel laboratories, one (farnesol) was found to be toxic. Lanosterol, a precursor of cholesterol in mitochondria and other cellular compartments of macrophages, has been found to be upregulated under increased oxidative stress conditions, suggesting a possible role of it in cellular response to stress (Andreyev et al., 2010). There is not much literature about lanosterol, however a recent study provided evidence that it might be a neuroprotective agent in a model of Parkinson's disease, acting through mitochondrial uncoupling induction and by promoting autophagy (Lim et al., 2012). In the present study, lanosterol significantly reduced ROS levels and also offered a small but significant protection against UVA-induced 8-oxoGua formation. Based on its spectral properties (Figure 2.5) as well as its high viscosity (very difficult to dilute and difficult to rinse following incubation, even after thorough washing with PBS), a sunscreen effect of lanosterol could not be excluded, although the inability to protect against UVA-induced CPD formation contradicts this hypothesis.

The phytosterol guggulsterone is a constituent of the Indian plant *Commiphora mukul*, and has been considered as a potent anti-inflammatory mediator (Deng, 2007). The repression of NF- $\kappa$ B activation by guggulsterone has been proposed as a mechanism of its anti-inflammatory properties (Shishodia and Aggarwal, 2004). Although a relatively recent study showed that guggulsterone attenuated H<sub>2</sub>O<sub>2</sub>-induced cytotoxicity and intracellular accumulation of ROS (Xu et al., 2008), this study did not find a significant effect of guggulsterone against UVA-induced ROS or UVA-induced DNA damage (Figures 3.33 and 3.35). Higher concentrations than the ones used here, might prove more beneficial (although cell viability assays showed a decline in cell survival with



high guggulsterone concentrations; Table 3.7).

In general, this study suggests a possible role of lanosterol in photoprotection, since it significantly protected against ROS and reduced oxidatively-induced DNA damage caused by UVA irradiation. Guggulsterone had no effect in the endpoints tested, but this could be attributed to low the concentrations used in the present study. Higher concentrations used in other studies with guggulsterone (none of which tested it against UVR-induced damage) could not be reached under this study's conditions, since the compound would not be thoroughly cleared from cell cultures prior to UVR.

## 4.8 General conclusions

This project generated a panel of quantitative techniques that measure UVR-induced damage and the photo-protective effects of various compounds against its deleterious effects. All studies were done under conditions of high cell viability with UVR doses that were environmentally and physiologically relevant.

A major finding was the beneficial effects of vitamin E when administered post-irradiation. This suggests that antioxidants may be useful in after-sun products, not only to counteract oxidative stress, but possibly aid in DNA repair. Vitamin E treatment, both before and after UVR, protected against ROS and 8-oxoGua formation, suggesting it is an ideal compound to counteract oxidatively generated damage by UVA irradiation. The results obtained by the T4endoV-modified comet assay also showed a protective effect of vitamin E against UVA-induced CPD, again both pre- and post-UVR. T $\rightarrow$ T measurement by the immuno-slot blot revealed the same protective effect of vitamin E for pre-UVA treatment, but no significant protection with the post-UVA treatment. As mentioned previously, a possible interpretation of this observation could be the lack of specificity of the T4endoV-modified comet assay for T $\rightarrow$ T (Dizdaroglu et al., 1996; Epe et al., 1993).

Although latest research has shown that UVA-induced CPD formation is due to direct absorption of UVA by DNA, this study along with recent literature highlights the importance of oxidative stress in DNA damage, indirectly, possibly by influencing DNA repair processes. Although UVA-induced ROS can cause direct oxidative damage to DNA, as evidenced by the increase in 8-oxoGua, they may also inhibit proteins

involved in the DNA repair process, enabling the accumulation of forms of DNA damage that are not directly caused by ROS, such as CPD (Halliday, 2010). Some results of this study suggested a role of ROS in the formation of UVA-induced CPD, as evidenced by the protection offered by vitamin E. However, post-UVR treatment with vitamin E did not protect against T<math>\rightarrow</math>T formation, as measured by the immuno-slot blot adding difficulty toward a definitive interpretation. Furthermore, mitochondrial ROS and NADPH oxidase were not found to be associated with UVA-induced CPD production, ruling out a direct involvement of ROS in their formation. Vitamin E might have a different mechanism of protection when applied pre- or post-UVR. Pre-UVR treatment may protect through partial absorption of UVB (0.2% UVB in the source used), thus reducing CPD formation (although the impact would be quite small), whereas post-UVR treatment could aid CPD repair.

In general, findings of this study show that vitamin E is an ideal compound for products that could be applied both before and after exposure to UVR, especially since recent findings showed that it is stable under UVR (long-wave UVA; 365 nm) for up to 6 h (Sabliov et al., 2009). However, the method of application and the vehicle used for its application on human skin are of great importance for its photostability.

Since data obtained in this project were produced with a (primarily UVAI) source containing 0.2% UVB, some CPD production could be attributed to UVB. However, the difference between CPD and 8-oxoGua levels when comparing data between obtained with the UVA source and the UVB source, suggest that the majority of CPD caused by the UVASPOT, was due to the UVA component.

A crucial point highlighted by the study of UVA-induced genes is the interpretation of *in vitro* data, as exemplified by the HO1 results *in vivo*. UVA-induced HO1 expression was analysed in more than one cell types with similar results, but this was not seen in the *in vivo* study which was conducted on 5 volunteers, offering a statistical significance to the obtained results.

Since recent evidence showed that CPD is the principal lesion produced by terrestrial sunlight (Besaratnia et al., 2011), photoprotection strategies should focus on how to inhibit its formation. Importance of photoprotection against UVA damage is also highlighted by latest findings that UVA-induced CPD are more mutagenic than those induced by UVB (Runger et al., 2012). Furthermore, it has been shown that UVA-induced T<math>\hookrightarrow</math>T formation is more abundant in the basal epidermis (Tewari et al., 2012a; Huang et al., 2009), an important finding, since that is where stem cells are located. Therefore, CPD in the basal layer could be an ideal marker of UVA-induced DNA damage, and possibly reflect other types of damage, such as 8-oxoGua. Another important aspect to bear in mind is the difference in CPD repair between *in vitro* and *in vivo* environments. Although UVA-induced T<math>\hookrightarrow</math>T were thought to be repaired less efficiently than UVB-induced T<math>\hookrightarrow</math>T as found *ex vivo* (Mouret et al., 2006), a more recent study showed that this was not the case *in vivo*, where a similar repair rate was observed between the two (Tewari et al., 2012a). Furthermore this study showed a relatively rapid repair of T<math>\hookrightarrow</math>T *in vitro*, compared to *in vivo* studies (Bykov et al., 1999; Tewari et al., 2012a; Young et al., 1996). This emphasizes the need to distinguish between *in vitro* and *in vivo* data.

Results of this project also indicated that NADPH is a key player in UVA-induced DNA damage. NADPH oxidase has been found to be inhibited by vitamin E *in vitro* (Wu et al., 2008). A recent study has pointed out a role of NADPH in tissue repair, through various signalling pathways (Chan et al., 2009). Therefore a possible mechanism of vitamin E photoprotection could be the enhancement of DNA repair, through downregulation of NADPH oxidase. A schematic representation of the main findings of this study is shown in Figure 4.2.

In the end, it is important to stress the variation of UVA spectra, doses, as well as fluence rate (irradiance) between different studies measuring UVA-induced CPD. High fluence rates of UVA have been shown to increase oxidatively-induced DNA damage in skin cells (Hoerter et al., 2008), therefore it is also important to note these measurements before comparing between studies. All these are highlighted by the disagreement regarding the relative yields of 8-oxoGua and CPD in the UVA range. Large UVA doses have been shown to give rise to more CPDs than oxidised purines, therefore, comparisons could be misleading (Pfeifer and Besaratinia, 2012). Furthermore, discrepancies in repair rates of CPD and 8-oxoGua induced by UVA irradiation are dependent on cell type (Sage et al., 2011).

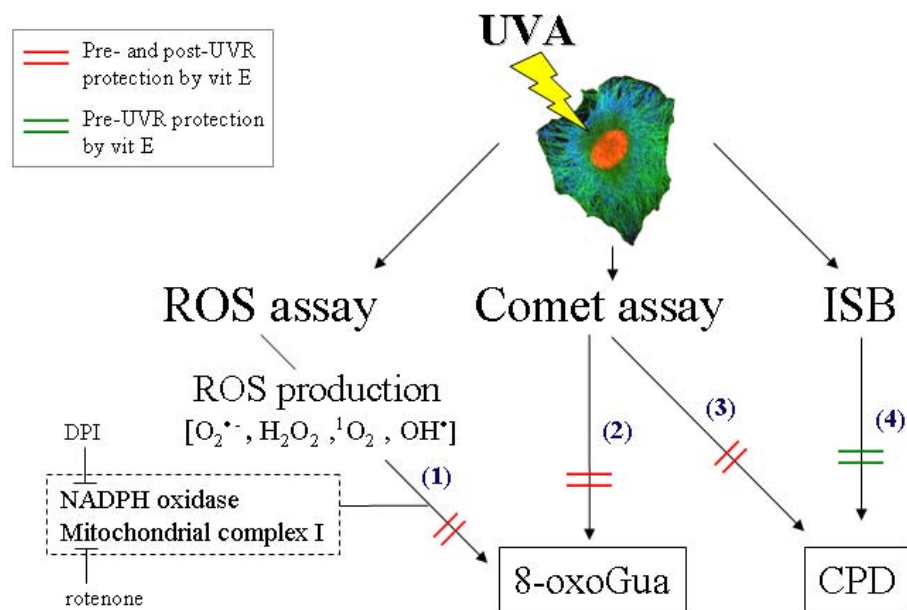


**Figure 4.2: UVA effects on human skin cells based on literature and findings of this thesis**

- (1) The  $H_2DCFDA/ROS$  assay demonstrated the production of various ROS following UVR. Some of these ROS were also present/generated up to 2 h post-irradiation, as indicated by the protection offered by vit E post-UVR. NADPH oxidase and mitochondrial complex I were found to be involved in UVA-induced production of ROS (and as a result, of 8-oxoGua), as shown by the ROS and comet assays with the use of DPI (NADPH oxidase inhibitor) and rotenone (mitochondrial complex I inhibitor).
- (2) The hOGG1-modified comet assay showed that UVA induces 8-oxoGua formation, an effect which is alleviated by vit E, both pre- and post-UVR.
- (3) The T4endoV-modified comet assay revealed the formation of CPD following UVA, which was reduced by pre- and post-UVR treatment with vit E.
- (4) The immuno-slot blot (ISB) showed the production of CPD due to UVA irradiation and demonstrated a significant protection by vit E pre-treatment. However, this was not the case for post-UVR treatment. This suggests that T4endoV is not totally specific for  $T \rightarrow T$ .

## 4.9 Further perspectives

The work presented in this thesis lends itself to further studies, both *in vitro* and *in vivo*. The data for induction of ROS and 8-oxoGua and their inhibition by vitamin E are generally consistent and the assays involved could be used to assess other potential antioxidants. Post-UVR treatment would be important to exclude protection by any UVR absorbing properties. The results for CPD are less clear cut and further experiments are necessary to establish any role of ROS in CPD induction and the effect of ROS on CPD repair, and indeed 8-oxoGua repair, as well as any effects of antioxidants on repair capacity. It would also be important to do comparative studies in skin cells with normal p53 status. Furthermore it would be informative to perform studies with pure UVB and UVAI sources (e.g. monochromatic radiation) as well as solar simulated radiation.

The DNA photolesion and gene expression studies developed here *in vitro* can be readily translated into the human skin in the *in vivo* situation. My colleague Dr Angela Tewari has a large amount of UVB (300 nm) and UVAI microarray data for the whole genome in human skin. These could be used, along with *in vitro* data, to identify UVR-induced genes and their proteins that might be modified by antioxidant treatment *in vivo*.

Some specific experiments that could be performed are listed below:

- The possible effects of vitamin E (and other antioxidants) can be studied *in vivo* against UVAI-induced CPD and 8-oxoGua formation. This could be done using antibody techniques which also allow the location of the damage in the epidermis and dermis, as well as double staining techniques to allow the identification of specific cell types (e.g. melanocytes).
- Further investigation could also be conducted on different repair rates between UVA- and UVB-induced DNA damage, since there are some discrepancies on the repair kinetics of CPD and 8-oxoGua in recent literature. Most importantly, great attention should be given to UVR spectra, in order to make comparisons between studies valid. ROS may interfere with DNA repair: thus it would be interesting to assess this possibility *in vitro* and *in vivo*.
- Recent literature has also pointed to the continued ROS formation following UVA irradiation. Although many hypotheses have been made about this phenomenon, it still remains to be fully elucidated, especially since the mechanism of activation of NADPH by UVA is still unknown. Further studies with inhibitors of ROS pathways and the consequences of such inhibition can also be conducted.
- A time-course experiment to measure ROS levels at different time points after irradiation is planned. This will provide further information on the involvement of secondary ROS production in UVA-induced DNA damage. This experiment will complete a manuscript in preparation.



## Bibliography

- Afaq, F., M.A.Zaid, N.Khan, M.Dreher, and H.Mukhtar. 2009. Protective effect of pomegranate-derived products on UVB-mediated damage in human reconstituted skin. *Experimental Dermatology*. 18(6):553-61.
- Afri, M., B.Ehrenberg, Y.Talmon, J.Schmidt, Y.Cohen, and A.A.Frimer. 2004. Active oxygen chemistry within the liposomal bilayer: Part III: Locating Vitamin E, ubiquinol and ubiquinone and their derivatives in the lipid bilayer. *Chemistry and Physics of Lipids* 131:107-121.
- Agar, N.S., G.M.Halliday, R.S.Barnetson, H.N.Ananthaswamy, M.Wheeler, and A.M.Jones. 2004. The basal layer in human squamous tumors harbors more UVA than UVB fingerprint mutations: A role for UVA in human skin carcinogenesis. *Proceedings of the National Academy of Sciences of the United States of America* 101:4954-4959.
- Alberti, A., L.Bolognini, D.Macciantelli, and M.Caratelli. 2000. The Radical Cation of N,N-Diethyl-para-Phenylendiamine : a Possible Indicator of Oxidative Stress in Biological Samples. *Research on Chemical Intermediates* 26:253-267.
- Allanson, M. and V.E.Reeve. 2004. Immunoprotective UVA (320-400 nm) Irradiation Upregulates Heme Oxygenase-1 in the Dermis and Epidermis of Hairless Mouse Skin. *J Invest Dermatol* 122:1030-1036.
- Andreyev, A.Y., E.Fahy, Z.Guan, S.Kelly, X.Li, J.G.McDonald, S.Milne, D.Myers, H.Park, A.Ryan, B.M.Thompson, E.Wang, Y.Zhao, H.A.Brown, A.Merrill, C.R.H.Raetz, D.W.Russell, S.Subramaniam, and E.Dennis. 2010. Subcellular organelle lipidomics in TLR 4-activated macrophages. *Journal of Lipid Research*: 2785–2797.

Applegate, L.A., A.Noel, G.Vile, E.Frenk, and R.M.Tyrrell. 1995. Two genes contribute to different extents to the heme oxygenase enzyme activity measured in cultured human skin fibroblasts and keratinocytes: implications for protection against oxidant stress. *Photochemistry & Photobiology*. 61(3):285-91.

Auletta, M., R.W.Gange, O.T.Tan, and E.Matzinger. 1986. Effect of cutaneous hypoxia upon erythema and pigment responses to UVA, UVB, and PUVA (8-MOP + UVA) in human skin. *Journal of Investigative Dermatology*. 86(6):649-52.

Autier, P., J.F.Dore, A.M.Eggermont, and J.W.Coebergh. 2011. Epidemiological evidence that UVA radiation is involved in the genesis of cutaneous melanoma. *Current Opinion in Oncology* 23:189-196.

Bachelor, M.A. and G.T.Bowden. 2004. UVA-mediated activation of signaling pathways involved in skin tumor promotion and progression. *Seminars in Cancer Biology* 14:131-138.

Baier, J., T.Maisch, M.Maier, M.Landthaler, and W.Baumler. 2007. Direct Detection of Singlet Oxygen Generated by UVA Irradiation in Human Cells and Skin. *J Invest Dermatol* 127:1498-1506.

Baran, R. and H.I.Maibach. 2004. Textbook of Cosmetic Dermatology, 3rd edn. Informa Healthcare.

Barrientos, A. and C.T.Moraes. 1999. Titrating the Effects of Mitochondrial Complex I Impairment in the Cell Physiology. *Journal of Biological Chemistry* 274:16188-16197.

Bartsch, H. and J.Nair. 2000. Ultrasensitive and specific detection methods for exocyclic DNA adducts: Markers for lipid peroxidation and oxidative stress. *Toxicology* 153:105-114.

Berton, T.R., C.J.Conti, D.L.Mitchell, C.M.Aldaz, R.A.Lubet, and S.M.Fischer. 1998. The effect of vitamin E acetate on ultraviolet-induced mouse skin carcinogenesis. *Molecular Carcinogenesis*. 23(3):175-84.

Besaratinia, A., J.i.Yoon, C.Schroeder, S.E.Bradforth, M.Cockburn, and G.P.Pfeifer. 2011. Wavelength dependence of ultraviolet radiation-induced DNA damage as determined by laser irradiation suggests that cyclobutane pyrimidine dimers are the principal DNA lesions produced by terrestrial sunlight. *The FASEB Journal* 25:3079-3091.

Bickers, D.R. and M.Athar. 2006. Oxidative stress in the pathogenesis of skin disease. [Review] [83 refs]. *Journal of Investigative Dermatology*. 126(12):2565-75.

Birch-Machin, M.A. and H.Swalwell. 2010. How mitochondria record the effects of UV exposure and oxidative stress using human skin as a model tissue. *Mutagenesis* 25:101-107.

Bissonnette, R. 2008. Update on sunscreens. *Skin Therapy Letter*. 13(6):5-7,-Aug.

Block, K.I., A.C.Koch, M.N.Mead, P.K.Tothy, R.A.Newman, and C.Gyllenhaal. 2007. Impact of antioxidant supplementation on chemotherapeutic efficacy: A systematic review of the evidence from randomized controlled trials. *Cancer Treat Rev* 33:407-418.

Boulton, S., A.Anderson, H.Swalwell, J.R.Henderson, P.Manning, and M.A.Birch-Machin. 2011. Implications of using the fluorescent probes, dihydrorhodamine 123 and 2',7'-dichlorodihydrofluorescein diacetate, for the detection of UVA-induced reactive oxygen species. *Free Radical Research*. 45(2):139-46.

Bovie, W.T. 1918a. The Localization of the Physiological Effects of Radiation within the Cell. *Journal of Medical Research*. 39(2):251-65.

Bovie, W.T. 1918b. The Physiological Action of Radiation. *Journal of Medical Research*. 39(2):271-7.

Bovie, W.T. and D.M.Hughes. 1918. The Effects of Quartz Ultra-Violet Light on the Rate of division of. *Paramecium Caudatum*. *Journal of Medical Research*. 39(2):223-31.

Brigelius-Flohe, R. 2006. Bioactivity of vitamin E. *Nutrition Research Reviews*. 19(2):174-186.

Bruge, F., L.Tiano, T.Cacciamani, F.Principi, and G.P.Littarru. 2003. Effect of UV-C mediated oxidative stress in leukemia cell lines and its relation to ubiquinone content. *Biofactors*. 18(1-4):51-63.

Bruls, W.A., H.Slaper, J.C.van der Leun, and L.Berrens. 1984. Transmission of human epidermis and stratum corneum as a function of thickness in the ultraviolet and visible wavelengths. *Photochemistry & Photobiology*. 40(4):485-94.

Burke, K.E., J.Clive, G.F.Combs, Jr., J.Commisso, C.L.Keen, and R.M.Nakamura. 2000. Effects of topical and oral vitamin E on pigmentation and skin cancer induced by ultraviolet irradiation in Skh:2 hairless mice. *Nutrition & Cancer*. 38(1):87-97.

Bykov, V.J., J.M.Sheehan, K.Hemminki, and A.R.Young. 1999. In Situ Repair of Cyclobutane Pyrimidine Dimers and 6-4 Photoproducts in Human Skin Exposed to Solar Simulating Radiation. 112:326-331.

Cadet, J., A.G.Bourdat, C.D'Ham, V.Duarte, D.Gasparutto, A.Romieu, and J.L.Ravanat. 2000. Oxidative base damage to DNA: specificity of base excision repair enzymes. *Mutation Research/Reviews in Mutation Research* 462:121-128.

Cadet, J., T.Douki, J.L.Ravanat, and P.Di Mascio. 2009. Sensitized formation of oxidatively generated damage to cellular DNA by UVA radiation. *Photochem. Photobiol. Sci.* 8:903-911.

Cario-Andr , M., S.Briganti, M.Picardo, O.Nikaido, Y.Gall, J.Ginestar, and A.Ta ieb. 2002. Epidermal reconstructs: a new tool to study topical and systemic photoprotective molecules. *Journal of Photochemistry and Photobiology B: Biology* 68:79-87.

Chadwick, C.A., C.S.Potten, O.Nikaido, T.Matsunaga, C.Proby, and A.R.Young. 1995. The detection of cyclobutane thymine dimers, (6-4) photolesions and the Dewar photoisomers in sections of UV-irradiated human skin using specific antibodies, and the demonstration of depth penetration effects. *Journal of Photochemistry and Photobiology B: Biology* 28:163-170.

Chan, E.C., F.Jiang, H.M.Peshavariya, and G.J.Dusting. 2009. Regulation of cell proliferation by NADPH oxidase-mediated signaling: Potential roles in tissue repair, regenerative medicine and tissue engineering. *Pharmacology & Therapeutics* 122:97-108.

Chatterjee, A., E.Mambo, M.Osada, S.Upadhyay, and D.Sidransky. 2006. The effect of p53-RNAi and p53 knockout on human 8-oxoguanine DNA glycosylase (hOgg1) activity. *The FASEB Journal* 20:112-114.

Chen, W., M.Barthelman, J.Martinez, D.Alberts, and H.L.Gensler. 1997. Inhibition of cyclobutane pyrimidine dimer formation in epidermal p53 gene of UV-irradiated mice by alpha-tocopherol. *Nutrition & Cancer*. 29(3):205-11.

Chen, Z., J.Y.Seo, Y.K.Kim, S.R.Lee, K.H.Kim, K.H.Cho, H.C.Eun, and J.H.Chung. 2004. Heat Modulation of Tropoelastin, Fibrillin-1, and Matrix Metalloproteinase-12 in Human Skin In Vivo. *J Investig Dermatol* 124:70-78.

Cheng, T.J., H.P.Kao, C.C.Chan, and W.P.Chang. 2003. Effects of ozone on DNA single-strand breaks and 8-oxoguanine formation in A549 cells. *Environmental Research*. 93(3):279-84.

Chung, J.H., J.Y.Seo, M.K.Lee, H.C.Eun, J.H.Lee, S.Kang, G.J.Fisher, and J.J.Voorhees. 2002. Ultraviolet Modulation of Human Macrophage Metalloelastase in Human Skin In Vivo. *119:507-512*.

Cleaver, J.E. 2002. Ultraviolet photobiology: its early roots and insights into DNA repair. *DNA Repair* 1:977-979.

Clingen, P.H., C.F.Arlett, L.Roza, T.Mori, O.Nikaido, and M.H.Green. 1995. Induction of cyclobutane pyrimidine dimers, pyrimidine(6-4)pyrimidone photoproducts, and Dewar valence isomers by natural sunlight in normal human mononuclear cells. *Cancer Research*. 55(11):2245-8.

Cocheme, H.M. and M.P.Murphy. 2010. Can antioxidants be effective therapeutics? *Current Opinion in Investigational Drugs*. 11(4):426-31.

Collins, A.R. and Horváthová E. 2001. Oxidative DNA damage, antioxidants and DNA repair: applications of the comet assay. *Biochem. Soc. Trans.* 29:337-341.

Cooke, M.S., M.D.Evans, M.Dizdaroglu, and J.Lunec. 2003. Oxidative DNA damage: mechanisms, mutation, and disease. [Review] [175 refs]. *FASEB Journal*. 17(10):1195-214.

Cooke, M.S., T.L.Duarte, D.Cooper, J.Chen, S.Nandagopal, and M.D.Evans. 2008a. Combination of azathioprine and UVA irradiation is a major source of cellular 8-oxo-7,8-dihydro-2'-deoxyguanosine. *DNA Repair* 7:1982-1989.

Cooke, M.S., M.D.Evans, R.M.Burd, K.Patel, A.Barnard, J.Lunec, and P.E.Hutchinson. 2001. Induction and Excretion of Ultraviolet-Induced 8-Oxo-2[prime]-deoxyguanosine and Thymine Dimers In Vivo: Implications for PUVA. *116*:281-285.

Cooke, M.S., R.Olinski, and S.Loft. 2008b. Measurement and Meaning of Oxidatively Modified DNA Lesions in Urine. *Cancer Epidemiology Biomarkers & Prevention* *17*:3-14.

Cotter, M.A., J.Thomas, P.Cassidy, K.Robinette, N.Jenkins, S.R.Florell, S.Leachman, W.E.Samlowski, and D.Grossman. 2007. N-Acetylcysteine Protects Melanocytes against Oxidative Stress/Damage and Delays Onset of Ultraviolet-Induced Melanoma in Mice. *Clinical Cancer Research* *13*:5952-5958.

Courdavault, S., C.Baudouin, M.Charveron, A.Favier, J.Cadet, and T.Douki. 2004. Larger yield of cyclobutane dimers than 8-oxo-7,8-dihydroguanine in the DNA of UVA-irradiated human skin cells. *Mutation Research/Fundamental and Molecular Mechanisms of Mutagenesis* *556*:135-142.

Couteau, C., O.Couteau, S.Alami-El Boury, and L.J.M.Coiffard. 2011. Sunscreen products: What do they protect us from? *International Journal of Pharmaceutics* *415*:181-184.

Cridland, N. and C.Driscoll. 2009. Ultraviolet Radiation. In *Environmental Toxicants*. John Wiley & Sons, Inc., *1121-1162*.

Cross, C.E., B.Halliwell, E.T.Borish, W.A.Pryor, B.N.Ames, R.L.Saul, J.M.McCord, and D.Harman. 1987. Oxygen radicals and human disease. [Review] [195 refs]. *Annals of Internal Medicine*. *107*(4):526-45.

D'Agostini, F., R.M.Balansky, A.Camoirano, and S.De Flora. 2005. Modulation of light-induced skin tumors by N-acetylcysteine and/or ascorbic acid in hairless mice. *Carcinogenesis* *26*:657-664.

Dahle, J., E.Kvam, and T.Stokke. 2005. Bystander effects in UV-induced genomic instability: antioxidants inhibit delayed mutagenesis induced by ultraviolet A and B radiation. *Journal of Carcinogenesis*. 4:11.

Dahle, J. and E.Kvam. 2003. Induction of Delayed Mutations and Chromosomal Instability in Fibroblasts after UVA-, UVB-, and X-Radiation. *Cancer Research* 63:1464-1469.

Damian, D.L., Y.J.Matthews, T.A.Phan, and G.M.Halliday. 2011. An action spectrum for ultraviolet radiation-induced immunosuppression in humans. *British Journal of Dermatology* 164:657-659.

Davies, M.J. 2004. Reactive species formed on proteins exposed to singlet oxygen. *Photochem. Photobiol. Sci.* 3:17-25.

de Boer, J. and J.H.Hoeijmakers. 2000. Nucleotide excision repair and human syndromes. [Review] [86 refs]. *Carcinogenesis*. 21(3):453-60.

de Gruijl, F.R. 1995. Action spectrum for photocarcinogenesis. [Review] [18 refs]. *Recent Results in Cancer Research*. 139:21-30.

de Gruijl, F.R. 1999. Skin cancer and solar UV radiation. *European Journal of Cancer* 35:2003-2009.

Deng, R. 2007. Therapeutic Effects of Guggul and Its Constituent Guggulsterone: Cardiovascular Benefits. *Cardiovascular Drug Reviews* 25:375-390.

Deng, Y.T., H.C.Huang, and J.K.Lin. 2010. Rotenone induces apoptosis in MCF-7 human breast cancer cell-mediated ROS through JNK and p38 signaling. *Mol. Carcinog.* 49:141-151.



Dianov, G., C.Bischoff, J.Piotrowski, and V.A.Bohr. 1998. Repair pathways for processing of 8-oxoguanine in DNA by mammalian cell extracts. *Journal of Biological Chemistry*. 273(50):33811-6.

Diffey, B. 2009. Sunscreens: expectation and realization. [Review] [29 refs]. *Photodermatology, Photoimmunology & Photomedicine*. 25(5):233-6.

Diffey, B.L. 2002. What is light?. [Review] [14 refs]. *Photodermatology, Photoimmunology & Photomedicine*. 18(2):68-74.

Dizdaroglu, M., T.H.Zastawny, J.R.Carmical, and R.S.Lloyd. 1996. A novel DNA N-glycosylase activity of E. coli T4 endonuclease V that excises 4,6-diamino-5-formamidopyrimidine from DNA, a UV-radiation- and hydroxyl radical-induced product of adenine. *Mutation Research*. 362(1):1-8.

Dong, K.K., N.Damaghi, S.D.Picart, N.G.Markova, K.Obayashi, Y.Okano, H.Masaki, S.Grether-Beck, J.Krutmann, K.A.Smiles, and D.B.Yarosh. 2008. UV-induced DNA damage initiates release of MMP-1 in human skin. *Experimental Dermatology* 17:1037-1044.

Doruk, S., H.Ozyurt, H.Inonu, U.Erkorkmaz, O.Saylan, and Z.Seyfikli. 2011. Oxidative status in the lungs associated with tobacco smoke exposure. *Clinical Chemistry and Laboratory Medicine*.

Douki, T., A.Reynaud-Angelin, J.Cadet, and E.Sage. 2003. Bipyrimidine Photoproducts Rather than Oxidative Lesions Are the Main Type of DNA Damage Involved in the Genotoxic Effect of Solar UVA Radiation. *Biochemistry* 42:9221-9226.

Douki, T., D.Perdiz, P.Grof, Z.+Kuluncsics, E.Moustacchi, J.Cadet, and E.Sage. 1999. Oxidation of Guanine in Cellular DNA by Solar UV Radiation: Biological Role. *Photochemistry and Photobiology* 70:184-190.

Dreher, D. and A.F.Junod. 1996. Role of oxygen free radicals in cancer development. [Review] [115 refs]. *European Journal of Cancer*. 32A(1):30-8.

Duan, M.R. and M.J.Smerdon. 2010. UV damage in DNA promotes nucleosome unwrapping. *Journal of Biological Chemistry*. 285(34):26295-303.

Eberlein-Konig, B., M.Placzek, and B.Przybilla. 1998. Protective effect against sunburn of combined systemic ascorbic acid (vitamin C) and d-alpha-tocopherol (vitamin E). *Journal of the American Academy of Dermatology*. 38(1):45-8.

Eberlein-Konig, B. and J.Ring. 2005. Relevance of vitamins C and E in cutaneous photoprotection. *Journal of Cosmetic Dermatology*. 4(1):4-9.

Edlich, R.F., K.L.Winters, H.W.Lim, M.J.Cox, D.G.Becker, J.H.Horowitz, L.S.Nichter, L.D.Britt, and W.B.Long. 2004. Photoprotection by sunscreens with topical antioxidants and systemic antioxidants to reduce sun exposure. [Review] [74 refs]. *Journal of Long-Term Effects of Medical Implants*. 14(4):317-40.

Eiberger, W., B.Volkmer, R.Amouroux, C.Dherin, J.P.Radicella, and B.Epe. 2008. Oxidative stress impairs the repair of oxidative DNA base modifications in human skin fibroblasts and melanoma cells. *DNA Repair*. 7(6):912-21.

Elmets, C.A., D.Singh, K.Tubesing, M.Matsui, S.Katiyar, and H.Mukhtar. 2001. Cutaneous photoprotection from ultraviolet injury by green tea polyphenols. *Journal of the American Academy of Dermatology* 44:425-432.

Epe, B., M.Pflaum, M.HΣring, J.Hegler, and H.Rndiger. 1993. Use of repair endonucleases to characterize DNA damage induced by reactive oxygen species in cellular and cell-free systems. *Toxicology Letters* 67:57-72.

Evans, M.D., M.S.Cooke, I.D.Podmore, Q.Zheng, K.E.Herbert, and J.Lunec. 1999. Discrepancies in the Measurement of UVC-Induced 8-Oxo-2'-deoxyguanosine: Implications for the Analysis of Oxidative DNA Damage. *Biochemical and Biophysical Research Communications* 259:374-378.

Fisher, G.J., T.Quan, T.Purohit, Y.Shao, M.K.Cho, T.He, J.Varani, S.Kang, and J.J.Voorhees. 2009. Collagen Fragmentation Promotes Oxidative Stress and Elevates Matrix Metalloproteinase-1 in Fibroblasts in Aged Human Skin. *The American Journal of Pathology* 174:101-114.

Fleck, O. and O.Nielsen. 2004. DNA repair. *Journal of Cell Science* 117:515-517.

Fourtanier, A., D.Moyal, and S.Seite. 2011. UVA filters in sun-protection products: regulatory and biological aspects. *Photochem. Photobiol. Sci* 11(1):81-9.

Frederick, J.E., H.E.Snell, and E.K.Haywood. 1989. Solar ultraviolet radiation at the earth's surface. *Photochemistry and Photobiology* 50:443-450.

Freyer, G.A., S.Davey, J.V.Ferrer, A.M.Martin, D.Beach, and P.W.Doetsch. 1995. An alternative eukaryotic DNA excision repair pathway. *Molecular & Cellular Biology*. 15(8):4572-7.

Friedberg, E.C. 2001. How nucleotide excision repair protects against cancer. [Review] [103 refs]. *Nature Reviews. Cancer*. 1(1):22-33.

Fuchs, J. and H.Kern. 1998. Modulation of UV-light-induced skin inflammation by D-alpha-tocopherol and L-ascorbic acid: a clinical study using solar simulated radiation. *Free Radical Biology & Medicine*. 25(9):1006-12.

Fuchs, J. 1998. Potentials and limitations of the natural antioxidants RRR-alpha-tocopherol, l-ascorbic acid and [beta]-carotene in cutaneous photoprotection. *Free Radical Biology and Medicine* 25:848-873.

Gallagher, R.P., J.J.Spinelli, and T.K.Lee. 2005. Tanning beds, sunlamps, and risk of cutaneous malignant melanoma. [Review] [28 refs]. *Cancer Epidemiology, Biomarkers & Prevention*. 14(3):562-6.

Gibbs, N.K. and M.Norval. 2011. Urocanic Acid in the Skin: A Mixed Blessing? *J Invest Dermatol* 131:14-17.

Gibbs, N.K., J.Tye, and M.Norval. 2008. Recent advances in urocanic acid photochemistry, photobiology and photoimmunology. *Photochem. Photobiol. Sci.* 7:655-667.

Girard et al,P.M. UVA-induced damage to DNA and proteins: direct versus indirect photochemical processes. *Journal of Physics: Conference Series* 261[1], 012002. 2011.  
Ref Type: Abstract

Girard, P.M. and S.Boiteux. 1997. Repair of oxidized DNA bases in the yeast *Saccharomyces cerevisiae*. *Biochimie* 79:559-566.

Godar, D.E. 1996. Preprogrammed and programmed cell death mechanisms of apoptosis: UV-induced immediate and delayed apoptosis. *Photochemistry & Photobiology*. 63(6):825-30.

Green, A., G.Williams, R.Neale, V.Hart, D.Leslie, P.Parsons, G.C.Marks, P.Gaffney, D.Battistutta, C.Frost, C.Lang, and A.Russell. 1999. Daily sunscreen application and betacarotene supplementation in prevention of basal-cell and squamous-cell carcinomas of the skin: a randomised controlled trial. *Lancet*. 354(9180):723-9.

Green, A.C., G.M.Williams, V.Logan, and G.M.Strutton. 2011. Reduced Melanoma After Regular Sunscreen Use: Randomized Trial Follow-Up. *Journal of Clinical Oncology* 29:257-263.

Greul, A.K., J.U.Grundmann, F.Heinrich, I.Pfützner, J.Bernhardt, A.Ambach, H.K.Biesalski, and H.Gollnick. 2002. Photoprotection of UV-irradiated human skin: an antioxidative combination of vitamins E and C, carotenoids, selenium and proanthocyanidins. *Skin Pharmacology & Applied Skin Physiology*. 15(5):307-15,-Oct.

Guenel, P., L.Laforest, D.Cyr, J.Fevotte, S.Sabroe, C.Dufour, J.M.Lutz, and E.Lynge. 2001. Occupational risk factors, ultraviolet radiation, and ocular melanoma: a case-control study in France. *Cancer Causes & Control*. 12(5):451-9.

Günter Speit and Andreas Hartmann. 2005. The Comet Assay: A Sensitive Genotoxicity Test for the Detection of DNA Damage and Repair. *In* DNA Repair Protocols: Mammalian Systems. 275-286.

Halliday, G.M. 2005. Inflammation, gene mutation and photoimmunosuppression in response to UVR-induced oxidative damage contributes to photocarcinogenesis. [Review] [99 refs]. *Mutation Research*. 571(1-2):107-20.

Halliday, G.M. 2010. Common Links among the Pathways Leading to UV-Induced Immunosuppression. *J Invest Dermatol* 130:1209-1212.

Halliday, G.M. and S.Rana. 2008. Waveband and Dose Dependency of Sunlight-induced Immunomodulation and Cellular Changes. *Photochemistry and Photobiology* 84:35-46.

Halliwell and Gutteridge. 1999. Free Radicals in Biology and Medicine. Oxford University Press, Oxford. 617-783 pp.

Hawkins, C.L., D.I.Pattison, and M.J.Davies. 2002. Reaction of protein chloramines with DNA and nucleosides: evidence for the formation of radicals, protein-DNA cross-links and DNA fragmentation. *Biochemical Journal*. 365(Pt 3):605-15.

He, Y.Y., J.L.Huang, M.L.Block, J.S.Hong, and C.F.Chignell. 2005. Role of Phagocyte Oxidase in UVA-Induced Oxidative Stress and Apoptosis in Keratinocytes. *J Invest Dermatol* 125:560-566.

He, Y.Y., J.L.Huang, D.C.Ramirez, and C.F.Chignell. 2003. Role of Reduced Glutathione Efflux in Apoptosis of Immortalized Human Keratinocytes Induced by UVA. *J. Biol. Chem.* 278:8058-8064.

Henri, P., S.Beaumel, A.Guezennec, C.Poumes, P.E.Stoebner, M.J.Stasia, J.Guesnet, J.Martinez, and L.Meunier. 2011. MC1R expression in HaCaT keratinocytes inhibits UVA-induced ROS production via NADPH oxidase- and cAMP-dependent mechanisms. *J. Cell. Physiol.*n/a.

Herrling, T., K.Jung, and J.Fuchs. 2006. Measurements of UV-generated free radicals/reactive oxygen species (ROS) in skin. *Spectrochimica Acta Part A: Molecular and Biomolecular Spectroscopy* 63:840-845.

Hochberg, M., R.Kohen, and C.D.Enk. 2006. Role of antioxidants in prevention of pyrimidine dimer formation in UVB irradiated human HaCaT keratinocytes. *Biomedicine & Pharmacotherapy* 60:233-237.

Hockberger, P.E. 2002. A history of ultraviolet photobiology for humans, animals and microorganisms. [Review] [340 refs]. *Photochemistry & Photobiology.* 76(6):561-79.

Hockberger, P.E., T.A.Skimina, V.E.Centonze, C.Lavin, S.Chu, S.Dadras, J.K.Reddy, and J.G.White. 1999. Activation of flavin-containing oxidases underlies light-induced production of H<sub>2</sub>O<sub>2</sub> in mammalian cells. *Proceedings of the National Academy of Sciences* 96:6255-6260.

Hoeijmakers, J.H.J. 2001. Genome maintenance mechanisms for preventing cancer. *Nature* 411:366-374.

Hoerter, J.D., C.S.Ward, K.D.Bale, A.N.Gizachew, R.Graham, J.Reynolds, M.E.Ward, C.Choi, J.L.Kagabo, M.Sauer, T.Kuipers, T.Hotchkiss, N.Banner, R.A.Chellson, T.Ohaeri, L.Gant, and L.Vanderhill. 2008. Effect of UVA fluence rate on indicators of oxidative stress in human dermal fibroblasts. *International Journal of Biological Sciences [Electronic Resource]*. 4(2):63-70.

Hoffmann, S., D.Spitkovsky, J.P.Radicella, B.Epe, and R.J.Wiesner. 2004. Reactive oxygen species derived from the mitochondrial respiratory chain are not responsible for the basal levels of oxidative base modifications observed in nuclear DNA of mammalian cells. *Free Radical Biology and Medicine* 36:765-773.

Huang, X.X., F.Bernerd, and G.M.Halliday. 2009. Ultraviolet A within Sunlight Induces Mutations in the Epidermal Basal Layer of Engineered Human Skin. *The American Journal of Pathology* 174:1534-1543.

Ikehata, H. and T.Ono. 2011. The Mechanisms of UV Mutagenesis. *Journal of Radiation Research* 52:115-125.

Javeri, A., J.Guy Lyons, X.X.Huang, and G.M.Halliday. 2011. Downregulation of Cockayne syndrome B protein reduces human 8-oxoguanine DNA glycosylase-1 expression and repair of UV radiation-induced 8-oxo-7,8-dihydro-2-deoxyguanine. *Cancer Science* 102:1651-1658.

Javeri, A., X.X.Huang, F.Bernerd, R.S.Mason, and G.M.Halliday. 2008. Human 8-oxoguanine-DNA glycosylase 1 protein and gene are expressed more abundantly in the superficial than basal layer of human epidermis. *DNA Repair* 7:1542-1550.

Jiang, Y., M.Rabbi, M.Kim, C.Ke, W.Lee, R.L.Clark, P.A.Mieczkowski, and P.E.Marszalek. 2009. UVA Generates Pyrimidine Dimers In DNA Directly. *Biophysical Journal* 96:1151-1158.

Jin, G.H., Y.Liu, S.Z.Jin, X.D.Liu, and S.Z.Liu. 2007. UVB induced oxidative stress in human keratinocytes and protective effect of antioxidant agents. *Radiation and Environmental Biophysics* 46:61-68.

Jones, D.P. 2006. Redefining Oxidative Stress. *Antioxidants & Redox Signaling* 8:1865-1879.

Kamal-Eldin, A. and L.A.Appelqvist. 1996. The chemistry and antioxidant properties of tocopherols and tocotrienols. [Review] [324 refs]. *Lipids*. 31(7):671-701.

Kaneko, K., U.Smetana-Just, M.Matsui, A.R.Young, S.John, M.Norval, and S.L.Walker. 2008. cis-Urocanic Acid Initiates Gene Transcription in Primary Human Keratinocytes. *The Journal of Immunology* 181:217-224.

Kaneko, K., S.L.Walker, J.Lai-Cheong, M.S.Matsui, M.Norval, and A.R.Young. 2011. cis-Urocanic Acid Enhances Prostaglandin E2 Release and Apoptotic Cell Death via Reactive Oxygen Species in Human Keratinocytes. *J Invest Dermatol* 131:1262-1271.

Kaneko, M., A.Matsuyama, and C.Nagata. 1979. Photosensitized formation of thymine dimers in DNA by tyramine, tyrosine and tyrosine-containing peptides. *Nucleic Acids Research*. 6(3):1177-87.

Kang, S., J.H.Chung, J.H.Lee, G.J.Fisher, Y.S.Wan, E.A.Duell, and J.J.Voorhees. 2003. Topical N-Acetyl Cysteine and Genistein Prevent Ultraviolet-Light-Induced Signaling That Leads to Photoaging in Human Skin in vivo. *J Investig Dermatol* 120:835-841.

Kappes, U.P., D.Luo, M.Potter, K.Schulmeister, and T.M.Runger. 2006. Short- and long-wave UV light (UVB and UVA) induce similar mutations in human skin cells. *Journal of Investigative Dermatology*. 126(3):667-75.

Kassam, S.N. and A.J.Rainbow. 2009. UV-inducible base excision repair of oxidative damaged DNA in human cells. *Mutagenesis* 24:75-83.



Kelly, F.J., R.Lee, and I.S.Mudway. 2004. Inter- and Intra-Individual Vitamin E Uptake in Healthy Subjects Is Highly Repeatable across a Wide Supplementation Dose Range. *Annals of the New York Academy of Sciences* 1031:22-39.

Kelly, F.J. 2004. Dietary antioxidants and environmental stress. *Proceedings of the Nutrition Society* 63:579-585.

Keyse, S.M. and R.M.Tyrrell. 1989. Heme oxygenase is the major 32-kDa stress protein induced in human skin fibroblasts by UVA radiation, hydrogen peroxide, and sodium arsenite. *Proceedings of the National Academy of Sciences* 86:99-103.

Kielbassa, C., L.Roza, and B.Epe. 1997. Wavelength dependence of oxidative DNA damage induced by UV and visible light. *Carcinogenesis* 18:811-816.

Kim, A.L., J.M.Labasi, Y.Zhu, X.Tang, K.McClure, C.A.Gabel, M.Athar, and D.R.Bickers. 2005. Role of p38 MAPK in UVB-induced inflammatory responses in the skin of SKH-1 hairless mice.[erratum appears in J Invest Dermatol. 2005 Dec;125(6):1320]. *Journal of Investigative Dermatology*. 124(6):1318-25.

Klein, E.A., I.M.Thompson, C.M.Tangen, J.J.Crowley, M.S.Lucia, P.J.Goodman, L.M.Minasian, L.G.Ford, H.L.Parnes, J.M.Gaziano, D.D.Karp, M.M.Lieber, P.J.Walther, L.Klotz, J.K.Parsons, J.L.Chin, A.K.Darke, S.M.Lippman, G.E.Goodman, F.L.Meyskens, and L.H.Baker. 2011. Vitamin E and the Risk of Prostate Cancer: The Selenium and Vitamin E Cancer Prevention Trial (SELECT). *JAMA: The Journal of the American Medical Association* 306:1549-1556.

Klotz, L.O., K.D.Kroncke, and H.Sies. 2003. Singlet oxygen-induced signaling effects in mammalian cells. *Photochem. Photobiol. Sci.* 2:88-94.

Kraemer, K.H., N.J.Patronas, R.Schiffmann, B.P.Brooks, D.Tamura, and J.J.DiGiovanna. 2007. Xeroderma pigmentosum, trichothiodystrophy and Cockayne syndrome: A complex genotype–phenotype relationship. *Neuroscience* 145:1388-1396.

Krinsky, N.I., I.C.Munro, S.P.Murphy, V.Young, and C.Garza. 2000. Dietary reference intakes for vitamin C, vitamin E, Selenium and carotenoids.

Kripke, M.L., P.A.Cox, L.G.Alas, and D.B.Yarosh. 1992. Pyrimidine dimers in DNA initiate systemic immunosuppression in UV-irradiated mice. *Proceedings of the National Academy of Sciences* 89:7516-7520.

Krol, E.S., K.A.Kramer-Stickland, and D.C.Liebler. 2000. Photoprotective actions of topically applied vitamin E. *Drug Metabolism Reviews* 32:413-420.

Kuluncsics, Z., D.Perdiz, E.Brulay, B.Muel, and E.Sage. 1999. Wavelength dependence of ultraviolet-induced DNA damage distribution: Involvement of direct or indirect mechanisms and possible artefacts. *Journal of Photochemistry and Photobiology B: Biology* 49:71-80.

Lee, E.H., D.Faulhaber, K.M.Hanson, W.Ding, S.Peters, S.Kodali, and R.D.Granstein. 2004. Dietary lutein reduces ultraviolet radiation-induced inflammation and immunosuppression.[Erratum appears in J Invest Dermatol. 2005 May;124(5):1092]. *Journal of Investigative Dermatology*. 122(2):510-7.

Lehman, T.A., R.Modali, P.Boukamp, J.Stanek, W.P.Bennett, J.A.Welsh, R.A.Metcalf, M.R.Stampfer, N.Fusenig, and E.M.Rogan. 1993. p53 mutations in human immortalized epithelial cell lines.[Erratum appears in Carcinogenesis 1993 Jul;14(7):1491]. *Carcinogenesis*. 14(5):833-9.

Li, W.G., F.J.Miller, Jr., H.J.Zhang, D.R.Spitz, L.W.Oberley, and N.L.Weintraub. 2001. H<sub>2</sub>O<sub>2</sub>-induced O<sub>2</sub> production by a non-phagocytic NAD(P)H oxidase causes oxidant injury. *Journal of Biological Chemistry*. 276(31):29251-6.

Lim, L., V.Jackson-Lewis, L.C.Wong, G.H.Shui, A.X.H.Goh, S.Kesavapany, A.M.Jenner, M.Fivaz, S.Przedborski, and M.R.Wenk. 2012. Lanosterol induces mitochondrial uncoupling and protects dopaminergic neurons from cell death in a model for Parkinson's disease. *Cell Death Differ.* 19: 416-427.

Lopez-Torres, M., J.J.Thiele, Y.Shindo, D.Han, and L.Packer. 1998. Topical application of  $\alpha$ -tocopherol modulates the antioxidant network and diminishes ultraviolet-induced oxidative damage in murine skin. *British Journal of Dermatology.* 138(2):207-15.

Markovitsi, D., T.Gustavsson, and A.Banyasz. 2004. Absorption of UV radiation by DNA: Spatial and temporal features. *Mutation Research/Reviews in Mutation Research* 704:21-28.

Marrot, L. and J.R.Meunier. 2008. Skin DNA photodamage and its biological consequences. *Journal of the American Academy of Dermatology* 58:S139-S148.

Masaki, H., Y.Okano, Y.Ochiai, K.Obayashi, H.Akamatsu, and H.Sakurai. 2002.  $\alpha$ -Tocopherol Increases the Intracellular Glutathione Level in HaCaT Keratinocytes. *Free Radic Res* 36:705-709.

Mason, R.S., V.B.Sequeira, K.M.Dixon, C.Gordon-Thomson, K.Pobre, A.Dilley, M.T.Mizwicki, A.W.Norman, D.Feldman, G.M.Halliday, and V.E.Reeve. 2010. Photoprotection by 1- $\alpha$ ,25-dihydroxyvitamin D and analogs: Further studies on mechanisms and implications for UV-damage. *The Journal of Steroid Biochemistry and Molecular Biology* 121:164-168.

Matsui, M.S., A.Hsia, J.D.Miller, K.Hanneman, H.Scull, K.D.Cooper, and E.Baron. 2009. Non-Sunscreen Photoprotection: Antioxidants Add Value to a Sunscreen. *J Invest Derm Symp P* 14:56-59.

Matsumura, Y. and H.N.Ananthaswamy. 2002. Short-term and long-term cellular and molecular events following UV irradiation of skin: implications for molecular medicine. *Expert Reviews in Molecular Medicine* 4:1-22.

Matsunaga, T., K.Hieda, and O.Nikaido. 1991. Wavelength dependent formation of thymine dimers and (6-4) photoproducts in DNA by monochromatic ultraviolet light ranging from 150 to 365 nm. *Photochemistry & Photobiology*. 54(3):403-10.

McArdle, F., L.E.Rhodes, R.Parslew, C.I.Jack, P.S.Friedmann, and M.J.Jackson. 2002. UVR-induced oxidative stress in human skin in vivo: effects of oral vitamin C supplementation. *Free Radical Biology & Medicine*. 33(10):1355-62.

McArdle, F., L.E.Rhodes, R.A.Parslew, G.L.Close, C.I.Jack, P.S.Friedmann, and M.J.Jackson. 2004. Effects of oral vitamin E and beta-carotene supplementation on ultraviolet radiation-induced oxidative stress in human skin. *American Journal of Clinical Nutrition*. 80(5):1270-5.

McVean, M. and D.C.Liebler. 1997. Inhibition of UVB induced DNA photodamage in mouse epidermis by topically applied alpha-tocopherol. *Carcinogenesis* 18:1617-1622.

McVean, M. and D.C.Liebler. 1999. Prevention of DNA photodamage by vitamin E compounds and sunscreens: roles of ultraviolet absorbance and cellular uptake. *Molecular Carcinogenesis*. 24(3):169-76.

Meewes, C., P.Brenneisen, J.Wenk, L.Kuhr, W.Ma, J.Alikoski, A.Poswig, T.Krieg, and K.Scharffetter-Kochanek. 2001. Adaptive antioxidant response protects dermal fibroblasts from UVA-induced phototoxicity. *Free Radical Biology and Medicine* 30:238-247.

Milatovic, D., T.J.Montine, and M.Aschner. 2011. Measurement of isoprostanes as markers of oxidative stress. *Methods in Molecular Biology*. 758:195-204.

Mitchell, D. and A.Fernandez. 2012. The photobiology of melanocytes modulates the impact of UVA on sunlight-induced melanoma. *Photochem. Photobiol. Sci.* 11:69-73.

Mitchell, D.L., J.Jen, and J.E.Cleaver. 1992. Sequence specificity of cyclobutane pyrimidine dimers in DNA treated with solar (ultraviolet B) radiation. *Nucleic Acids Research* 20:225-229.

Miyamae, Y., K.Zaizen, K.Ohara, Y.Mine, and Y.F.Sasaki. 1997. Detection of DNA lesions induced by chemical mutagens by the single cell gel electrophoresis (Comet) assay. 1. Relationship between the onset of DNA damage and the characteristics of mutagens.[Republished in *Mutat Res.* 1998 Jul 31;415(3):229-35; PMID: 9714818]. *Mutation Research.* 393(1-2):99-106.

Montaner, B., P.O'Donovan, O.Reelfs, C.M.Perrett, X.Zhang, Y.Z.Xu, X.Ren, P.Macpherson, D.Frith, and P.Karran. 2007. Reactive oxygen-mediated damage to a human DNA replication and repair protein. *EMBO Rep* 8:1074-1079.

Morabito, K., N.C.Shapley, K.G.Steeley, and A.Tripathi. 2011. Review of sunscreen and the emergence of non-conventional absorbers and their applications in ultraviolet protection. *International Journal of Cosmetic Science* 33:385-390.

Moriwaki, S.I. and K.H.Kraemer. 2001. Xeroderma pigmentosum - bridging a gap between clinic and laboratory. *Photodermatology, Photoimmunology & Photomedicine* 17:47-54.

Morley, N., A.Curnow, L.Salter, S.Campbell, and D.Gould. 2003. N-acetyl-l-cysteine prevents DNA damage induced by UVA, UVB and visible radiation in human fibroblasts. *Journal of Photochemistry and Photobiology B: Biology* 72:55-60.

Mosmann, T. 1983. Rapid colorimetric assay for cellular growth and survival: application to proliferation and cytotoxicity assays. *Journal of Immunological Methods.* 65(1-2):55-63.

Mouret, S., M.Charveron, A.Favier, J.Cadet, and T.Douki. 2008. Differential repair of UVB-induced cyclobutane pyrimidine dimers in cultured human skin cells and whole human skin. *DNA Repair*. 7(5):704-12.

Mouret, S., C.Philippe, J.Gracia-Chantegrel, A.Banyasz, S.Karpati, D.Markovitsi, and T.Douki. 2010. UVA-induced cyclobutane pyrimidine dimers in DNA: a direct photochemical mechanism? *Organic & Biomolecular Chemistry*. 8(7):1706-11.

Mouret, S., C.Baudouin, M.Charveron, A.Favier, J.Cadet, and T.Douki. 2006. Cyclobutane pyrimidine dimers are predominant DNA lesions in whole human skin exposed to UVA radiation. *Proceedings of the National Academy of Sciences* 103:13765-13770.

Mouret, S., A.Forestier, and T.Douki. 2012. The specificity of UVA-induced DNA damage in human melanocytes. *Photochem. Photobiol. Sci.* 11:155-162

Murdoch, W.J. and J.F.Martinchick. 2004. Oxidative damage to DNA of ovarian surface epithelial cells affected by ovulation: carcinogenic implication and chemoprevention. *Experimental Biology & Medicine*. 229(6):546-52.

Murray, J.C., J.A.Burch, R.D.Streilein, M.A.Iannacchione, R.P.Hall, and S.R.Pinnell. 2008. A topical antioxidant solution containing vitamins C and E stabilized by ferulic acid provides protection for human skin against damage caused by ultraviolet irradiation. *Journal of the American Academy of Dermatology* 59:418-425.

Norval, M. 2006. The mechanisms and consequences of ultraviolet-induced immunosuppression. *Progress in Biophysics and Molecular Biology* 92:108-118.

Nusgens, B.V., P.Humbert, A.Rougier, A.C.Colige, M.Haftek, C.A.Lambert, A.Richard, P.Creidi, and C.M.Lapiere. 2001. Topically applied vitamin C enhances the mRNA level of collagens I and III, their processing enzymes and tissue inhibitor of matrix metalloproteinase 1 in the human dermis. *Journal of Investigative Dermatology*. 116(6):853-9.

Obermuller-Jevic, U.C., P.I.Francz, J.Frank, A.Flaccus, and H.K.Biesalski. 1999. Enhancement of the UVA induction of haem oxygenase-1 expression by beta-carotene in human skin fibroblasts. *FEBS Letters* 460:212-216.

Odeleye, O.E., C.D.Eskelson, S.I.Mufti, and R.R.Watson. 1992. Vitamin E inhibition of lipid peroxidation and ethanol-mediated promotion of esophageal tumorigenesis. *Nutrition & Cancer*. 17(3):223-34.

Offer, H., M.Milyavsky, N.Erez, D.Matas, I.Zurer, C.C.Harris, and V.Rotter. 2001. Structural and functional involvement of p53 in BER in vitro and in vivo. *Oncogene*.581-589.

Oresajo, C., M.Yatskayer, A.Galdi, P.Foltis, and S.Pillai. 2010. Complementary effects of antioxidants and sunscreens in reducing UV-induced skin damage as demonstrated by skin biomarker expression. *Journal of Cosmetic & Laser Therapy*. 12(3):157-62.

Ouedraogo, G.D. and R.W.Redmond. 2003. Secondary reactive oxygen species extend the range of photosensitization effects in cells: DNA damage produced via initial membrane photosensitization. *Photochemistry & Photobiology*. 77(2):192-203.

Padayatty, S.J., M.Levine, A.L.Briley, L.Poston, A.H.Shennan, C.A.Crowther, A.R.Rumbold, J.Robinson, and the ACTS Study Group. 2006. Vitamins C and E and the Prevention of Preeclampsia. *N Engl J Med* 355:1065-1066.

Panich, U., V.nan, T.Onkoksoong, K.Kongtaphan, K.Kasetsinsombat, P.Akarasereenont, and A.Wongkajornsilp. 2011. Inhibition of UVA-mediated melanogenesis by ascorbic acid through modulation of antioxidant defense and nitric oxide system. *Archives of Pharmacal Research* 34:811-820.

Pedrelli, V.F., M.M.Lauriola, and P.D.Pigatto. 2011. Clinical evaluation of photoprotective effect by a topical antioxidants combination (tocopherols and tocotrienols). *Journal of the European Academy of Dermatology and Venereology*.

Perdiz, D., P.Gróf, O.Nikaido, E.Moustacchi, and E.Sage. 2000. Distribution and Repair of Bipyrimidine Photoproducts in Solar UV-irradiated Mammalian Cells. *Journal of Biological Chemistry* 275:26732-26742.

Perluigi, M., F.Di Domenico, C.Blarzino, C.Foppoli, C.Cini, A.Giorgi, C.Grillo, F.De Marco, D.Butterfield, M.Schinina, and R.Coccia. 2010. Effects of UVB-induced oxidative stress on protein expression and specific protein oxidation in normal human epithelial keratinocytes: a proteomic approach. *Proteome Science* 8:13.

Peter, W. 2007. Fluorescent and luminescent probes for measurement of oxidative and nitrosative species in cells and tissues: Progress, pitfalls, and prospects. *Free Radical Biology and Medicine* 43:995-1022.

Petersen, A.B., R.Gniadecki, J.Vicanova, T.Thorn, and H.C.Wulf. 2000. Hydrogen peroxide is responsible for UVA-induced DNA damage measured by alkaline comet assay in HaCaT keratinocytes. *Journal of Photochemistry and Photobiology B: Biology* 59:123-131.

Pfeifer, G.P. and A.Besaratinia. 2012. UV wavelength-dependent DNA damage and human non-melanoma and melanoma skin cancer. *Photochem. Photobiol. Sci.* 11:90-97



Phillipson, R.P., S.E.Tobi, J.A.Morris, and T.J.McMillan. 2002. UV-A induces persistent genomic instability in human keratinocytes through an oxidative stress mechanism. *Free Radical Biology and Medicine* 32:474-480.

Pinnell, S.R. 2003. Cutaneous photodamage, oxidative stress, and topical antioxidant protection. *Journal of the American Academy of Dermatology* 48:1-19.

Placzek, M., S.Gaube, U.Kerkmann, K.P.Gilbertz, T.Herzinger, E.Haen, and B.Przybilla. 2005. Ultraviolet B-induced DNA damage in human epidermis is modified by the antioxidants ascorbic acid and D-alpha-tocopherol. *Journal of Investigative Dermatology*. 124(2):304-7.

Podda, M., M.G.Traber, C.Weber, L.J.Yan, and L.Packer. 1998. UV-irradiation depletes antioxidants and causes oxidative damage in a model of human skin. *Free Radical Biology & Medicine*. 24(1):55-65.

Possel,H., H.Noack, W.Augustin, G.Keilhoff, and G.Wolf. 2,7-Dihydrodichlorofluorescein diacetate as a fluorescent marker for peroxynitrite formation. *FEBS Letters* 416[2], 175-178. 1997.

Rangwala, S. and K.Y.Tsai. 2011. Roles of the Immune System in Skin Cancer. *British Journal of Dermatology* 165:953-965.

Rassool, F.V., T.J.Gaymes, N.Omidvar, N.Brady, S.Beurlet, M.Pla, M.Reboul, N.Lea, C.Chomienne, N.S.B.Thomas, G.J.Mufti, and R.A.Padua. 2007. Reactive Oxygen Species, DNA Damage, and Error-Prone Repair: A Model for Genomic Instability with Progression in Myeloid Leukemia? *Cancer Research* 67:8762-8771.

Reardon, J.T., T.Bessho, H.C.Kung, P.H.Bolton, and A.Sancar. 1997. In vitro repair of oxidative DNA damage by human nucleotide excision repair system: possible explanation for neurodegeneration in xeroderma pigmentosum patients. *Proceedings of the National Academy of Sciences of the United States of America*. 94(17):9463-8.

Reelfs, O., R.M.Tyrrell, and C.Pourzand. 2004. Ultraviolet a radiation-induced immediate iron release is a key modulator of the activation of NF-kappaB in human skin fibroblasts. *Journal of Investigative Dermatology*. 122(6):1440-7.

Reeve, V.E., D.Domanski, and M.Slater. 2006. Radiation Sources Providing Increased UVA/UVB Ratios Induce Photoprotection Dependent on the UVA Dose in Hairless Mice. *Photochemistry and Photobiology* 82:406-411.

Reeve, V.E., M.Allanson, S.J.Arun, D.Domanski, and N.Painter. 2010. Mice drinking goji berry juice (*Lycium barbarum*) are protected from UV radiation-induced skin damage via antioxidant pathways. *Photochem. Photobiol. Sci.* 9:601-607.

Remacle, J., D.Lambert, M.Raes, E.Pigeolet, C.Michiels, and O.Toussaint. 1992. Importance of various antioxidant enzymes for cell stability. Confrontation between theoretical and experimental data. *Biochemical Journal*. 286 ( Pt 1):41-6.

Ridley, A.J., J.R.Whiteside, T.J.McMillan, and S.L.Allinson. 2009. Cellular and sub-cellular responses to UVA in relation to carcinogenesis. *Int J Radiat Biol* 85:177-195.

Rizwan, M., I.Rodriguez-Blanco, A.Harbottle, M.A.Birch-Machin, R.E.B.Watson, and L.E.Rhodes. 2011. Tomato paste rich in lycopene protects against cutaneous photodamage in humans in vivo: a randomized controlled trial. *British Journal of Dermatology* 164:154-162.

Roberts, L.J. and J.D.Morrow. 2000. Measurement of F2-isoprostanes as an index of oxidative stress in vivo. *Free Radical Biology and Medicine* 28:505-513.

Robinson, K.S., N.J.Traynor, H.Moseley, J.Ferguson, and J.A.Woods. 2010. Cyclobutane pyrimidine dimers are photosensitised by carprofen plus UVA in human HaCaT cells. *Toxicology in Vitro* 24:1126-1132.

Rochette, P.J., S.Lacoste, J.P.Therrien, N.Bastien, D.E.Brash, and R.+Drouin. 2009. Influence of cytosine methylation on ultraviolet-induced cyclobutane pyrimidine dimer formation in genomic DNA. *Mutation Research/Fundamental and Molecular Mechanisms of Mutagenesis* 665:7-13.

Rochette, P.J., J.-P.Therrien, R.Drouin, D.Perdiz, N.Bastien, E.A.Drobetsky, and E.Sage. 2003. UVA-induced cyclobutane pyrimidine dimers form predominantly at thymine-thymine dipyrimidines and correlate with the mutation spectrum in rodent cells. *Nucleic Acids Research* 31:2786-2794.

Rumbold, A., L.Duley, C.A.Crowther, and R.R.Haslam. 2008. Antioxidants for preventing pre-eclampsia. [Review] [65 refs]. *Cochrane Database of Systematic Reviews*. (1):CD004227.

Runger, T.M., B.Farahvash, Z.Hatvani, and A.Rees. 2012. Comparison of DNA damage responses following equimutagenic doses of UVA and UVB: A less effective cell cycle arrest with UVA may render UVA-induced pyrimidine dimers more mutagenic than UVB-induced ones. *Photochem. Photobiol. Sci.* 11:207-215

Saarialho-Kere, U., E.Kerkela, L.Jeskanen, T.Hasan, R.Pierce, B.Starcher, R.Raudasoja, A.Ranki, A.Oikarinen, and M.Vaalamo. 1999. Accumulation of Matrilysin (MMP-7) and Macrophage Metalloelastase (MMP-12) in Actinic Damage. *113:664-672*.

Sabliov, C., C.Fronczek, C.Astete, M.Khachaturyan, L.Khachatryan, and C.Leonardi. 2009. Effects of Temperature and UV Light on Degradation of  $\alpha$ -Tocopherol in Free and Dissolved Form. *Journal of the American Oil Chemists' Society* 86:895-902.

Sage, E. 1993. Distribution and repair of photolesions in DNA: genetic consequences and the role of sequence context. [Review] [153 refs]. *Photochemistry & Photobiology*. 57(1):163-74.

Sage, E., P.M.Girard, and S.Francesconi. 2011. Unravelling UVA-induced mutagenesis. *Photochem. Photobiol. Sci.* 11:74-80.

Sakagami, H., K.Satoh, Y.Makino, T.Kojima, and M.Takeda. 1997. Effect of alpha-tocopherol on cytotoxicity induced by UV irradiation and antioxidants. *Anticancer Research*. 17(3C):2079-82.

Scharffetter-Kochanek, K., M.Wlaschek, P.Brenneisen, M.Schauen, R.Blaudschun, and J.Wenk. 1997. UV-induced reactive oxygen species in photocarcinogenesis and photoaging. [Review] [118 refs]. *Biological Chemistry*. 378(11):1247-57.

Scharffetter-Kochanek, K., M.Wlaschek, K.Briviba, and H.Sies. 1993. Singlet oxygen induces collagenase expression in human skin fibroblasts. *FEBS Letters*. 331(3):304-6.

Schauen, M., H.T.Hornig-Do, S.Schomberg, G.Herrmann, and R.J.Wiesner. 2007. Mitochondrial electron transport chain activity is not involved in ultraviolet A (UVA)-induced cell death. *Free Radical Biology and Medicine* 42:499-509.

Schuchmann, S. and U.Heinemann. 2000. Increased mitochondrial superoxide generation in neurons from trisomy 16 mice: a model of Down's syndrome. *Free Radical Biology and Medicine* 28:235-250.

Seyedrezazadeh, E., A.Ostadrahimi, S.Mahboob, Y.Assadi, J.Ghaemmagami, and M.Pourmogaddam. 2008. Effect of vitamin E and selenium supplementation on oxidative stress status in pulmonary tuberculosis patients. *Respirology*. 13(2):294-8.

Shindo, Y., E.Witt, D.Han, W.Epstein, and L.Packer. 1994. Enzymic and non-enzymic antioxidants in epidermis and dermis of human skin. *J. Inv. Derm.* 102(1):122-4.

Shishodia, S. and B.B.Aggarwal. 2004. Guggulsterone Inhibits NF-kB and I $\kappa$ B $\alpha$  Kinase Activation, Suppresses Expression of Anti-apoptotic Gene Products, and Enhances Apoptosis. *Journal of Biological Chemistry* 279:47148-47158.

Shklar, G., J.L.Schwartz, D.P.Trickler, and S.Reid. 1990. Prevention of experimental cancer and immunostimulation by vitamin E (immunosurveillance). *Journal of Oral Pathology & Medicine*.60-64.

Silvers, A.L., M.A.Bachelor, and G.T.Bowden. 2003. The role of JNK and p38 MAPK activities in UVA-induced signaling pathways leading to AP-1 activation and c-Fos expression. *Neoplasia (New York)*. 5(4):319-29,-Aug.

Simone, C.B., N.L.Simone, V.Simone, and C.B.Simone. 2007. Antioxidants and other nutrients do not interfere with chemotherapy or radiation therapy and can increase kill and increase survival. [Review] [130 refs]. *Alternative Therapies in Health & Medicine*. 13(1):22-8,-Feb.

Singh, N.P., M.T.McCoy, R.R.Tice, and E.L.Schneider. 1988. A simple technique for quantitation of low levels of DNA damage in individual cells. *Experimental Cell Research* 175:184-191.

Slatore, C.G., A.J.Littman, D.H.Au, J.A.Satia, and E.White. 2008. Long-Term Use of Supplemental Multivitamins, Vitamin C, Vitamin E, and Folate Does Not Reduce the Risk of Lung Cancer. *Am. J. Respir. Crit. Care Med*. 177:524-530.

Smith, A.M. 1996. Ptolemy's Theory of Visual Perception: An English Translation of the Optics With Introduction and Commentary. American Philosophical Society.

Smith, C.C., M.R.O'Donovan, and E.A.Martin. 2006. hOGG1 recognizes oxidative damage using the comet assay with greater specificity than FPG or ENDOIII. *Mutagenesis* 21:185-190.

Son, Y., Y.K.Cheong, N.H.Kim, H.T.Chung, D.G.Kang, and H.O.Pae. 2011. Mitogen-Activated Protein Kinases and Reactive Oxygen Species: How Can ROS Activate MAPK Pathways? *Journal of Signal Transduction*. 792639.

Stahl, W. and H.Sies. 2012. Photoprotection by dietary carotenoids: Concept, mechanisms, evidence and future development. *Mol. Nutr. Food Res.* 56:287-295.

Steenvoorden, D.P. and G.M.van Henegouwen. 1997. The use of endogenous antioxidants to improve photoprotection. [Review] [134 refs]. *Journal of Photochemistry & Photobiology. B - Biology.* 41(1-2):1-10.

Steinhubl, S.R. 2008. Why Have Antioxidants Failed in Clinical Trials? *The American Journal of Cardiology* 101:S14-S19.

Streilein, J.W., J.R.Taylor, V.Vincek, I.Kurimoto, T.Shimizu, C.Tie, and C.Golomb. 1994. Immune surveillance and sunlight-induced skin cancer. [Review] [53 refs]. *Immunology Today.* 15(4):174-9.

Sutherland, J.C. and K.P.Griffin. 1981. Absorption spectrum of DNA for wavelengths greater than 300 nm. *Radiation Research.* 86(3):399-409.

Tavani, A., C.Bosetti, S.Franceschi, R.Talamini, E.Negri, and C.La Vecchia. 2006. Occupational exposure to ultraviolet radiation and risk of non-Hodgkin lymphoma. *European Journal of Cancer Prevention.* 15(5):453-7.

Tewari, A., R.Sarkany, and A.R.Young. 2012a. UVA1 induces cyclobutane pyrimidine dimers but not 6-4 photoproducts in human skin *in vivo*. *Journal of Investigative Dermatology.* 132:394-400.

Tewari,A., C.Lahmann, R.P.Sarkany, J.Bergemann, and A.R.Young. 2012b. Human erythema and matrix metalloproteinase-1 mRNA induction, *in vivo*, share an action spectrum which suggests common chromophores. *Photochem. Photobiol. Sci.* 11:216-223

The Alpha-Tocopherol Beta Carotene Cancer Prevention Study Group. 1994. The Effect of Vitamin E and Beta Carotene on the Incidence of Lung Cancer and Other Cancers in Male Smokers. *N Engl J Med* 330:1029-1035.

Thompson, S.C., D.Jolley, and R.Marks. 1993. Reduction of Solar Keratoses by Regular Sunscreen Use. *N Engl J Med* 329:1147-1151.

Trevithick, J.R., D.T.Shum, S.Redae, K.P.Mitton, C.Norley, S.J.Karlik, A.C.Groom, and E.E.Schmidt. 1993. Reduction of sunburn damage to skin by topical application of vitamin E acetate following exposure to ultraviolet B radiation: effect of delaying application or of reducing concentration of vitamin E acetate applied. *Scanning Microscopy.* 7(4):1269-81.

Trickler, D. and G.Shklar. 1987. Prevention by vitamin E of experimental oral carcinogenesis. *Journal of the National Cancer Institute.* 78(1):165-9.

Tyrrell, R.M. 2004. Solar ultraviolet A radiation: an oxidizing skin carcinogen that activates heme oxygenase-1. [Review] [37 refs]. *Antioxidants & Redox Signaling.* 6(5):835-40.

Vaalamo, M., A.L.Kariniemi, S.D.Shapiro, and U.Saarialho-Kere. 1999. Enhanced Expression of Human Metalloelastase (MMP-12) in Cutaneous Granulomas and Macrophage Migration. *112:499-505.*

Valencia, A. and I.E.Kochevar. 2008. Nox1-based NADPH oxidase is the major source of UVA-induced reactive oxygen species in human keratinocytes. *Journal of Investigative Dermatology.* 128(1):214-22.

- Valencia, A., A.Rajadurai, A.B.Carle, and I.E.Kochevar. 2006. 7-Dehydrocholesterol enhances ultraviolet A-induced oxidative stress in keratinocytes: roles of NADPH oxidase, mitochondria, and lipid rafts. *Free Radical Biology & Medicine*. 41(11):1704-18.
- Valeur, B. and J.C.Brochon. 2001. New Trends in Fluorescence Spectroscopy: Applications to Chemical and Life Sciences. Springer-Verlag, Berlin.
- Valgimigli, L., G.F.Pedulli, and M.Paolini. 2001. Measurement of oxidative stress by EPR radical-probe technique. *Free Radical Biology and Medicine* 31:708-716.
- van den Broeke, L.T. and G.M.J.Beijersbergen van Henegouwen. 1995. Topically applied N-acetylcysteine as a protector against UVB-induced systemic immunosuppression. *Journal of Photochemistry and Photobiology B: Biology* 27:61-65.
- Vasavi, H., M.Thangaraju, and P.Sachdanandam. 1994. Effect of alpha-tocopherol on lipid peroxidation and antioxidant system in fibrosarcoma bearing rats. *Molecular & Cellular Biochemistry*. 131(2):125-9.
- Vile, G.F., S.Basu-Modak, C.Waltner, and R.M.Tyrrell. 1994. Heme oxygenase 1 mediates an adaptive response to oxidative stress in human skin fibroblasts. *Proceedings of the National Academy of Sciences* 91:2607-2610.
- von Thaler, A.K., Y.Kamenisch, and M.Berneburg. 2010. The role of ultraviolet radiation in melanomagenesis. *Experimental Dermatology* 19:81-88.
- Vrablic, A.S., C.D.Albright, C.N.Craciunescu, R.I.Salganik, and S.H.Zeisel. 2001. Altered mitochondrial function and overgeneration of reactive oxygen species precede the induction of apoptosis by 1-O-octadecyl-2-methyl-rac-glycero-3-phosphocholine in p53-defective hepatocytes. *FASEB Journal*. 15(10):1739-44.



Walker, S.L. and A.R.Young. 2007. An action spectrum (290-320 nm) for TNFalpha protein in human skin in vivo suggests that basal-layer epidermal DNA is the chromophore. *Proceedings of the National Academy of Sciences of the United States of America*. 104(48):19051-4.

Webb, A.R. and M.F.Holick. 1988. The Role of Sunlight in the Cutaneous Production of Vitamin D3. *Annu. Rev. Nutr.* 8:375-399.

Webb, A.R., H.Slaper, P.Koepke, and A.W.Schmalwieser. 2011. Know Your Standard: Clarifying the CIE Erythema Action Spectrum. *Photochemistry & Photobiology*. 87(2):483-6.

Werninghaus, K., M.Meydani, J.Bhawan, R.Margolis, J.B.Blumberg, and B.A.Gilchrest. 1994. Evaluation of the photoprotective effect of oral vitamin E supplementation. *Archives of Dermatology*. 130(10):1257-61.

Widyarini, S., D.Domanski, N.Painter, and V.E.Reeve. 2012. Photoimmune protective effect of the phytoestrogenic isoflavonoid equol is partially due to its antioxidant activities. *Photochem. Photobiol. Sci.(In press)*.

Wiseman, H. and B.Halliwell. 1996. Damage to DNA by reactive oxygen and nitrogen species: role in inflammatory disease and progression to cancer. [Review] [213 refs]. *Biochemical Journal*. 313 (Pt 1):17-29.

Wolf, P., H.Maier, R.R.Mullegger, C.A.Chadwick, R.Hofmann-Wellenhof, H.P.Soyer, A.Hofer, J.Smolle, M.Horn, L.Cerroni, D.Yarosh, J.Klein, C.Bucana, K.Dunner, Jr., C.S.Potten, H.Honigsmann, H.Kerl, and M.L.Kripke. 2000. Topical treatment with liposomes containing T4 endonuclease V protects human skin in vivo from ultraviolet-induced upregulation of interleukin-10 and tumor necrosis factor-alpha. *Journal of Investigative Dermatology*. 114(1):149-56.

Wölfle, U., P.R.Esser, B.Simon-Haarhaus, S.F.Martin, J.Lademann, and C.M.Schempp. 2011. UVB-induced DNA damage, generation of reactive oxygen species, and inflammation are effectively attenuated by the flavonoid luteolin in vitro and in vivo. *Free Radical Biology and Medicine* 50:1081-1093.

Wondrak, G.T., M.K.Jacobson, and E.L.Jacobson. 2006. Endogenous UVA-photosensitizers: mediators of skin photodamage and novel targets for skin photoprotection. *Photochem. Photobiol. Sci.* 5:215-237.

Woollons, A., C.Kipp, A.R.Young, C.Petit-Frere, C.F.Arlett, M.H.Green, and P.H.Clingen. 1999. The 0.8% ultraviolet B content of an ultraviolet A sunlamp induces 75% of cyclobutane pyrimidine dimers in human keratinocytes in vitro. *British Journal of Dermatology*. 140(6):1023-30.

World Health Organisation. 1992. IARC monographs on the evaluation of carcinogenic risks to humans. Solar and ultraviolet radiation. *IARC monographs on the evaluation of carcinogenic risks to humans / World Health Organization, International Agency for Research on Cancer*. 55 (pp 1-316),1-316.

Wu, S., J.Gao, Q.T.Dinh, C.Chen, and S.Fimmel. 2008. IL-8 production and AP-1 transactivation induced by UVA in human keratinocytes: Roles of d-[alpha]-tocopherol. *Molecular Immunology* 45:2288-2296.

Xu, H.B., L.Li, and G.Q.Liu. 2008. Protection against hydrogen peroxide-induced cytotoxicity in PC12 cells by guggulsterone. *Yao Hsueh Hsueh Pao - Acta Pharmaceutica Sinica*. 43(12):1190-7.

Xue, C., W.Liu, J.Wu, X.Yang, and H.Xu. 2011. Chemoprotective effect of N-acetylcysteine (NAC) on cellular oxidative damages and apoptosis induced by nano titanium dioxide under UVA irradiation. *Toxicology in Vitro* 25:110-116.

Yakes, F.M. and B.Van Houten. 1997. Mitochondrial DNA damage is more extensive and persists longer than nuclear DNA damage in human cells following oxidative stress. *Proceedings of the National Academy of Sciences of the United States of America*. 94(2):514-9.

You, Y.H., D.H.Lee, J.H.Yoon, S.Nakajima, A.Yasui, and G.P.Pfeifer. 2001. Cyclobutane pyrimidine dimers are responsible for the vast majority of mutations induced by UVB irradiation in mammalian cells. *Journal of Biological Chemistry*. 276(48):44688-94.

Young, A.R. 2004. Tanning devices--fast track to skin cancer?. [Review] [69 refs]. *Pigment Cell Research*. 17(1):2-9.

Young, A.R., C.A.Chadwick, G.I.Harrison, J.L.Hawk, O.Nikaido, and C.S.Potten. 1996. The in situ repair kinetics of epidermal thymine dimers and 6-4 photoproducts in human skin types I and II. *Journal of Investigative Dermatology*. 106(6):1307-13.

Young, A.R. 2010. Some Light on the Photobiology of Vitamin D. *J Invest Dermatol* 130:346-348.

Young, A.R., C.A.Chadwick, G.I.Harrison, O.Nikaido, J.Ramsden, and C.S.Potten. 1998. The Similarity of Action Spectra for Thymine Dimers in Human Epidermis and Erythema Suggests that DNA is the Chromophore for Erythema. *III*:982-988.

Zhang, X., B.S.Rosenstein, Y.Wang, M.Lebwohl, and H.Wei. 1997. Identification of Possible Reactive Oxygen Species Involved in Ultraviolet Radiation-Induced Oxidative DNA Damage. *Free Radical Biology and Medicine* 23:980-985.

Ziegler, A., A.Jonason, J.Simon, D.Leffell, and D.E.Brash. 1996. Tumor Suppressor Gene Mutations and Photocarcinogenesis. *Photochemistry and Photobiology* 63:432-435.

## Appendix

Presentations and posters produced by the work presented in this thesis:

Delinassios G.J., Cooke M.S. and Young A.R. Inhibition of cellular oxidative stress in keratinocytes by  $\alpha$ -tocopherol. The 13<sup>th</sup> Congress for the European Society for Photobiology (Wroclaw, Poland; 2009)

Delinassios G.J., Cooke M.S. and Young A.R. Inhibition of UVA-induced DNA damage by Vitamin E. British Society for Investigative Dermatology, Annual Meeting (Edinburgh, Scotland; 2010)

Delinassios G.J., Cooke M.S. and Young A.R. Antioxidant treatment after UVAI exposure offers protection against ROS and DNA photodamage. The 14<sup>th</sup> Congress for the European Society for Photobiology (Geneva, Switzerland; 2011)

The following manuscript has also been produced and will be submitted for publication by the end of November 2011:

Delinassios G.J., Karbaschi M., Cooke M.S. and Young A.R. DNA photolesions and reactive oxygen species in human keratinocytes *in vitro* are inhibited by vitamin E treatment after ultraviolet radiation exposure